APPLICATION OF VORTEX TUBES IN AN UNDERGROUND MINE VENTILATION SYSTEM

By

Nelson K. Dumakor-Dupey, B.S., MPhil.

A Thesis Submitted in Partial Fulfillment of the Requirements
for the Degree of

Master of Science
in
Mining Engineering

University of Alaska Fairbanks

December 2021

APPROVED:

Sampurna N. Arya, Ph.D., Committee Chair
Tathagata Ghosh, Ph.D., Committee Co-Chair
Gang Chen, Committee Member
Tathagata Ghosh, Ph.D., Department Chair
Department of Mining and Mineral Engineering
William E. Schnabel, Ph.D., Dean
College of Engineering and Mines
Richard Collins, *Director of the Graduate School*

ABSTRACT

A major challenge for deep underground mines in tropical regions is high-temperature climate conditions at a working face. The high-temperature conditions can cause discomfort to people working underground and lead to health and safety issues. In some instances, airflow from primary ventilation and central refrigeration systems is not adequate to reduce the ambient temperature below a permissible limit at remotely located working faces. In some mines, mobile cooling systems are used in conjunction with an existing central cooling system. However, mining companies are often skeptical about implementing the combined cooling system due to its high operating costs involved with refrigeration infrastructure. This research examines the potential of a low-cost, maintenance-free vortex tube spot cooling system that operates on compressed air and can work with or without a central cooling system. Using an underground metal mine in Ghana as a case study, the impact of a vortex tube cooling system at a working face was evaluated using the computational fluid dynamics (CFD) technique. An integrated CFD model of vortex tube, ventilation duct, and development heading was developed. The airflow was simulated within the CFD model with a varying number of vortex tubes and locations. The simulation result shows that the mine can achieve a decent temperature drop from 28°C (82.4°F) to 24°C (75.2°F) with 20 vortex tubes at the working face.

TABLE OF CONTENTS

Page

LIST OF FIGURES

Page

LIST OF TABLES

Page

LIST OF APPENDICES

Page

DEDICATION

To my family and teachers

ACKNOWLEDGEMENT

I am most grateful to Dr. Sampurna N. Arya for his excellent academic guidance and support throughout my academic journey at the University of Alaska Fairbanks. I extend profound gratitude to the advisory committee members: Dr. Tathagata Ghosh and Dr. Gang Chen for their support and intellectual input.

I acknowledge the generous financial support from the Institute of Northern Engineering and the Department of Mining and Mineral Engineering towards my graduate studies. I also appreciate the encouragement and selfless contribution of the following individuals: Banabas Dogah, Fahimeh Dehghani, Utpal Avro Mozumder, and Benny Acquah. A special thanks to Jill Riddle, the department's office manager for her assistance.

CHAPTER 1 INTRODUCTION

1.1 Background and Problem Statement

Mine ventilation serves as a respiratory system for an underground mine. It provides adequate quality and quantity of fresh air to dilute and exhaust contaminated air, maintains an ambient temperature within a regulatory threshold, and ensures a comfortable and safe working environment for both workers and mine equipment. Generally, fresh air from the atmosphere is drawn to the working faces with the aid of mechanical fans to remove heat loads and control high temperatures at a working face [1]. However, as mining operation advances, at certain depths, the cooling effect of atmospheric air becomes ineffective due to excessive strata heat. In other words, the total heat load from the geothermal gradient, auto-compression, mine machinery, human metabolism, and blasting exceeds the thermal capacity of atmospheric air, resulting in high temperatures and humidity in the mine [2]. Exposure to such unconducive working conditions can cause deleterious health effects to workers and impede production [3], [4]. At this point, artificial air-cooling is required to regulate the air temperature in the working areas. Among the available artificial cooling methods, spot cooling (also referred to as decentralized, tertiary, face, or in-stope air cooling systems) is considered an efficient and cost-effective strategy because cooled air is directly delivered where it is needed. The idea behind this strategy is that the cooling unit is in direct contact with the airflow at the place where cooling is required (*i.e.*, mining face), and the absorbed heat is dumped directly to the return air [5]. The advantages of this system include immediate cooling at the spot [5] and positional efficiency [6]. This system can be used exclusively when the heat load is low. It can also be applied in conjunction with other cooling systems such as central cooling.

Due to the large energy consumption of conventional vapor-compression cooling systems, some alternative cooling systems are being investigated for spot cooling in industrial processes. One of these techniques is the use of vortex tubes. A vortex tube is a low-cost, maintenance-free thermal device that separates a high-pressure air/gas stream into cold and hot air/gas streams [7]. This phenomenon takes place without the help of any moving parts. Despite the relatively low refrigeration capacity of vortex tubes, they can be a potential candidate for underground spot

cooling for many reasons, such as being lightweight, usable when electricity is not available, low initial cost, instantaneous operation, and no need for an expert operator [5], [8], [9].

Vortex Tubes have a wide range of spot cooling applications on machines, assembly lines, and processes. EXAIR Corporation, NexFlow Air Products Corp., and several other manufacturers produce different types of vortex tubes on a commercial scale for varied industrial needs. Notwithstanding its wide implementation in industries and processes, such as welding, brazing, solidifying polymers, and controlling air climate, there is a lack of study and information about its application or implementation in mining operations, particularly in underground mine ventilation. So far, two theoretical studies have investigated the feasibility of vortex tube refrigeration in underground mine ventilation. Wang & Jiao [10] estimated the heat load of an underground mine and suggested a vortex tube refrigeration system as an excellent prospect for meeting the cooling requirement of the mine. The benefits of this refrigeration system include the availability of compressed gas at a working face, the possibility of moving the vortex tube system with the working face, no need for long piping, major cost-saving, and an overall reduction in greenhouse gas emissions. Zhai [11] also investigated the feasibility of vortex tube refrigeration in a mine cooling jacket. Nonetheless, Kamyar et al. [5] believe that work on this type of cooling strategy is still immature and should be examined further for future potentials in mining applications. This thesis aims to numerically investigate the cooling potential of a vortex tube system and ascertain its sufficiency in controlling high temperatures at a working face of an underground mine.

The mine considered in this study is an underground metal mine located in the Western Region of Ghana. Mechanized shrinkage stoping is used to exploit the gold deposit, producing about 650 tonnes/day (717 tons/day). The mine is experiencing extreme thermal conditions as it extends to exploit deeper ore zones at depths exceeding 900 m (2,953 ft). Due to excessive heat, mainly from the strata (estimated at 30–31°C) and the long travel time of airflow, wet bulb temperature in working areas is approaching 30°C (86°F). The Ghanaian mining regulations require that wet-bulb temperature in the working areas must not exceed 32.5°C (90.5°F). Therefore, artificial air cooling will be required as the mine develops to greater depths.

1.2 Research Objectives

This research aims to use computational fluid dynamics (CFD) to evaluate the cooling potential of a vortex tube system at a working face of an underground metal mine. The specific objectives of the research are as follows:

i. Use CAD software to design a 3D model of a development heading and auxiliary ventilation system.
ii. Model air velocity and temperature in a ventilation duct and a development heading.
iii. Determine the appropriate number and location of vortex tubes required to achieve sufficient cooling at the working face.
iv. Evaluate the airflow dynamics for the different number of vortex tubes and locations.

1.3 Research Methods

The methods adopted include the following:

i. Review of relevant literature on vortex tube cooling system and numerical modeling;
ii. Acquisition of mine data through review of mine reports and the Ghana mining regulations, and interview with mine personnel.
iii. 3D model design of the vortex tube, development heading, and ventilation duct for numerical simulation.
iv. CFD modeling and simulation of the ventilation system.
v. Numerical analyses of the simulation results using velocity and temperature contours.

1.4 Organization of Thesis

There are five main chapters in this thesis. Chapter 1 introduces the research. It contains the problem statement, research objectives, methods adopted for the research, and organization of the thesis. Chapter 2 reviews existing literature on vortex tubes, design considerations, classification, and applications. The chapter also presents a brief review of numerical modeling in the mining industry. Chapter 3 provides a detailed description of the materials and methods, boundary conditions, and numerical simulation of the ventilation system. Chapter 4 presents and discusses the results obtained. The final chapter, Chapter 5, provides conclusions and scope for future research.

CHAPTER 2 OVERVIEW OF VORTEX TUBE

2.1 Introduction

This chapter reviews pertinent literature about mine ventilation and vortex tubes (VTs). It describes the working principles, components, and industrial applications of VTs. The chapter also presents theoretical studies on VT applications in the mining industry and numerical modeling tools for addressing mining-related fluid flow problems.

2.2 Overview of Underground Mining

Underground mining involves the extraction of mineral deposits whereby the exploitation activities are located below ground without exposure to the atmosphere. The extraction is done using an appropriate mining method, which is selected among a pool of suitable alternatives. This mode of mining is applicable to deeply buried deposits with excessive stripping ratio (i.e., depths greater than 500 m) that are otherwise not exploitable with surface mining techniques [12]. Typical depths of some deep underground mines in the world are presented in Figure 2.1. The depth of these mines ranges from 1,280 m in Canada to over 4,800 m in South Africa.

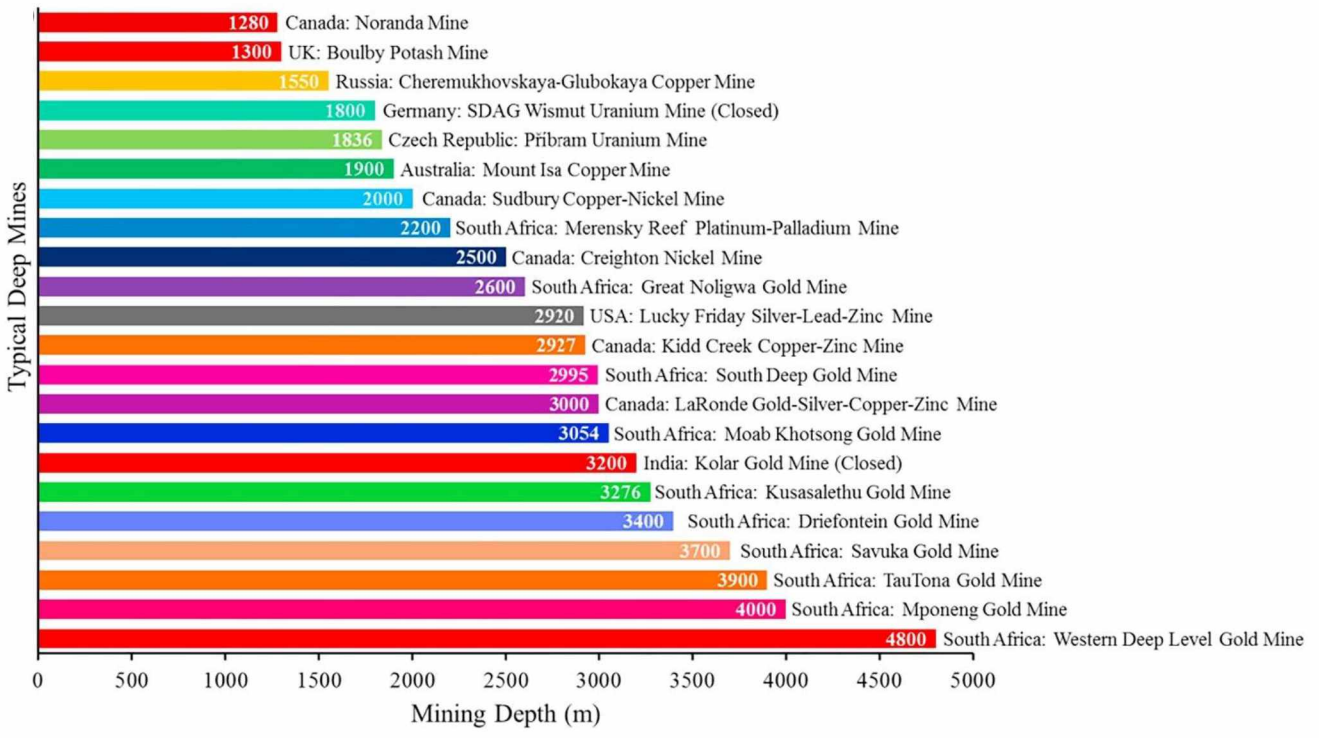

Figure 2.1 Typical Ultra-deep Mines in the World [13]

Prior to exploitation, the deposit is probed, delineated, and developed. The development entails the construction of a series of vertical, lateral, and or inclined excavations to access the orebody for exploitation, auxiliary operations, and exploration where necessary. Colloquially, these different openings are called adit, ramp, decline, incline, shaft, winze, raise, drift/drive, or crosscut, depending on its geometry, orientation, and purpose. A significant number of openings are excavated before stoping, and many more are excavated as exploitation progresses. Excavation of these openings is termed development. There are two categories of development: primary development and secondary development. Primary development deals with the excavation of principal entrances (e.g., shaft, adit, and ramp) of the mine through which the orebody is accessed and extracted. Any other opening which does not serve the purpose of the main entry is considered as a secondary development. This could be a drift, raise or internal shaft.

There are several mining methods (Figure 2.2) in practice for exploiting mineral deposits. These methods are extensively covered in the literature. The methods have not changed since their inception though some modifications are applied based on the unique characteristics of a particular deposit. Generally, there are two methods of classifying underground mining methods based on (i) the type of ground support and (ii) the nature of the stope room and ground treatment for support. The latter method, which is not widely used, considers the nature of stoping room (drift or chamber) together with the type treatment for ground support (i.e., pillars, pillars and filling, filling, filling and self-filling, or self-filling) and assign a coding system. The former method, signifying the importance of ground support, is the most widely accepted classification method. In this method, there are three classes based on the extent of support utilized, namely the supported, unsupported and caving methods. Each method is differentiated by the type of wall and roof supports used, the configuration of production openings, and the direction in which mining operations progress [14].

The unsupported class consists of those underground methods that are essentially self-supporting and require no major artificial system of support to carry the super incumbent load, relying instead on the walls of the openings and natural pillars. The superincumbent load is the weight of the overburden and any tectonic forces acting at depth. This definition of unsupported methods does not preclude the use of rock or roof bolts or light structural sets of timber or steel, provided that

such artificial support does not significantly alter the load-carrying ability of the natural structure. Unsupported methods of mining are used to extract mineral deposits that are roughly tabular, flat or steeply dipping and generally in contact with competent wall rock. This class consists of five methods: room and pillar mining, stope and pillar mining, shrinkage stoping, sublevel stoping, and vertical crater retreat mining.

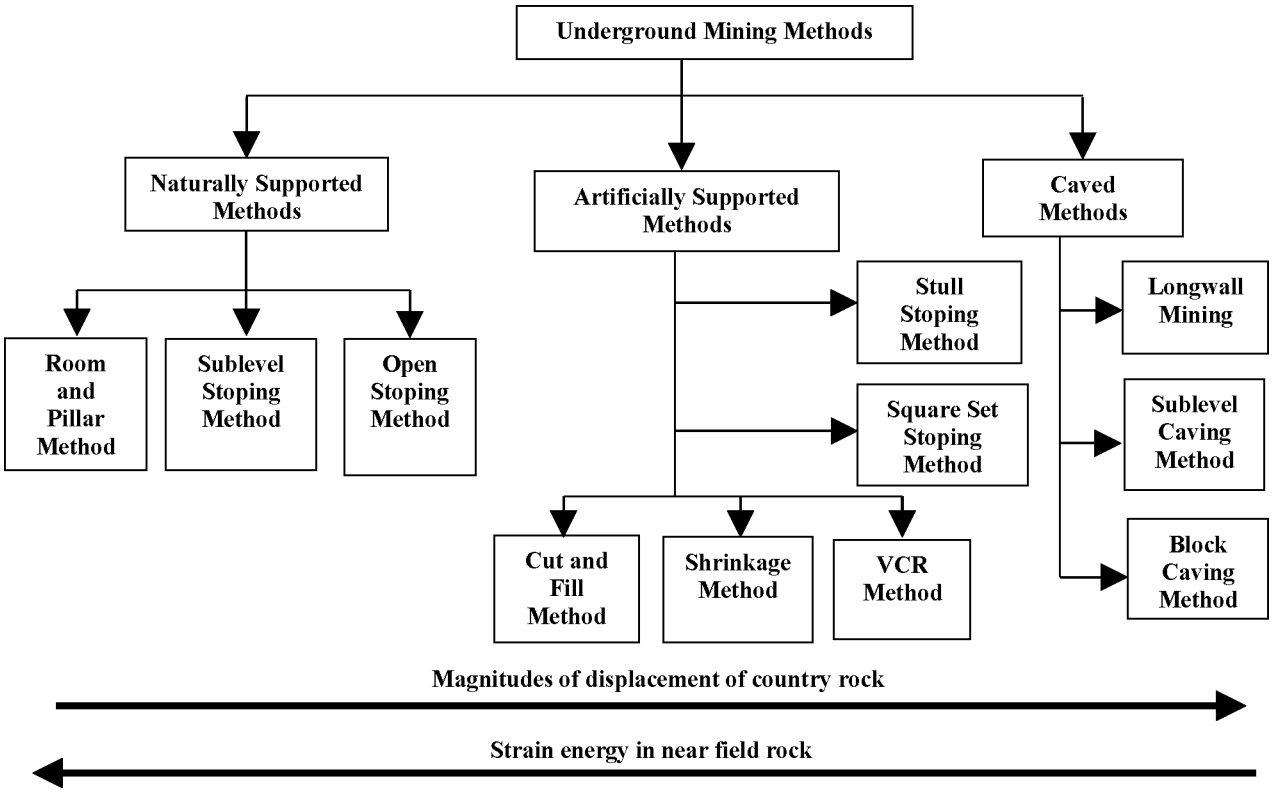

Figure 2.2 Classification of Underground Mining Methods [15]

The supported mining method consists of those methods that require substantial amounts of artificial support to maintain stability in exploitation openings and systematic ground control throughout the mine. Supported methods are used when production openings will not remain standing during their active life and when major caving or subsidence to the surface cannot be tolerated. In other words, the supported class is employed when the other two categories of methods, unsupported and caving, are not applicable. The supported class of mining methods is intended for application to rock ranging in competency from moderate to incompetent. A competent rock is defined as a rock that, because of its physical and geologic characteristics, is capable of sustaining openings without any heavy structural support.

Caving methods may be defined as those associated with induced, controlled, massive caving of the ore body, the overlying rock, or both, concurrent with and essential to the conduct of mining. Subsidence of the surface eventually follows. There are three major caving methods: longwall mining, sublevel caving, and block caving. Table 2.1 summarizes the mining methods for various deposit characteristics.

Table 2.1 Underground Mining Methods for Different Deposit Types [15]

Support System	Method	Rock strength		Geological characteristics	
		Ore	**Waste**	**Type of deposit**	**Dip of orebody**
Naturally supported	Room & pillar	Medium to strong	Medium to strong	Thick or thin stratified beds	Flat to inclined
	Sublevel stoping	Medium to strong	Medium to strong	Narrow or wide veins Massive	Steep
Artificially supported	Cut & fill	Medium to strong	Medium to strong	Narrow or wide veins Massive	Inclined to steep
	Shrinkage	Medium to strong	Medium to strong	Narrow or wide veins	Inclined to steep
	Square set	Weak	Weak to medium	Narrow or wide veins Massive	Inclined to steep
	Block caving	Weak	Weak to medium	Wide vein Massive	Steep
	Sublevel caving	Medium to strong	Medium to strong	Wide vein Massive	Steep
	Longwall	Weak to medium	Weak to medium	Thin stratified beds	Flat to steep

In addition to the productive phases of the actual mining cycle, certain auxiliary unit operations must also be performed. In underground mining, these operations consist of providing and maintaining adequate health and safety, roof support, ventilation, power supply, pumping, communications, and handling of materials and supplies. Generally, the important auxiliary operations in mining are health and safety, ground control, and atmospheric environmental control. When planning production cycles, these auxiliary operations are scheduled to support but not interfere with the production operations. Some may, however, be conducted as an integral part of the cycle if they are essential to health and safety or overall efficiency.

2.3 Mine Ventilation

Mine ventilation serves as life support for underground mining, providing continuous fresh air to and removing contaminated air from working areas. It is important to maintain sufficient and good quality air in the working areas to ensure a safe working environment for workers and equipment. The design and operation of a mine ventilation system have a significant impact on the morale of the workforce, capital and operating costs, productivity, and health and safety. Poor ventilation in underground mining can also cause serious occupational hazards and diseases such as thermal stress, silicosis, asbestosis, and other degenerative lung diseases [16], [17]. Further, concerns about exposure to unfavorable thermal conditions are growing as mines expand to explore orebodies located at great depth [18]. According to Brake [19], the most frequent complaints (e.g., heat, humidity, fumes, gases, and dust) from underground personnel are ventilation-related.

2.3.1 Sources of Heat in Underground Mines

There are several different heat sources that contribute to hot environmental conditions in underground mines. These factors may be greatly increased or decreased based on the mine and mining methods [18]. Some common sources of heat in underground metal mines include auto compression or adiabatic compression (i.e., as air descends through vertical openings), geothermal gradient (strata heat or rock wall temperature), blasting (explosive detonation), electrical and diesel machinery, mine water influx, human metabolism, oxidation of the orebody or timber, and ground movement (friction between falling rock). Figure 2.3 shows the percentage contribution of the major heat sources. The relative contributions of the major heat sources are affected by several factors, including depth of the mine, mechanization, mine power sources, geothermal activity, and rock thermal properties [20].

As indicated in Figure 2.3, the geothermal gradient is often the greatest contributor to the overall hot conditions, as the virgin rock temperature increases with depth [18]. The virgin rock temperature surrounding the excavations has a significant role in the ambient air temperature throughout the mine. For example, at a depth of 900 m in a mine in Germany, the average temperature is 41°C, and at the mining depth of 1,712 m, the maximum temperature is 50°C. In South Africa's Carletonville gold deposit, the mining depth is 4,000 m, and the ground temperature is 70°C. China is also encountering the problem of high temperatures in deep mines such as

Shandong Sun Cun mine, Tongling Shizishan copper mine, and Fushun Hongtoushan copper mine, where the mining depth is more than 1,000 m, and the geothermal temperature is 45°C [21].

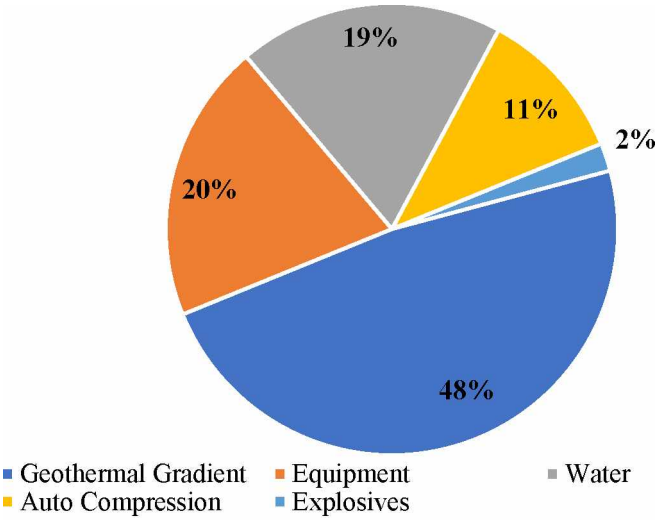

Figure 2.3 Heat Sources in Deep Underground Mines [21]

When cool air passes through mine airways, its temperature usually increases due to the natural geothermal heat being conducted through the rock formations towards the airway. Freshly exposed rock surface has a high temperature; thus, there is a relatively high rate of initial heat release into the mine air. However, this declines in time and as the rock surface gradually cools approaching an equilibrium state when its temperature equals that of the air [22]. In auto compression, when fresh air from the surface flows down an airway, the air experiences compression; that is, the increase in the depth causes the air pressure to increase. This means that the volume of air reduces while descending, but the heat content remains the same resulting in a relatively hotter air than the original air from the surface [23]. According to the principles of air compression and heat release, the air releases a certain amount of heat during the compression process [21]. The temperature increase due to auto compression can be up to 10ºC per kilometer of vertical depth, whether in a shaft or in a decline [24].

Machineries used in the mining process also contribute significantly to the total heat in an underground mine. Production equipment, service vehicles, transformers, and fans are all devices that convert an input power via a useful effect into heat. For any given mining equipment, the total heat produced is simply the rate at which power is supplied, less any work done against gravity

[25]. For instance, the efficiency of internal combustion engines of diesel equipment is 33%, the remaining two-third ($2/3^{rd}$) dissipates as heat through the radiator, exhaust gases, and frictional processes. Additionally, groundwater from hot fissures and natural rock reservoirs is an inexhaustible source of heat in underground mines. As the water flows into the mine, it absorbs heat from the surrounding rock until its temperature reaches equilibrium or sometimes it may exceed that of the rock. The water transfers heat to the airflow through evaporation, increasing the latent heat in the air. Similarly, mine service water also contributes to the latent heat of the mine air because it absorbs heat from the surrounding rock [23].

2.3.2 Heat Exposure and Heat Stress Control

Heat is a major concern in mining, especially in underground metal mines operating at great depths. Because heat renders the work area uncomfortable for human occupancy, reduces worker and equipment productivity, and causes heat-related illness, injury, or death. Naturally, the human body regulates its core temperature by means of conduction, convection, radiation, and evaporation of sweat. This process is referred to as thermoregulation. Just like a black body, the human body can exchange heat with its surroundings readily through absorption and radiation to establish equilibrium.

However, the body can experience heat stress when its ability to maintain a constant temperature is affected by exposure to excessive heat that cannot be dissipated to the environment. This heat stress can result in heat-related illness, injury, or potential death. The onset of heat stress begins with fatigue, loss of concentration, and slowed thinking. Long-term exposure can lead to more serious heat illnesses such as rash, cramps, syncope, exhaustion, heat stroke, and death. Studies have shown that exposure of mine workers to extremely hot conditions is unhealthy, inefficient, and unproductive [3], [26].

To ensure that workers' health is protected, many countries have promulgated heat stress management policies and standards to regulate working in hot environments. Generally, heat stress management regulations provide information and guidance for employers in developing policies and procedures to protect workers in hot environments. The regulations include allowable air temperature in a work environment, temperature monitoring procedures, work area classification,

personal training, and reporting. In the mining industry, these standards are enforced by special government-designated institutions, such as Mine Safety and Health Administration (MSHA) in the USA, Minerals Commission in Ghana, and the Department of Mineral Resources and Energy (DMRE) in South Africa. Table 2.2 presents a summary of heat stress management codes for underground mines in the USA, Australia, Canada, South Africa, and Ghana.

Table 2.2 Summary of Heat Control Regulations in Some Mining Jurisdictions [27]

Country	Regulation
USA	1. Any combination of air temperature, humidity, radiant temperature, or air velocity exceeding a wet-bulb globe temperature (WBGT) of 26.1°C for men, and 24.4°C for women. 2. Employees should not be subjected to any combination of thermal conditions or physical work that raises the core body temperature above 38°C.
Australia	1. Responsible employees must ensure that all other employees do not suffer from extreme hot or cold temperatures underground. 2. If hot or humid conditions are to be encountered, all employees must be provided with training to avoid any heat illness or harmful effects 3. If the underground air temperature in an area where a worker is residing exceeds 28°C wet-bulb temperature, then the manager must exhaust all measures to reduce the risk of heat-related injuries or accidents.
Canada	The regulations are based on threshold limit values (TLVs), which provide a limit to ensure the core temperature of a worker's body does not exceed 38°C.
South Africa	1. The South African Mine Health and Safety Act in 1996 defines the temperature range of an "abnormally hot environment" in an underground mine to be dry-bulb temperature (ta) > 37°C and wet-bulb temperature (twb) >32.5°C. 2. Employees are not allowed to work in areas where conditions may induce heat stroke unless the working practice follows a code approved by the Principal Inspector of Mines

Table 2.2 continued.

Ghana	Regulation 180 1. A manager of a mine shall ensure that in the mine, the wet bulb temperature at any working place or any traveling way does not exceed 32.5°C except (a) in the course of attempting to lower the temperature; (b) in the course of undertaking emergency response training or, (c) during an emergency. 2. The manager of a mine shall provide longer breaks and a reduced working time for workmen in the mine if the wet bulb temperature in the mine exceeds 27°C.

2.3.3 Heat Control Strategies

There are different techniques available for mitigating or reducing heat load in underground mining. The choice of heat control technique can change the operating cost of an underground mine drastically because ventilation consumes a significant portion of mines' energy demand and is responsible for a large percentage of the total operating costs. Studies show that ventilation is among the top energy consumers on a mine, accounting for approximately 40% of the total energy consumption and up to 60% of underground operating costs [28], [29]. Thus, deciding between different mitigation techniques is a critical task with enormous cost implications. It is essential to monitor the climatic conditions in the mine to understand where the heat is coming from in order to identify and design the most appropriate method of cooling. In most cases, the primary ventilation (i.e., fresh air from the surface) is sufficient to remove the heat produced during the mining processes without any form of external cooling. However, in ultra-deep metal mines, heat removal, which is often the dominant environmental problem, may necessitate the use of some level of air-conditioning. Other heat management strategies include refrigeration (bulk air cooling), localized refrigeration (spot coolers), ventilation, administrative controls (air-conditioned cabins, cooling vests, acclimatization, rest areas), engineering controls (controlling/reducing heat at source, shielding, insulation), and identifying and applying a heat stress index [18], [27].

In addition to diluting dust and gases in spent air, ventilation serves as a primary technique to remove heat from the underground mine environment. It allows for the movement of fresh air from the surface through underground airways to replace spent air or return air (contaminated with dust, diesel particulate matter, gases, heat) in the development and production workings. The fresh air replaces the spent air with the aid of a mechanical device (fan) which either pushes or pulls the fresh air into the mine workings [22]. Primary ventilation planning involves extensive development that is integrated with the mine design process and upgraded throughout the life of the mine. Even though the ventilation concept is the same industry-wide, the actual ventilation system, which comprises a ventilation network, equipment, and airway, can vary drastically because each mine is unique.

A good mine ventilation system must supply quality and sufficient air to keep the climatic conditions in the working area within acceptable limits. And if, for any reason, the system fails to achieve its intended purpose, then it must be redesigned or upgraded. In cases where ventilation cannot adequately remove the heat to acceptable conditions, some form of artificial cooling is incorporated into the ventilation system to increase the cooling capacity of the fresh air (Figure 2.4). Typically, air ventilation itself will not be enough to remove heat generated by the surrounding rock, mining equipment, and drilling/blasting equipment throughout the life of mine because as the mine extends deeper, the heat load increases to exceed the cooling capacity of the fresh air [29], as illustrated in Figure 2.4. At some point, air-conditioning will be required. When the temperature goes beyond its comfort zone, the air-conditioning system ensures that the regulatory limits are met throughout the mine at operating costs to a minimum.

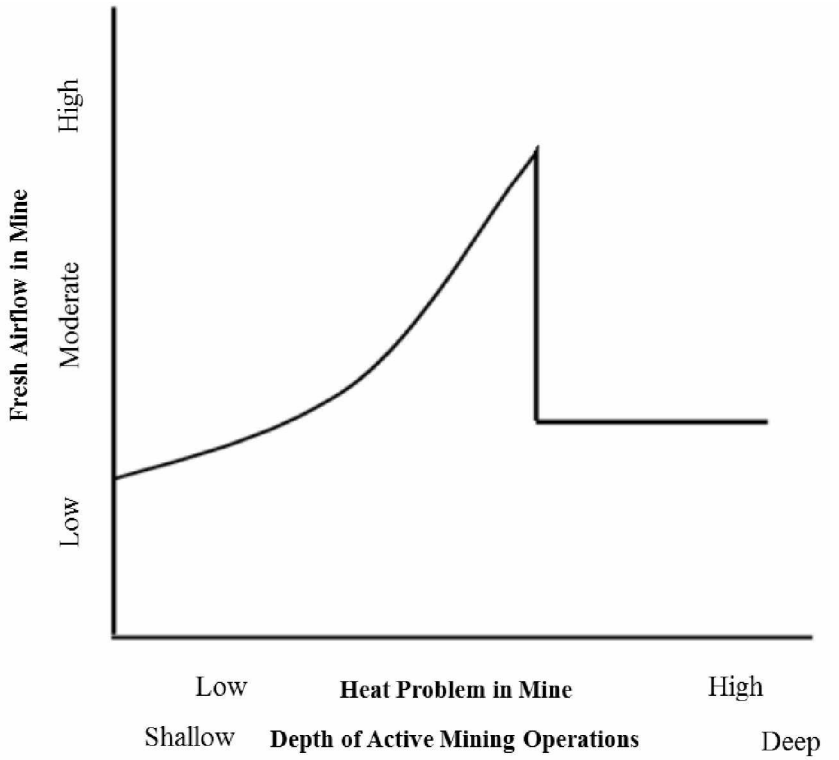

Figure 2.4 Fresh Airflow Delivery Demand [6]

According to Dong et al. [13], when mining depth increases, high temperature is adjusted to normal climatic conditions through conventional ventilation systems, air cooling systems, water cooling system, and ice cooling systems, as shown in Figure 2.5. From Figure 2.5, the ventilation system can reduce air temperature to a comfortable working climate when mining depth is 400 – 800 m. At a mining depth of 800 – 1,500 m, the ventilation system alone would not achieve the cooling requirements. Therefore, a compressed air refrigeration system is often added to lower the temperature. When the depth reaches 1,500 – 2,500 m, the water supply refrigeration system is applied to cool. The water output from the surface refrigeration plant is generally 2 – 4 °C. When the depth exceeds 2,500 m, the surface ice making system is introduced, the ice cubes are broken and then transported through the pipeline to the underground cold storage. Then the air and water are cooled through the heat exchange system [13]. The pumping cost is reduced, and the cooling effect is more significant. The Mponeng gold mine in South Africa, for example, uses the dissolved heat of ice to regulate the operating temperature [13]

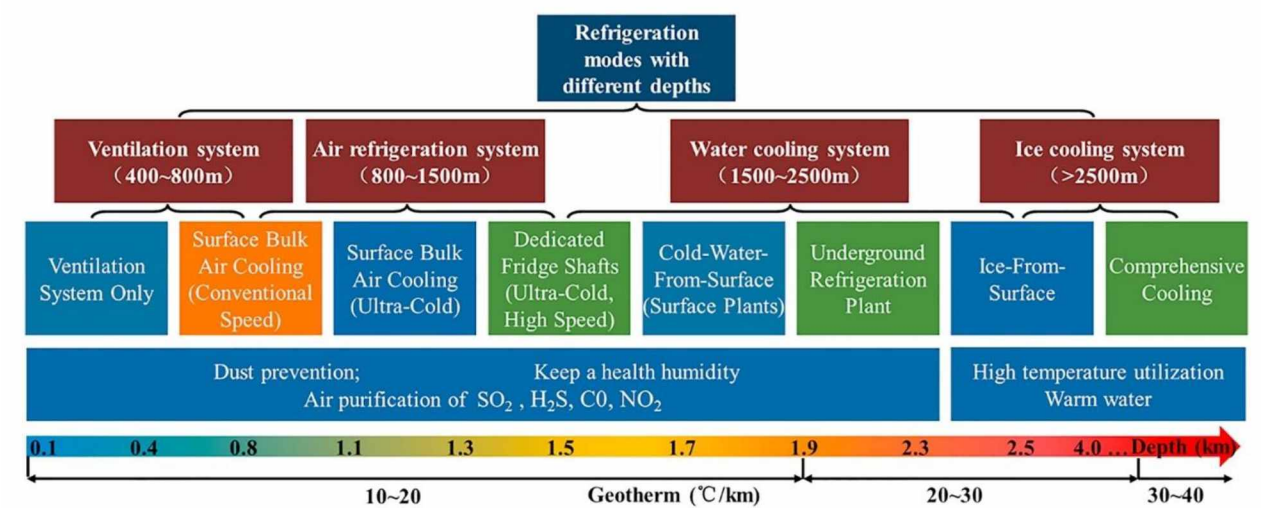

Figure 2.5 Mine Air Cooling Modes with Different Depths [13]

The principles applied in mine air cooling are not any different from refrigeration/air-conditioning in domestic and other industrial applications. Fundamentally, the aim of a mine cooling system is to remove unwanted heat from one place and discharge it into another. The cooling process is based on the vapor compression cycle (Figure 2.6), where a refrigerant (e.g., water, Ammonia, Hydrocarbons, etc.) is compressed to a high temperature and high-pressure vapor before sending it to a condenser (a heat exchanger) where it reaches a liquid form. Condensation is done with the aid of cold water coming from cooling towers. The high-pressure liquid then flows into a receiver, followed by an expansion valve. Upon passing through the valve (e.g., thermal expansion valve or capillary tube), the liquid refrigerant experiences an abrupt drop in pressure (along with a dramatic drop in temperature) and sudden expansion (flash off), resulting in the evaporation of the liquid. The low-pressure liquid then flows to the surge drum, which separates the liquid and gas phases to ensure only vapor is sent to the compressor. The liquid refrigerant passes through the evaporator (another heat exchanger), where it absorbs the heat from air or water and boils [5]. All these happen in a closed cycle to keep the refrigerant from becoming contaminated and control its flow. This principle is employed in underground mine refrigeration systems. Currently, there are different underground mine refrigeration systems and cooling practices being utilized around the world. The cooling practices are central cooling or bulk cooling, spot cooling, and microclimate cooling. A summary of the various cooling practices is shown in Table 2.3.

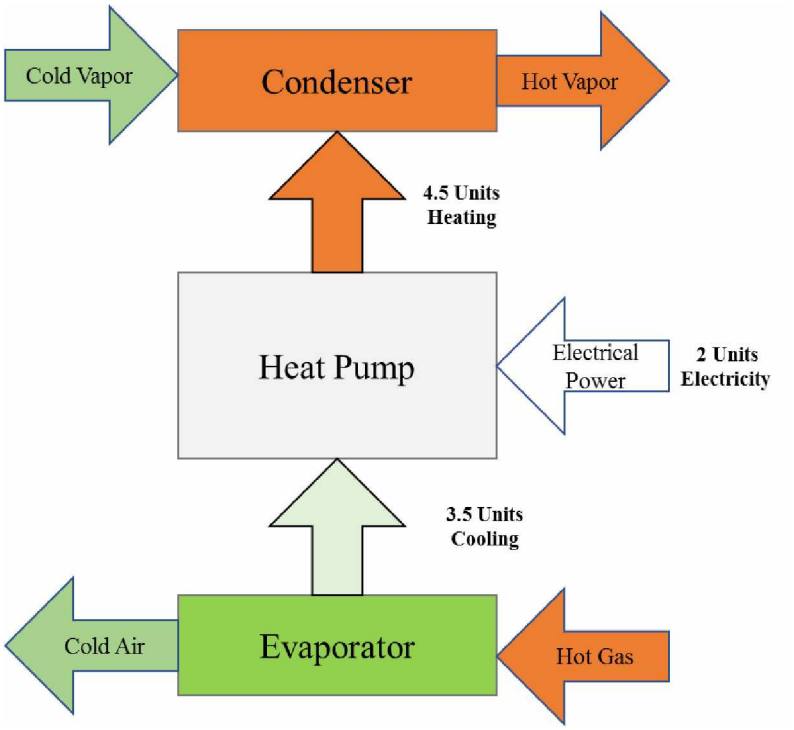

Figure 2.6 Typical Vapor Compression Cycle Energy Balance

Table 2.3 Mine Refrigeration Systems and Cooling Practices in the Mining Industry [30]

Cooling System	Strategy	Description
Surface bulk cooling	The intake shaft draws air through a spray chamber known as a bulk air cooler (BAC) to chill the air. A dedicated fridge shaft may be used entirely for ultra-cold air.	Located on the surface, largest cooling capacity, lowest positional efficiency, can dissipate heat directly to the atmosphere, and limited by the depth of the mine.
Underground bulk cooling	Utilize a BAC or cooling-coil coolers to chill the main intake air. Secondary underground BACs may be set up along the main intake.	Located underground in main airways, large cooling capacity, low positional efficiency, limited by space underground, and reject heat into a return airway or through return water lines to the surface.

Table 2.3 continued.

Spot cooling	These small, mobile units are placed in problem areas to mitigate heat or to supplement the central cooling system when necessary.	Located in areas away from main airways, low cooling capacity, high positional efficiency, low capital investment, mobile, and reject heat into a return airway.
Micro-climate cooling	These cooling systems serve the purpose of cooling the area directly around the worker. Examples of this include air-conditioned cabs and cooling garments.	Located where the miners work and travel, Maximum positional efficiency, low capital investment, mobile, air conditioned cabs, and cooling garments.

The central cooling system has two configurations; bulk air cooler (BAC) and condenser cooling tower (CCT). The BAC system includes a cooling tower that sprays chilled water over the air which is drawn from the surface. The CCT system includes the refrigeration plant, which acts as a condenser where heat is rejected in the form of air or water to the surrounding area. Both systems can be installed on the surface as a surface bulk cooling system or underground as an underground bulk cooling system. The application of surface BAC is common in the mining industry as the primary artificial air-cooling method. The mine refrigeration system at Mount Isa Copper Mine in Australia with an installed refrigeration capacity of 36 MWR is an example of a surface BAC. The infrastructure of a surface BAC is located on the surface. The ventilation system draws air from the surface and passes it to the BAC system to cool before it is circulated to the underground workings. The advantage of this system is that it has no space restriction and size limitation; hence, it can cool a larger amount of air and deliver a large cooling capacity depending on its complexity. Also, it is convenient for maintenance but is often located far from the working areas. Hence it has low positional efficiency compared to the cooling system. The large height difference and the long transportation distance between the cooling units and the working areas lead to high pressure and a large loss of cold energy. The temperature of the fresh air will increase significantly by the time it reaches the working area due to auto compression and heat from the surrounding strata as the cooled travels the intake shaft to the mine workings. This limitation can be addressed by using a

dedicated downcast shaft that utilizes ultra-cold surface bulk cooling. By accommodating auto-compression and strata heat, the ultra-cold air will reach safe limits by the time it reaches the bottom [6], [31], [32].

For underground BAC systems, the refrigerator is placed below the surface, often in the main airway, where it can draw a large quantity of air and transform it to adapt to the mine, while the cooling tower is installed on the surface to discharge heat. All the equipment can be located underground if the heat is being discharged to the return air. With the BAC system located underground, the transport distance is shortened, and the quantity of cold energy loss is reduced. At the same time, the cooling tower on the ground avoids the difficulty of heat discharge [32]. The primary underground BAC is generally placed in the main intake. Secondary underground BACs (secondary cooling) may be placed deeper in the mine and used to re-cool fresh intake air or to re-cool recirculated air. Cooling-coil heat exchangers may be used in place of BAC's for secondary cooling if the cooling requirements are low (less than 1.5 MW) [6]. Unlike BACs, a cooling-coil heat exchanger can be moved, but they also require a washing system as the coils can become dirty and less efficient. Underground BACs can utilize either an underground or surface refrigeration plant. Underground refrigeration plants perform at a higher efficiency than surface plants as they are closer to where cooling is required underground. A surface plant providing cold water to an underground BAC requires a large system of insulated pipes, pumps, and water dams [6].

Ice (granular or slurry) has also been used to cool mine air since the 1920s. Ice-cooling system involves the production of granular ice or slurry ice (a mixture of ice and water) by an ice-making plant on the ground and then transported underground into a melting pool, releasing the cold energy when melting into cold water which is used for the working face cooling by cooler [32]. In cold regions, ice can be created and stored stopes during the winter season and then used during warmer months to cool the intake air. South African Mponeng mine successfully implemented the application of ice to provide cooling at a depth of 4 km with rock temperatures reaching 55°C. It produces slurry ice (4,200 t/day) using vacuum ice technology and water as the sole refrigerant. The ice plant has the capacity to produce 6,985 t/day or 27 MWR [5], [31]. Belle and Biffi [31] and Guo et al. [32] observed that the advantage of using ice include lower pumping costs of chilled water, a large cold source, and convenience for maintenance since part of the system can be located on the surface. Greth et al. [6] also reported that in 2012, a prototype portable surface ice stope,

called the Modular Thermal Transfer Unit (MMTU), was designed to emulate an ice stope. The unit consists of stacked shipping containers with the tops and bottoms removed to store the ice like a stope. Water sprays were used to accumulate ice, allowing for easier maintenance and greater control over heating and cooling. It is believed that MMTU has a high potential to be employed in cold region mines with large heat loads.

A microclimate cooling system involves the cooling of the area directly surrounding the mine worker. This system is ideally the most efficient way to keep the mine workers cool in a hot underground mine environment as the positional efficiency can be 100%. An example of this system is utilizing air-conditioned cabins on mining equipment which allows mine workers to stay out of the heat. This has resulted in a reduction of heat-related injuries and increased productivity. Yet, the issue of heat stress is not eliminated as not all tasks can be completed from inside of an air-conditioned cabin, as many operations underground may not be fully mechanized. A less common microclimate cooling system is the use of cooling garments that a mine worker would wear. In the 1970s, the U.S. Bureau of Mines investigated ice-cooled vests and liquid-cooled clothing for mine workers. The liquid-cooled clothing consists of a vest, hood, and a heat sink which pumps liquid coolant through the clothing to cool the mine worker [6]. Presently, there are more advanced personnel cooling garments that can cool the worker through air cooling, water circulation, gas expansion, and more.

Studies such as Ngô et al. [33], [34] and Al Sayed et al. [35], [36] investigated these garments specifically for use in underground mines and concluded that no current portable cooling technology is perfectly suited to deep and ultra-deep mining environments. Moreover, these cooling technologies alone can protect a mine worker from excess heat exposure underground. However, they can be employed to mitigate heat exposure. For example, Al Sayed et al. [32] developed a prototype personal cooling garment (Figure 2.7) for personnel exposed to a hot and humid climate in deep mining activities. The garment is made of three main parts, the layers forming the garment, the air treatment system, and the distribution channels. It weighs 5.1 kg and uses the atmospheric discharge of highly pressurized CO_2 to create a cool microclimate between the body (torso) and its surrounding environment. The garment showed improvements in terms of heart rate, internal body temperature, perceived well-being, and thermal comfort at 30°C and 60% relative humidity while their participants were exercising on a stationary bicycle. Overall, the

findings suggest strong evidence of the cooling garment's ability to reduce heat stress in deep mines. Ernst and Garimella [37] also designed and tested a wearable cooling system for use in elevated temperature environments by military, fire-fighting, chemical-response, and other hazardous duty personnel. The cooling system consists of an engine-driven R134a vapor compression system, which is a backpack configuration with a cooling garment containing refrigerant lines.

To ensure that these garments meet the constraints and requirements of miners in deep mines, Ngô et al. [34] created a matrix of criteria that will eventually be used to design a personal cooling garment. The usability matrix was later validated, improved, and structured into a mind map representing all relevant criteria and their relationships in a recent study [33] by the authors.

Figure 2.7 Sectional Views and Air Treatment System of Cooling Garment [35]

Presently, spot cooling systems or mobile cooling units (MCU) are among the cheapest and efficient cooling techniques for mine application. These are cooling systems where the evaporator of the refrigeration unit or the cooling device is in direct contact with the airflow at the place where cooling is required (i.e., face cooling or in-stope), the absorbed heat in the condenser is also dumped directly into the return air. These systems are used in areas where heat problems are localized and often are away from main airways [6]. Often these remote areas include actively mined faces or development headings where ventilation air cannot adequately remove the heat generated from equipment and exposed rock. Therefore, a spot cooler can be located at the working face to remove the heat. This cooler can also be moved from one working face to another as production progresses. The main benefits of this system include immediate cooling at the face, no

loss in efficiency, mobility, high positional efficiency, less cost per kilowatt of cooling, and cooling opportunities for remote areas [5].

Additionally, the mobility of spot coolers and their location underground gives them a. However, one drawback is that its size limits its cooling capacity. Spot cooling systems are often used in conjunction with central cooling, but they can be used exclusively in small mines where the overall mine heat load is relatively low and highly localized [6]. The type of spot coolers in the application are spray chambers and closed-circuit cooling-coil heat exchangers. The evaporator portion of the spot cooler can be installed in a ventilation duct, while the condenser portion is positioned outside of the ventilation duct in the return airway, where the spot cooler rejects its heat. A typical example is an air cooling unit (ACU) is a mobile refrigeration unit consisting of a vapor compression system in a chassis mounted on rolling stock, as shown in Figure 2.8. With the rolling stock, the cooling source can be moved closer to the working areas [38]. Another option is to use an underground refrigeration plant to provide chilled water to spot coolers. In this case, the refrigeration plant is set up in an area where it can directly reject heat into a return airway. Chilled water is then pumped to where the spot cooler is situated. An example of this system is conventional cooling cars (CC). CCs are air-to-water heat exchangers mounted in a chassis on rolling stock, which enables them to be moved and installed in different areas of the mine [38]. The application of these systems is not always ideal as new airways may not be close to the return airways [6].

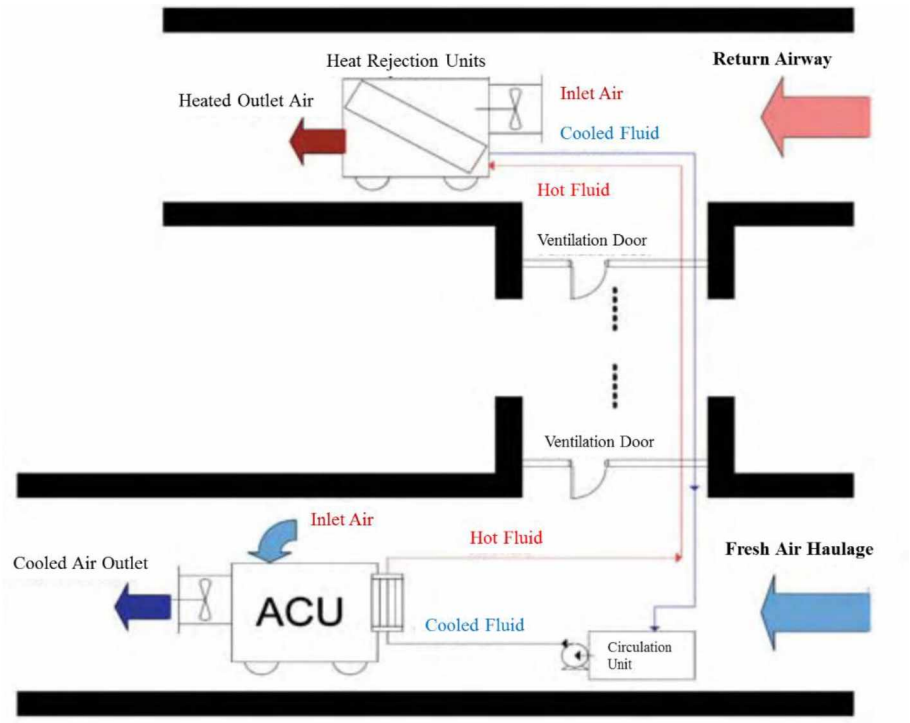

Figure 2.8 Closed Loop ACU Configuration [38]

Studies have designed, tested, and implemented different variations of spot coolers in underground mining. For instance, Van Eldik [39] designed a prototype modular air cooling unit that can be deployed at different locations of a mine to establish a suitable working environment. The modular air-cooling unit is based on heat-pump technology for use as a localized refrigeration unit. The author also evaluated the techno-economic impact of wide-scale implementation in deep mines and observed that this system is energy efficient, cost effective and practical alternative to conventional cooling methods for deep mines. Stanton [40] also developed a mobile refrigeration unit that used mobile cooling units in the evaporator and condenser circuits. The mobile refrigeration plant chills water, which is then circulated through the evaporator MCU and returned to the mobile refrigeration plant for re-use. The refrigerant of the mobile refrigeration plant is cooled using a condenser MCU.

The different mine cooling systems discussed are suitable for varied cooling needs, and no signal cooling system is perfect for every mining operation. Each system varies widely by cooling capacity, operating cost, capital investment, efficiency, and more. And their performance and efficiency also vary between different mine sites based on a variety of factors such as mine design, mining method, heat load, and more. Table 1 shows a comparison of the different cooling systems

with respect to cooling capacity, mobility, positional efficiency, and cost. Table 2.4 and 2.5 demonstrates the benefits and limitations of current cooling system strategies.

Table 2.4 Comparison of the Cooling Systems Used in Underground Mining [6]

Cooling System	Cooling Capacity	Mobility	Positional Efficiency	Cost
Surface Bulk Cooling	High	Stationary	Low	High
Underground Bulk Cooling	Medium-High	Stationary	Low-Medium	High
Ice Storage	Medium-High	Stationary	Low-Medium	Medium-Low
Spot	Low-Medium	Partially Mobile	Medium-High	Medium-Low
Micro-Climate	Low	Fully Mobile	Maximum	Low

Table 2.5 Benefits and limitation of the Cooling Systems Used in Underground Mining [6]

Cooling System	Advantages	Disadvantages
Surface Bulk Cooling	Provides the greatest amount of cooling	Limited by the depth of the mine
Underground Bulk Cooling	Generates the largest amount of cooling capable underground	Must reject heat to a return airway or through return waterlines to the surface
Ice Storage	Utilizes natural cooling processes to reduce operating costs	Limited to cold climates
Spot	Mitigates heat in localized areas	Must reject heat to a return airway or through return waterlines to the surface
Micro-Climate	Cools area directly around the mine worker	Workers are unable to always remain in air-conditioned cabs Current cooling garments are not optimal for use in the mine environment

From Tables 2.4 and 2.5, each cooling system provides a unique set of capabilities that can be utilized to reduce the heat load in deep mines. Though a single system may be able to reduce the heat load to appropriate levels, a cooling system strategy is often developed which utilizes multiple systems. As the mine continues to deepen and become more mechanized, more cooling is implemented either by upgrading current cooling infrastructure and/or by implementing more or other cooling systems. Most often, a surface bulk air cooling system is utilized solely or first when implementing cooling due to its large cooling capacity, ease of maintenance, and lower installation costs relative to underground cooling infrastructure. This is only the case when the mine design allows for the chilled air to be directly moved to specific areas underground, experiencing excess heat. Other cooling methods would need to be employed if the chilled air from the surface BAC is unable to remove the heat at deeper parts of the mine [6].

Another refrigeration technology that can be applied in mine air cooling is vortex tubes. A vortex tube is a simple thermal device that separates compressed air into cold and hot air without any moving part and external energy source. Presently, this device is being utilized for small-scale refrigeration needs in many industrial applications. Despite the relatively low refrigeration capacity of vortex tubes, they can be a potential candidate for localized cooling in underground working face.

2.4 Vortex Tube

VT, also known as the Ranque-Hilsch vortex tube, is a simple thermal device that simultaneously splits a compressed gas or air into hot and cold streams without any moving part. The separation of fluid flow into low and high-temperature regions is called the temperature (or energy) separation effect [7]. The device was first invented by French metallurgist and physicist George Ranque in 1931 and later improved by German physicist Rudolph Hilsch in 1945 [41]. It consists of entry nozzles to admit the compressed air, a vortex generation chamber to create swirling tangential flow, working length of tube, cold exit, hot exit, and flow control valve.

Given its cooling capabilities and mechanical robustness, VTs are being applied commercially in a wide range of applications, such as cooling machines parts, set solders, dehumidify gas samples, cool electric or electronic control cabinets, chill environmental chambers, cool food, test

temperature sensors, separating gas mixtures, DNA application, liquefying natural gas and other purposes. The increased research interest and popularity in industrial applications of VTs is because VTs' are small, simple and compact, easy-to-make, maintenance-free, require no electrical or chemical power, and no use of environmentally detrimental refrigerants such as CFCs and HCFCs [42]. According to Xue et al. [43], these significant benefits of VT have encouraged increased investigations into the working mechanism of VT on how to improve performance and identify operational parameters. The main drawback of VT is its low thermal efficiency, limiting its application for specific high refrigeration needs.

Several studies proposed hypotheses explaining the working principle of a vortex tube. A working fluid (e.g., compressed gas) is injected tangentially via a nozzle into a vortex chamber, which undergoes transformation and exhausts the VT at the cold and hot ends. The fraction of the gas that leaves the tube in either direction is controlled by a valve. Because of the tangential injection, the gas velocity has a high rotational component in the vortex chamber. The fluid splits up into hot gas that exhausts at the right side (hot end) periphery and cold gas that exhausts at the left-center part (cold end) of the vortex chamber [44]. The gas exhausting from the hot end can reach temperatures of 200°C (392°F), and that of the cold end can reach -50°C (-58°F) [41], [44], [45]. A vortex tube can produce refrigeration up to 2.39 hp (6,000 BTU/h) using 0.05 m^3/s (100 scfm) of compressed air at 689 kPa (100 psi) [7].

2.4.1 Vortex Tube Components

The main components of VT include compressed air inlet, inlet nozzle, vortex chamber, cold air/gas exit, hot end tube, hot air/gas exit, hot valve, and internal counterbore. Compressed air expands in the nozzle and enters the vortex tube tangentially with high speed, utilizing whirl, then the inlet gas splits in low-pressure hot and cold temperature streams [42]. The compressed air inlet is an entry for the compressed gaseous fluid into the VT from the supply. The supply piping of the compressed air is connected and tightened to the inlet of the VT. A vortex chamber is a portion where the diaphragm and nozzle are placed inside the VT to facilitate the high-pressure air stream to gain velocity and form a free vortex [41]. The shape of the nozzle is designed such that the compressed air enters tangentially into the vortex tube to form a vortex flow. The nozzles play a critical role in obtaining the spiral motion of the air stream [41]. Figure 2.9 shows the schematic

diagram of a VT, while Figure 2.10 is a 3D image of commercially available counterflow VT with its components.

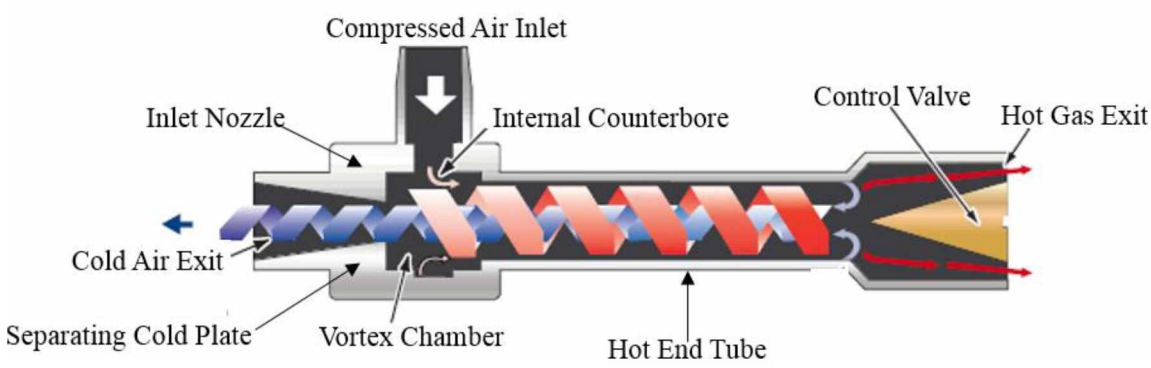

Figure 2.9 Sectional Schematic of a Vortex Tube [46]

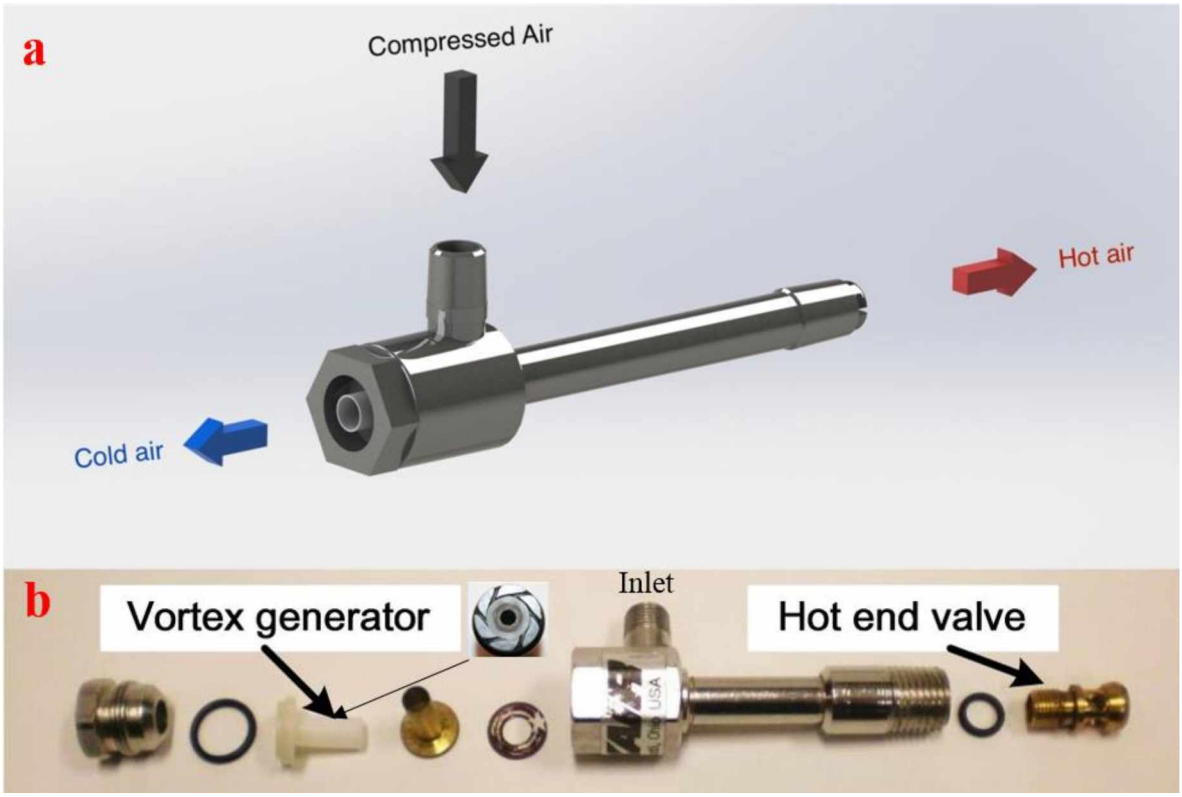

Figure 2.10 Commercial Vortex Tubes with Components (modified after [47])

Under a spiral motion, the compressed air leaves the vortex chambers towards the hot gas outlet. The compressed air experiences an increase in temperature (hot stream) during this motion. Karthikeya Sharma et al. [41] reports that a hot stream is generated due to a free vortex moving close to the tube periphery. As the free vortex moves close to the wall, it undergoes compression

due to the expansion of the forced vortex to the walls, where it gains heat and leaves through the hot gas outlet. The separating cold plates (diaphragms) are small circular plates with a hole at the center that works like a throttle valve to reduce the temperatures of the cold streams further, leaving towards the cold end. The diaphragm is placed very next to the nozzle towards the cold end. The diameter of the diaphragm hole affects the cold end temperatures to a considerable extent. The control valve is a conically shaped valve installed at the hot end to deflect the free vortex to the other end. The control valve's conical angle plays a significant role in splitting the air streams into cold and hot streams. It also controls the quantity of air or gas to be exhausted from the hot end or deflected towards the cold end. The cold fractions can be decided by controlling the valve opening and closing towards the hot end [41].

The various components influence the overall performance of a VT. Many researchers have investigated the effect of geometrical parameters on VT performance, considering components such as length and shape of the tube, size and number of inlet nozzle, size of hot and cold ends, types of vortex chamber, and structure of the tube. Other variables of influence include cold mass fraction, overall mass flow rate, inlet pressure, inlet temperature, gas density at tube inlet, type of fluid, gas viscosity, gas thermal conductivity, the heat capacity of the gas at constant pressure, static pressure at the cold exit, static pressure at the hot exit, swirl velocity at tube inlet, the material of the tube, internal roughness, and gas molecular mass [7], [8], [43]. Yilmaz et al. [8] summarized the effect of tube length, diameter, and length/diameter (L/D) ratio on performance characteristics. They reported that the optimal length of the tube should be longer than its diameter to achieve significant temperature separation within the vortex tube. For example, Saidi & Allaf Yazdi [48] found that increasing tube length increases temperature differences and decreases exergy (entropy-free energy) destruction significantly. A CFD experiment by Aljuwayhel et al. [49] revealed that increasing the length of the vortex tube from 10 to 30 cm resulted in a temperature drop of 0.7 K (2.6%) in the cold air. However, a further increase in length to 40 cm does not change the energy separation. Khazaei et al. [50] also conducted a numerical analysis to examine the effects of five different gases (Helium, Ammonia, Water vapor, Nitrogen, Air, Oxygen, and Carbon dioxide) on the performance of VT. They found that helium produces the largest energy separation with the coldest temperature difference than other gases. They attributed the performance of helium to its maximum value of specific heat capacity ratio and minimum molecular weight.

2.4.2 Vortex Tube Working Principle

Since the invention of VT in 1931, extensive research has been conducted to understand its working principle or optimize its performance. However, to date, the energy separation mechanism of VT, which is dominated by the complex coupled interaction of the viscous thermo-fluid characteristics and geometrical properties [51], is not fully understood, and no clear theory or widely accepted understanding has been proposed [7]. Initially, Ranque believed that compression and expansion effects were the main reasons for the temperature separation. Later, Hilsch investigated the geometrical parameters and performance optimization of the tube and added the effect of inner friction [52]. Hilsch proposed that the gradients of angular velocity in the radial direction will lead to the formation of frictional torque between different layers of the rotating flow, thus, transferring energy by the shear work from the inner layers toward the outer layers [51].

There are varying and opposing energy separation hypotheses about VT due to the complexity of the flow structure in the tube. These hypotheses have been proposed based on results obtained from different theoretical, experimental, and numerical studies. Some of the theoretical explanations proposed that the energy separation mechanism is mainly due to temperature gradient theory [53], momentum transfer theory [54], pressure gradient theory [55], [56], acoustic flow theory [57], and secondary flow heat pump theory [58]. Some experimental research attributed the separation energy to viscous compression and expansion processes across different layers [52], viscous shear separation across the layers at different speeds [59], cold mass fraction [60], and geometrical properties [45]. In recent years, computational fluid dynamics (CFD) have also been widely applied to determine VT's energy separation mechanism and flow structure. These numerical studies include prediction of temperature separation using comparison of different turbulence models (e.g., Reynolds Averaged Navier Stokes (RANS), renormalization group (RNG) standard $k\varepsilon$, shear stress transport (SST $k\omega$) k-w, standard $k\omega$, and Reynolds stress equation model (RSM), Large eddy simulation (LES)), and influence of different geometries of VT and hot-end control valve on temperature separation [60]–[63]. Xue et al. (2010) opined that the energy separation in the VT involves several different factors, among which expansion and friction between the flow layers could be considered as the most important. Xue et al. (2013) also believes that the temperature drop in VT is mainly due to pressure drop near the inlet, and the temperature

rise is caused by partial stagnation and mixture due to the structure of multi-circulation (illustrated in Figure 2.11) near the hot end.

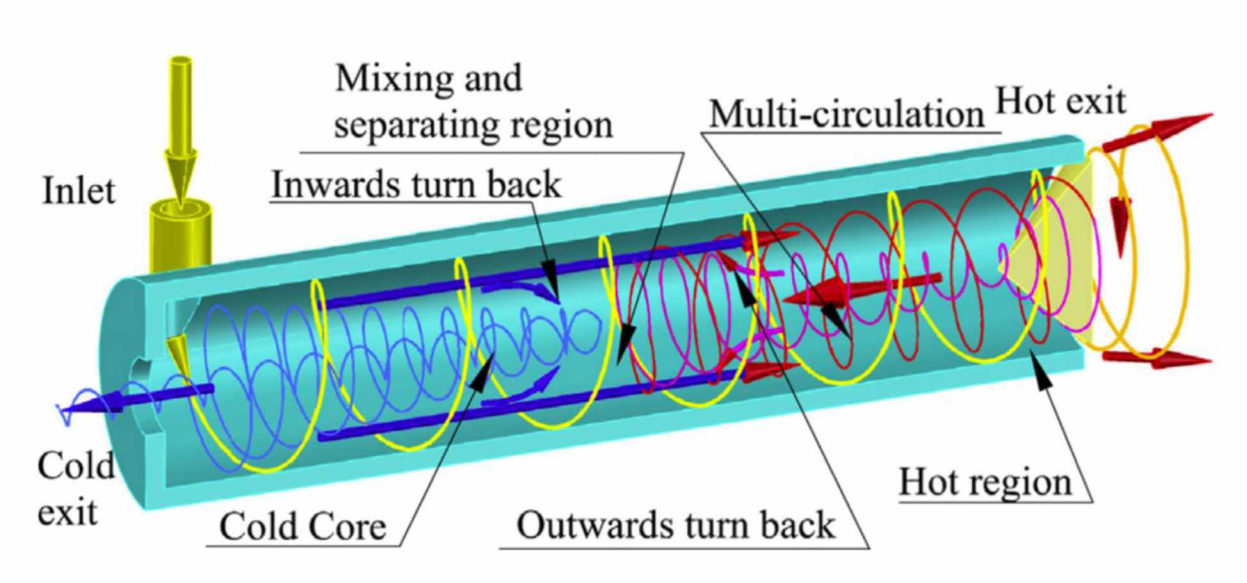

Figure 2.11 Flow Structure Inside a Counterflow Vortex Tube [43]

A general description of the energy separation is presented based on work done by Xue et al. [43] and Karthikeya Sharma et al. [41]. When a compressed air gas is injected through the tangential inlet nozzle, it undergoes expansion and accelerates through the nozzle of the vortex generator resulting in a spiral airflow stream. The spiral airflow stream (vortex flow or free vortex) moves close to the periphery of the VT towards the hot end of the tube. The control valve at the end of the hot side deflects the free vortex creating a forced vortex diverted back towards the cold end. The deflected airstream travels at the central axis of the tube with speed reaching 1,000,000 rpm [41]. A sectional view of the flow dynamics in a VT is illustrated in Figure 2.12, where the red and blue spiral streams represent hot and cold air, respectively. This part of the flow gets expanded due to the low pressure in the central part of the tube and escapes from the cold nozzle at a lower temperature than the injected compressed air [43].

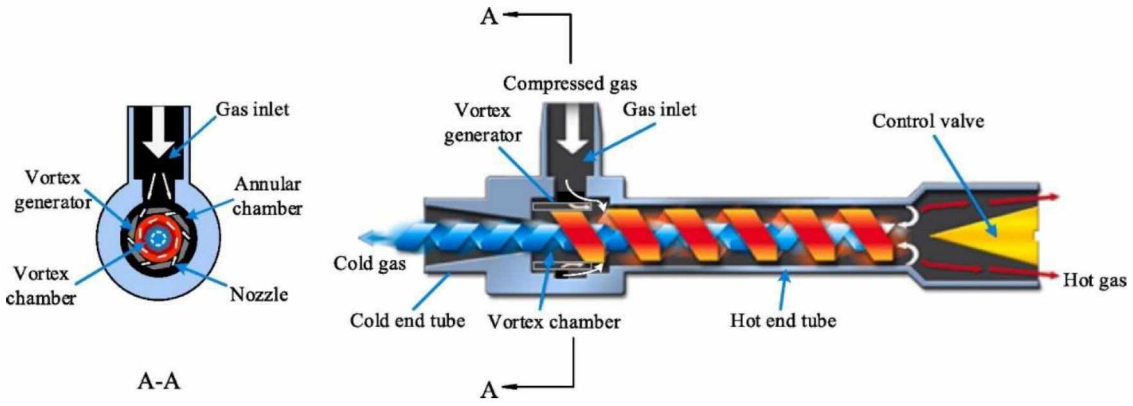

Figure 2.12 Working Fluid Flow Structure in a VT [53]

The control valve restricts the flow and helps in setting the cold mass fraction. Closing the control valve partially increases the pressure of air near the valve than the outside air. Energy transfer takes place between the free and forced vortex streams because of the difference in their pressures and as the free vortex is compressed against the walls of the vortex tube due to expansion of the forced vortex. The free vortex absorbs heat and leaves the vortex tube through the hot end, and the forced vortex loses heat and leaves through the cold end. The cold stream escapes through the hole of the diaphragm, reducing their temperatures further into the cold side, while the hot stream is passed through the opening of the control valve [41].

2.4.3 Classifications and Types of Vortex Tubes

VTs are mainly classified based on geometrical configuration, flow characteristics, method of heat supply (removal), and organization of low-pressure streams.

Table **2.6** presents a summary of the classification categories of VT. Uniflow VT, counterflow VT, and conical VT are widely applied in research and industrial applications. Both uniflow and counterflow VTs can be cylindrical.

Counterflow VTs have the cold and hot exhaust placed at the opposite ends of the tube, as shown in Figure 2.9 and Figure 2.12. The inlet nozzle is positioned on the cold side, where the working gas is injected tangentially into the VT. The cold and hot airstreams flow in opposite directions. The counterflow VT is very efficient because heat exchange takes place in opposite directions of the airstreams [41]. It is the most used VT for industrial applications.

Table 2.6 Classification of Vortex Tubes [8]

Method	Classification
Geometrical configuration	Cylindrical vortex tubes
	Conical vortex tubes
Flow characteristics	Parallel flow (uniflow) vortex tubes
	Counterflow vortex tubes
Heat supply (removal)	Uncooled (adiabatic) vortex tubes
	Cooled (nonadiabatic)vortex tubes
Removal of low-pressure gas streams	Dividing vortex tubes
	Self-evacuating vortex tubes
	Vortex ejectors

In the uniflow VT, both cold and hot exhausts are placed at the same side of the tube, hence the name uniflow or parallel flow. The flow of hot air and cold air is in the same direction, ejecting at one end of the tube (Figure 2.13). The other tube adjacent to the inlet nozzle is sealed. Less heat exchange takes place between the same direction flowing air streams, making it less efficient [41]. Studies found the performance of the uniflow system is less efficient than that of the counterflow system. Hence, most of the time, the counter flow geometry was chosen [8].

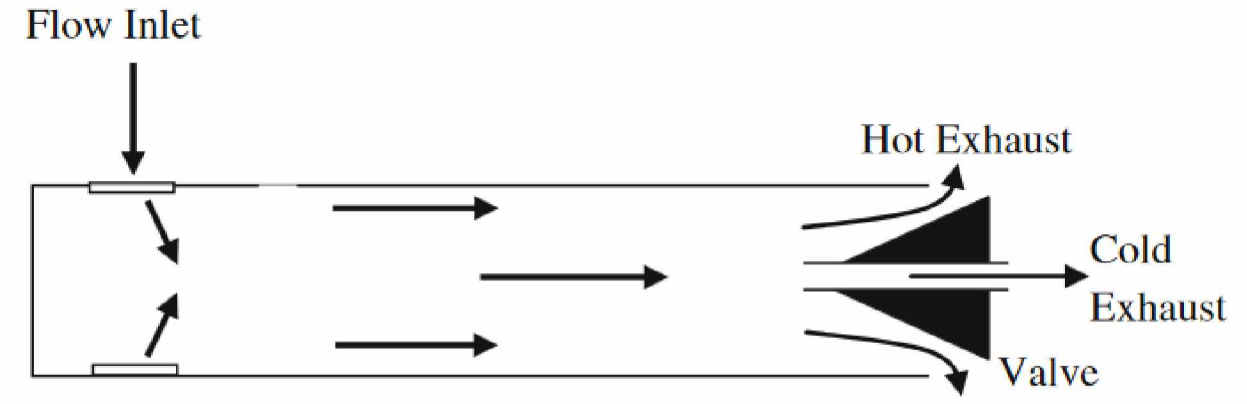

Figure 2.13 Uniflow Vortex Tube [8]

The conical or divergent VTs have a conical geometry, as shown in Figure 2.14, instead of a cylindrical shape (Figure 2.9). This type was first designed in 1961 by Paruleker [41]. By varying

the conical angle, the parameter L/D can be as small as three. The conical type vortex tube can reduce the need for lengthy vortex tubes to get the required drop in temperature [41].

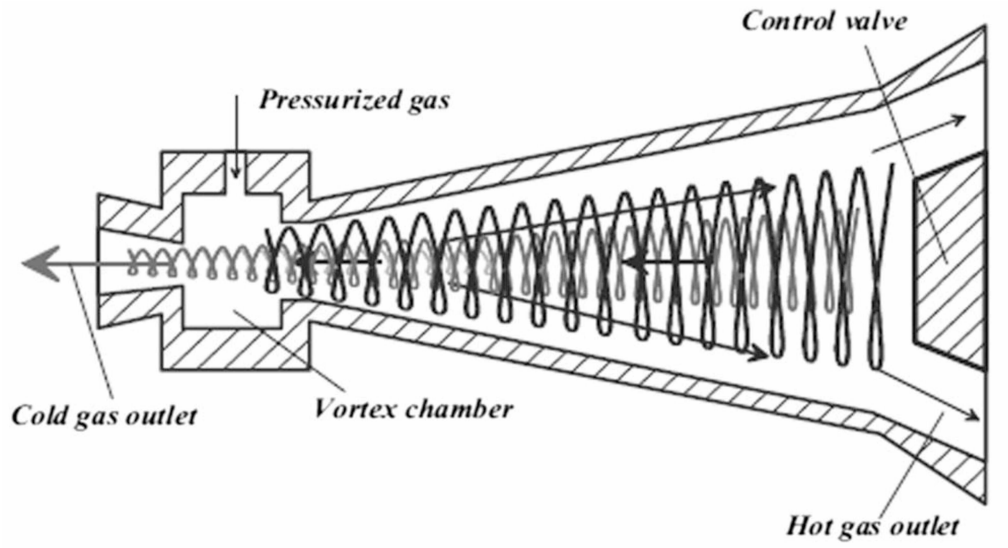

Figure 2.14 Conical Vortex Tube [41]

2.4.4 Vortex Tube Performance Indices

The performance of VT is evaluated based on several metrics. The following are some performance criteria presented by Yilmaz et al. [8]:

i. Cold flow mass ratio (cold mass fraction)

The cold mass fraction is the percentage of input compressed air that is released through the cold end of the tube. It is the mass flow rate of cold gas divided by mass flow rate of the inlet gas, mathematically calculated as;

$$\varepsilon = \frac{\dot{m}_c}{\dot{m}_{in}} \tag{2.1}$$

where $\dot{m}_c$ represents the mass flow rate of the cold stream released, $\dot{m}_{in}$ represents the inlet or total mass flow rate of the pressurized inlet working fluid. Therefore, ε changes in the range $0 \le \varepsilon \le 1.0$.

ii. Cold and hot temperature difference

The cold side temperature gradient or temperature reduction is the difference between inlet air temperature and cold side air temperature:

$$\Delta T_c = T_{in} - T_c \tag{2.2}$$

where T_{in} is the inlet flow temperature and T_c is the cold flow temperature. Similarly, the hot side temperature gradient is the difference between inlet air temperature and hot side air temperature:

$$\Delta T_h = T_i - T_{in} \tag{2.3}$$

where T_{in} is the inlet flow temperature and T_h is the hot flow temperature.

iii. Normalized temperature gradient (drop/rise).

The normalized cold temperature drop is the ratio of cold temperature difference to inlet temperature:

$$\frac{\Delta T_c}{T_{in}} = \frac{\left(T_c - T_{in}\right)}{T_{in}} \tag{2.4}$$

Also, normalized hot temperature rise is the ratio of hot temperature difference to inlet temperature:

$$\frac{\Delta T_h}{T_{in}} = \frac{\left(T_h - T_{in}\right)}{T_{in}} \tag{2.5}$$

iv. Cold orifice diameter

Cold orifice diameter ratio (β) is defined as the ratio of cold orifice diameter (d_c) to vortex tube diameter (D):

$$\beta = \frac{d_c}{D} \tag{2.6}$$

v. Isentropic efficiency

Assuming isentropic expansion process inside the VT, then isentropic efficiency is:

$$\eta_{is} = \frac{T_{in} - T_c}{T_{in}\left[1 - \left(p_{atm}/p_{in}\right)^{(k-1)/k} - 1\right]} \tag{2.7}$$

where η_{is}, p_{in}, p_{atm}, and k are the isentropic efficiency, inlet air pressure, atmosphere pressure and specific heat ratio, respectively.

vi. Coefficient of performance

The coefficient of performance (COP) is defined as the ratio of the cooling power gained by the system to the work power. It is mathematically computed for VT as a heat pump:

$$COP_{hp} = \frac{k}{k-1} \frac{(1-\varepsilon)(T_h - T_{in})}{T_{in}\left(\ln \frac{p_{in}}{p_c}\right)} \tag{2.8}$$

2.5 Commercial Applications of Vortex Tubes

VT has several advantages, including simple design, no moving part, long life expectancy, low maintenance, lightweight and compact, low initial cost, maintenance-free, no expert attendant required, and low operating cost. Its main drawbacks are the poor coefficient of performance (COP), limited capacity, and unsuitable for large capacity refrigeration applications.

The utility of VT for small capacity applications is always justified if compressed air or working gas is readily available. Currently, VTs are widely considered for commercial low-temperature applications such as cooling electronic components, testing thermal sensors, cooling of controlling cabins, local heating of enclosures, cooling of cutting tools, and cooling off spots under thermal stresses [7]. Other applications include extensive uses in fast starting up the steam power stations, liquefying natural gas, nuclear reactors, gas separations, and cooling the laboratories used to store low-temperature materials [64]. Examples of a few specific applications of VTs are described below.

2.5.1 Personnel Cooling Clothing

VTs have been integrated into personnel safety clothing to provide reasonable thermal comfort and protection to workers working in environments or confined areas with the risk of exposure to high temperatures, toxic gases, fumes, or dust. Workers commonly use it in coal mines, vessels, tanks, pits, and foundries. Most often, it is not always economical to refrigerate work areas where the heat can be considerably large. Thus, the only economical way is to isolate the worker from the ambient climate by air-conditioning the operators working near the hot places [41].

Presently, the largest single use is a cooling unit for protective clothing and helmets for such jobs as sandblasting, welding, and handling toxic materials. These garments/vests can be cooled simply by connecting a vortex tube to an airline and attaching it to the suit. Alexander et al. [65] designed a portable refrigerator using VT to be worn by personnel wearing industrial protective clothing. The cooling device is light and small and can be strapped to the body where it does not interfere

with the physical movements of the workers. The tube operates on 20 to 25 cfm of compressed air at 80 to 100 psig and delivers from 15 to 18 cfm of air-cooled 50 to 80°F below the inlet air temperature. Today, there are a variety of commercial air-cooled vests available on the market for different applications. Figure 2.15 illustrates a VT-based cooling vest. The cold air outlet of the VT is attached to the lower section of the vest. Cold air is supplied to the mask and the top half of the vest to maintain the normal body temperature. Warm air from the hot outlet of the VT can also be used in the vest, depending on the prevailing ambient temperature.

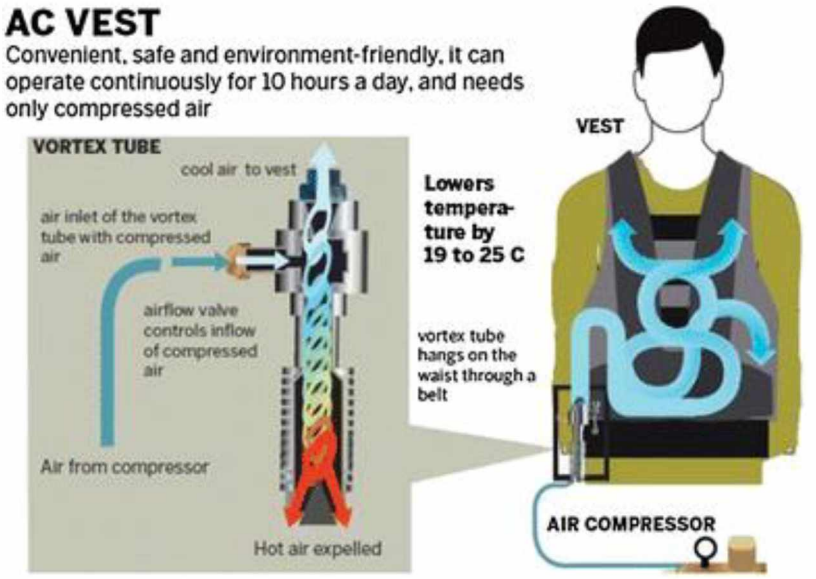

Figure 2.15 Working Process of a Vortex Tube Personnel Cooling Vest [41]

Compressed air is circulated through the suit from the lower to the top half of the suit to maintain the normal body temperature. The air supplied to the unit can be cooled or warmed by the vortex tube. Additionally, the supply of air can also be adjusted quickly and easily. The safety and comfort provided by such a suit can result in considerable cost savings because the operator is encased in the suit, eliminating the need to ventilate the entire work area. This is an ideal application of VT, where lightness, compactness, and simplicity are of prime importance [41].

2.5.2 Vortex Tube Based Refrigeration and Cooling Systems

Refrigeration of food and medicine is an extensive problem. Fishing communities living on the coastline are also dependent on cold storage facilities for storing a day's catch. Usually, conventional cold storage rooms are expensive for a local fisherman to afford. Conventional

refrigerators are expensive to buy for an average person. Another important problem is the transport of medicines, specifically vaccines from one place to another. Several vaccines require storage at low temperatures, and the distance a medicine can be delivered via road is very limited, particularly in remote areas. Cooling of tools and instruments such as electronic controls, variable speed drives, and servos in confined enclosures is also a major refrigeration issue. These components are extremely sensitive to heat and contamination, while their confined enclosures make temperature control difficult. Excessive heat causes components to cook, digital displays to misread, starters and breakers to trip below rated loads, and controls to drift. Fans often provide inadequate cooling and commonly pull in dirty, humid air creating another source of failure.

One suitable and less expensive solution to the various needs described above is the application of VT. For instance, ITW Vortec's Vortex Cooler™ Enclosure Coolers (Figure 2.16a) are the low-maintenance alternative for keeping enclosures cool and clean without Freon or other refrigerants. The Hampden Model H-6826 (Figure 2.16b) is also a VT refrigerator manufactured by Bestech Australia for the study of the characteristics of VT refrigerating effects. The compact size of VT cooling systems makes them ideally suited for small enclosures. Powered by compressed air (typically 100 psig, not to exceed 150 psig), VT coolers generate chilled air without refrigerants or moving parts. These coolers provide exceptional reliability with minimal maintenance in even the hottest environmental conditions [41].

Figure 2.16 Vortex Tube Refrigeration Units: (a) Vortex Cooler™ Enclosure Cooler, and (b) Hampden Model H-6826 Vortex Tube Refrigerator [66], [67]

2.5.3 Spot Cooling for Machining Operations

VTs are viable alternatives to traditional cooling technologies used in machining operations. There are many VTs for cooling metal machining processes such as drilling, cutting, milling, and turning. Traditional liquid coolants used in metal machining are known to contain chemical carcinogens that could present serious health risks for machine operators and have inherent waste disposal concerns on the environment [68]. Studies by Boswell [68] found that the VT-based air jet cooling provides a highly efficient heat removal mechanism for metal cutting and delivers thermal cooling performance comparable to traditional liquid coolants without the inherent chemical exposure risks to machine operators and harmful impact on the environment.

For example, Nex Flow Air Products Corporation offers a range of VT tool coolers for metal machining. The company also utilizes a combination of VT cooling technology with lubrication for mist cooling and lubrication. In this case, the mist is cooled to about 41°F, reducing the amount of lubricant or coolant used by up to 20%. These new VT cooling devices improve the environment and minimize the cost of liquid coolants. Figure 2.17 shows a VT-based cooler for dry machining operation.

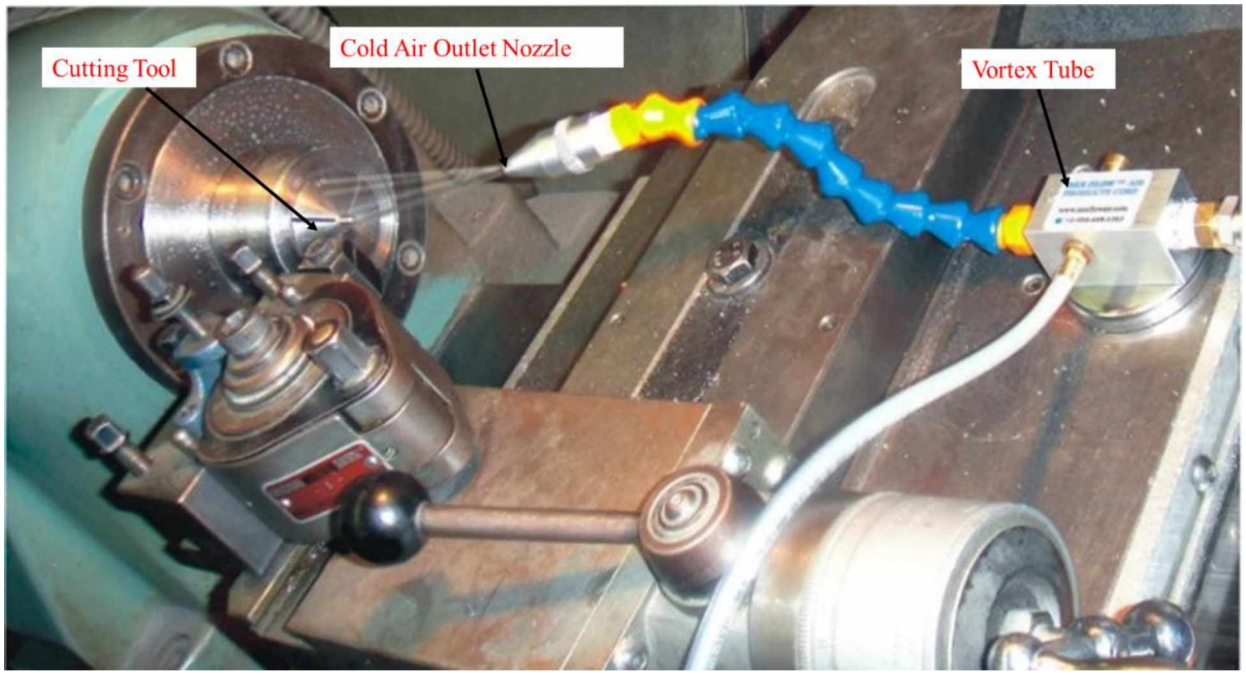

Figure 2.17 Vortex Tube Spot Cooling Device [69]

2.5.4 Other Applications of Vortex Tubes

In aviation, the cabins of high-speed gas turbine-powered airplanes are cooled with the use of a bootstrap air cycle. Usage of VT, especially in military aircraft, would result in an overall reduction in weight, which is of prime importance. The VT can also be used for the same purpose with less efficiency because more air would have to be bled off from the compressor at high pressure compared with a bootstrap cycle for the same cooling capacity [41].

VT can find its application in gasses separation based on the density differences. A specific gas can be separated from a combination of two or more gasses having control over the temperature drop at which a particular gas can be liquefied [41], [70]. Research and demonstration are ongoing of a unique gas-liquid contactor design for the separation of carbon dioxide from natural gas and flue gas using VT.

Another promising application of VT is the cooling of gas turbine rotor blades. Currently, the cooling of blades of gas turbines used for aircraft and marine purposes is achieved by passing the air through several radial holes. The cycle efficiency and specific output of the current method can be improved with the same quantity of air but at a lower temperature which can be made available with the help of VT. The compressed air can be bled from the main compressor [41].

2.6 Vortex Tubes for Mining Applications

Workers in underground metal and coal mines are often exposed to extreme conditions characterized by high temperatures, heat, and elevated levels of dust and fumes. Heat concerns are severe, especially in deep underground mines where increasing depth leads to high temperatures from the geothermal gradient, auto compression, machinery, and oxidation processes. Excessive heat can impede production and result in serious related health hazards such as heat stroke, heat exhaustion, heat syncope, heat cramp, heat rash, and transient heat fatigue. It can cause equipment malfunction. Traditionally, heat in working areas is usually removed by ventilating the mine with atmospheric air. In cases where the heat load is severe, the atmospheric air is further cooled through artificial refrigeration. This method is capital intensive and associated with adverse effects on the environment. Many refrigerants used in artificial refrigeration, such as chlorofluorocarbons (CFCs), damage the ozone layer, while others are extremely potent greenhouse gases. Therefore, in recent years ongoing research is focused on finding cost-effective and environmentally benign

alternatives to mitigate heat damage at mine workings. Considering the beneficial features of VT, it can be a suitable heat control device in underground mines.

It is worth mentioning that the application of VT in mining is lagging despite its wide usage in other industries. Recently, three theoretical studies have investigated the feasibility of a VT cooling system in underground mining and concluded that VT could provide sufficient cooling with better economic efficiency, less energy, and minimal environmental impacts [10], [11], [71]. Given that compressed air is readily available at underground working areas, VT-based cooling technologies can be integrated into the mine ventilation system. In hot underground mines, workers can wear VT personal cooling vests (described in Section 2.3.1) to prevent heat damage while working at the face. Additionally, VT can provide spot cooling at the working face, whereby cold air from the VT is channeled into the auxiliary ventilation system before the air gets to the face.

2.7 Numerical Modeling in Mining

Numerical modeling tools such as computational fluid dynamics (CFD) have been widely applied to the mining industry to solve mine ventilation, mine drainage, dewatering, wastewater treatment, and safety and health problems. CFD is a branch of fluid mechanics that employs physics, numerical mathematics, and computer sciences to simulate, analyze and solve fluid flow problems. It is based on a set of governing equations, including Navier-Stokes equations, continuity, and any additional conservation equations, such as energy or species concentrations. These equations describe the fundamental physical behavior of the fluid flow.

CFD is a powerful tool for research and design in the mining industry. It helps in understanding and analysis of fluid mechanism or gas flow in order to improve efficiency, safety, and health [72]. CFD enables researchers to conduct numerical experiments to determine difficult metrics from laboratory or full-scale experiments. The numerical experiments also further the interpretation of physical experiments and enhance the understanding of phenomena that are observed during physical experimentation [72]. CFD modeling has been used in the mining industry in several areas, including airflow-dust-gas dispersion and interaction [73], [74], coal dust control [75], [76], methane dispersion [77], line brattice ventilation system [78], mine fires and explosions [79], acid mine drainage [80], and mineral processing [81].

The development of CFD models involves many complex steps, depending upon the specific problems to be addressed. The most crucial step is to understand the issues to be investigated, the engineering concepts, and the results to be expected from the modeling studies. For mining-related health and safety problems such as gas management, this would typically require visits to the mine site to discuss the problem with the engineers and examine relevant data to clarify any technical issues before developing the CFD models. In summary, the following steps would be involved in the process of any CFD models [82]:

i. Field studies to obtain fundamental data and information. Depending on the problems to be studied, this stage typically involves gathering of mine design plans, ventilation layout, gas monitoring data, gas drainage systems, and geological and geotechnical reports;

ii. Construction of CFD model geometry and computational mesh/grid. The raw data collected from the field studies must be simplified to produce the model geometry and grid (2D or 3D), which must be conceptually sophisticated enough to represent the real case to be investigated. This is usually done using a CAD style mesh generator or preprocessor of a CFD package;

iii. Setup of CFD model. The above computational mesh will be brought into the CFD processor or the solver for the definition of computational models, boundary conditions, flow properties, and other functions that need to be performed by user-defined programs or functions (UDF). This step may also involve the refinement of meshing, mesh quality, and boundary checking, and in some cases, the complete re-meshing of the initial model;

iv. Initial model simulations. Once the CFD model setup has been completed, an initial run of the CFD model with a few iterations is often performed to check the stability and convergence of the model. 'Engineering judgment' is needed at this stage to examine if the model is producing meaningful results. In many cases, modifications are needed to modify boundary conditions, computational models, UDF functions, and mesh improvements. A good base model should be characteristic of good convergence and meaningful results independent of computational mesh;

v. Base-model simulation and validation using field or experimental data. The above base model needs to be calibrated and validated against real data, typically ventilation survey

data or gas monitoring data. The base model will be fine-tuned to produce results that show reasonably good agreement with the real case; and

vi. Parametric studies to investigate various 'what if' scenarios of the problems and solutions. The fine-tuned base model can now be used to carry out a wide range of parametric or sensitivity studies to investigate the problems when changing one or two design parameters and develop solutions or optimum strategies.

CHAPTER 3 NUMERICAL MODELING AND SIMULATION

3.1 Introduction

This chapter presents the materials and methods used in gathering data and conducting the numerical experiments in the research. The data gathered include vortex tube temperature ranges, working face temperature, and geothermal gradient of the mine. The chapter also discusses the vortex tube model considered, its geometry, dimensions, and operating conditions. The data gathered served as input parameters for the numerical model. Following the model creation, numerical simulation was also performed under various conditions to generate corresponding contour diagrams which were subjected to further analyses.

CFD modeling is a numerical technique for solving complex fluid dynamics problems, including heat transfer. In this research, the numerical analysis includes modeling air velocity and temperature in a ventilation duct and a development heading. The simulation was conducted in two stages. Stage one involved modeling a ventilation duct equipped with a vortex tube cooling system. The result obtained from stage one was used in stage two to simulate the airflow dynamics in the development heading of the mine. In both stages, different scenarios, including variation in location and number of vortex tubes, were considered to determine their corresponding cooling effects.

A thermo-fluid analysis software, Cradle SC/Tetra 14, was used for this study. The geometry of the auxiliary ventilation system was generated using a computer-aided design (CAD) package, Solidworks. The 3D design includes features of the ventilation duct and development heading. The simulations were performed on a Windows 7 operating system with 3.60-GHz, Intel microprocessors (Intel core i7-4790), and 16 GB of memory.

3.2 Mine Model

The mine has operated for over 100 years with current mining depth exceeding 900 m (2,953 ft) and more than 6 km (3.7 miles) in strike length. Access to the mine is through two shafts, which also serve as the main intake for fresh air. The shafts are equipped with cages for transporting workers and a skip for hoisting ore and materials. One of the shafts serves as the primary hoisting shaft. The distance between the two shafts is approximately 4 km, and the ore zone is between the

shafts. Previously, the mining methods used were non-mechanized shrinkage stoping, conventional cut and fill, and rill mining along the narrow gold-bearing vein. However, with recent advances in technology, the mine has adopted mechanized shrinkage stoping called Alimak stoping to exploit the West Reef narrow vein orebody. Small Load Haul Dumps (LHD) transfer the ore to rail cars for transport to the primary shaft. The daily production from the West Reef is 650 tonnes per day. Current production is at Level 24, which is approximately 900 m below the primary shaft collar. Figure 3.1 shows the layout of the mine and reef orientation.

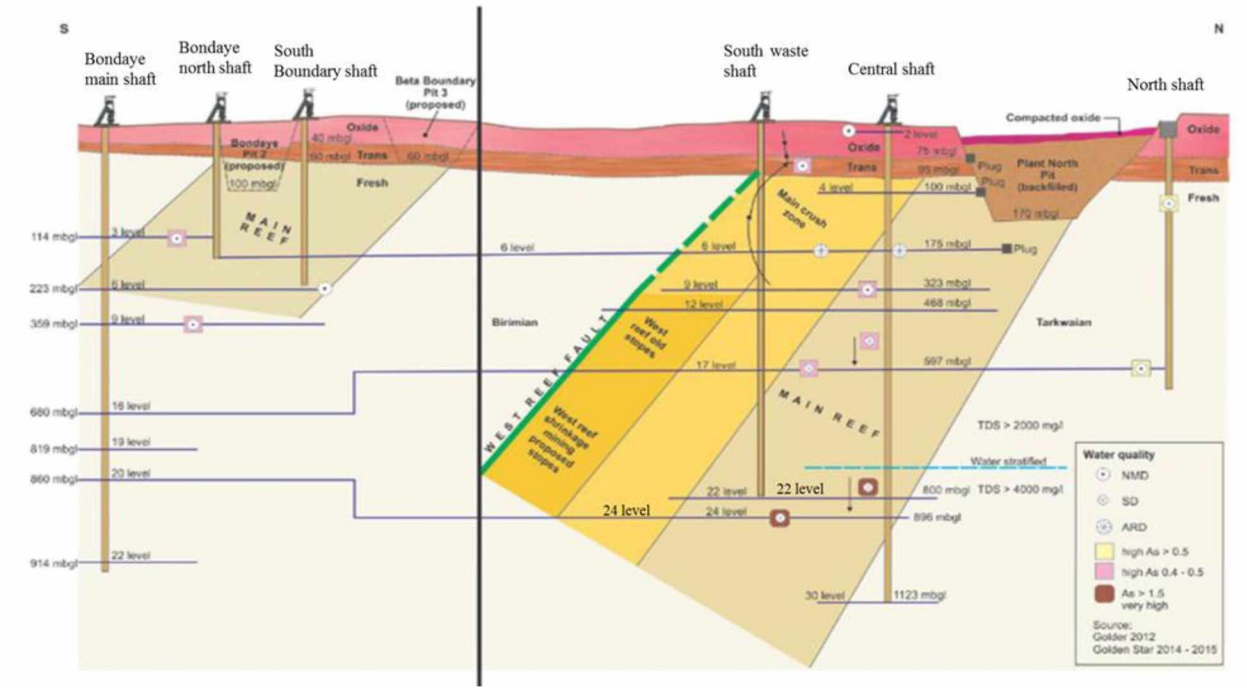

Figure 3.1 Mine Layout [83]

The mechanized shrinkage stoping employs Alimak raises to mine the orebody. First, Alimak raises are excavated, and blastholes are drilled along the strike of the orebody. Pillars are left between the Alimak stopes along with a crown pillar left for ground stability between vertical stopes. Figure 3.2 shows the basic concept for the mining system and airflow design values for the stopes. The figure shows the various stages of stope development, that is, one stope near completion, one full of broken ore to be removed from the base of the stope, two being blasted, two being drilled to prepare for blasting, and two under construction. The pattern is repeated across the strike length. During development, the Alimak is ventilated by compressed air lines, then once complete, 2.5 m^3/s of airflow through the open raise [83].

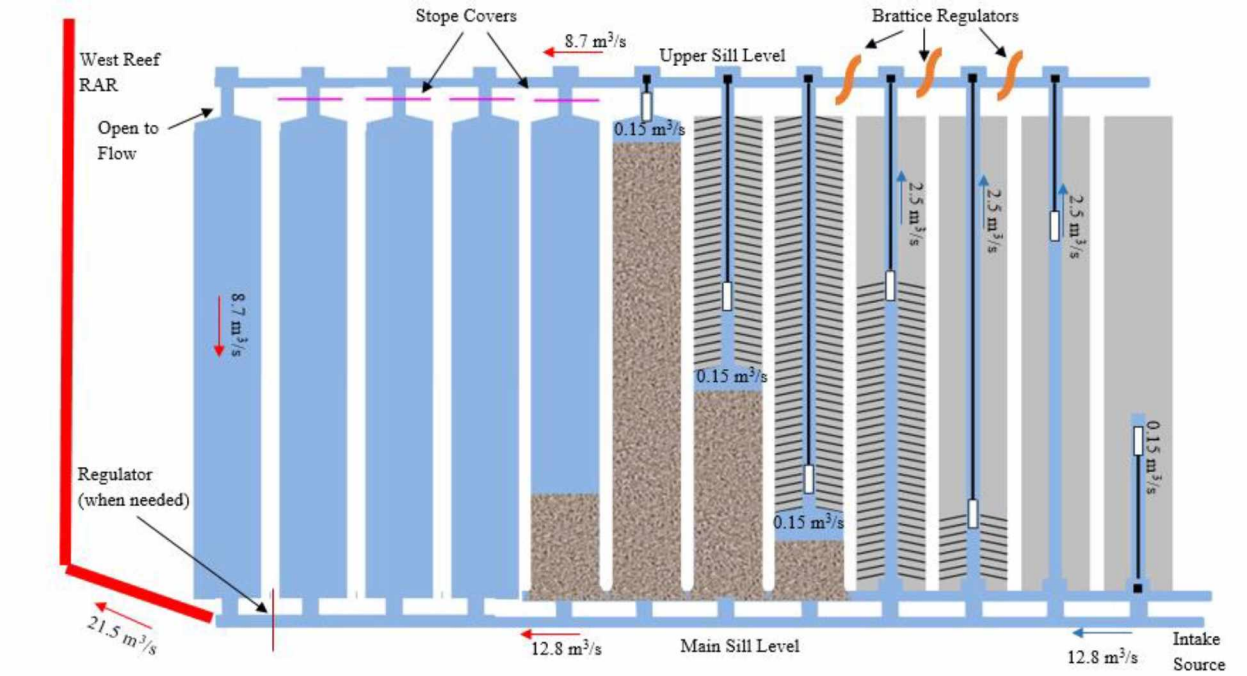

Figure 3.2 Schematic of Stope Sequencing and Airflow Distribution at West Reef [83]

The ventilation system for West Reef consists of two main exhaust fans installed on the surface, a booster fan, and regulators. The 250-kW motor axial fan with variable speed drive exhausts 93 m^3/s of air at 1.4 kPa. To provide sufficient airflow to support mining of the West Reef, a 35 m^3/s booster fan with 2.15 kPa was installed at 23 Level to supply about 20 m^3/s across 24 Level. Intake air from the primary shafts passes through the booster fan, then to working areas and exhausts via the return airway to the surface.

3.3 Vortex Tube Model

The VT model applied in this study is based on Exair Corporation's standard large vortex tube product (50 – 150 scfm) with a cold fraction of 80% (Exair, 2020). This model has an operating length of 279 mm and a vortex chamber outer diameter of 54 mm. The vortex tube can produce a temperature drop of 28°C (82.4°F) at 345 kPa (80 psi) inlet air pressure. A summary of the VT's dimension is provided in Table 3.1. The reason for choosing this VT model is that it is already available for commercial and industrial applications. Exair Corporation and other VT companies manufacture it for commercial purposes, and samples can be purchased from the market for experimental studies or field applications.

Table 3.1 Summary of Vortex Tube Geometry

Parameter	Value	Units
Working tube length	279 (11)	mm (in)
Vortex chamber diameter	54 (2.12)	mm (in)
Nozzle inlet diameter	1/2	NPT
Supply pressure	80	psig
Temperature drop	10 (50)	°C (°F)
Temperature rise	82 (180)	°C (°F)
Cold fraction	80	%

3.4 Geometry Creation

The geometry of the ventilation duct and the development heading were developed using Solidworks 3D computer-aided design software. The diameter and length of the ventilation duct are 0.75 m (2.46 ft) and 36.21 m (118.8 ft), respectively. Figure 3.3 depicts a 3D model of the ventilation duct with the different cold air injection points. There are five injection points named Location 1, Location 2, Location 3, Location 4, and Location 5. Cold air from the VT is released into the ventilation duct at these different locations one after another, starting with Location 1. Injecting cold air at different points would help to ascertain the best location along the ventilation duct to achieve optimal mixing of the cold air and the fresh airflow. Additionally, the location would also inform the exhaust region of the hot air stream from the VT.

The ventilation duct is located at the roof of the development heading, and it ends at 40 ft away from the working face. The face is ventilated with the aid of a ventilation duct connected to an auxiliary fan. A fraction (14.16 m^3/s or 30,000 cfm) of the fresh air is pulled into the ventilation duct from a ramp with 23.6 m^3/hr (50,000 cfm) of airflow. The inlet temperature of the fresh air is 28°C (82.4°F). As illustrated in Figure 3.3, cold air from the vortex tubes was injected at different locations (one after another) in the ventilation duct. The first injection point (Location 1) is 3 m (10 ft) from the ventilation duct outlet, while the remaining points were placed at 6 m (20 ft) intervals.

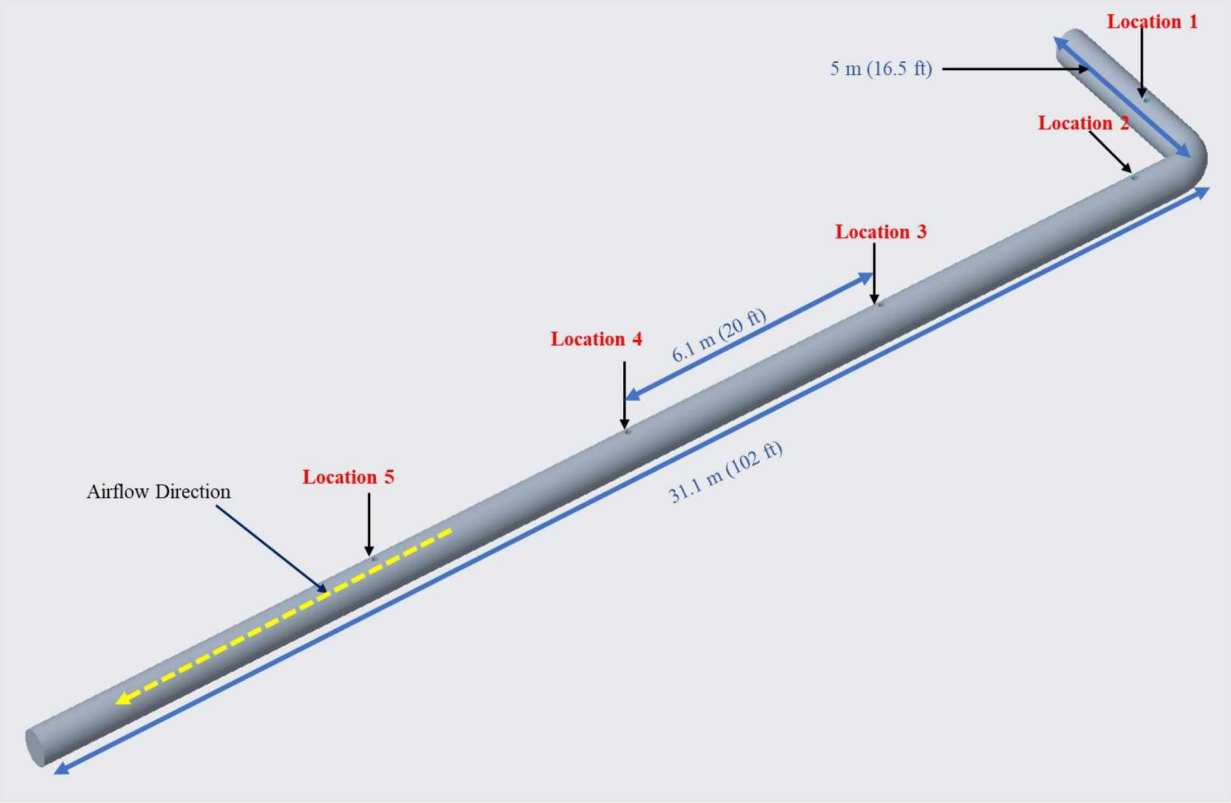

Figure 3.3 3D Model of Ventilation Duct with Different Cold Air Injection Locations

The design process integrates the ventilation duct into the development heading to complete the auxiliary ventilation system. Conventionally, in underground metal mines, ventilation ducts or hardlines are installed at the roof of mine excavations to promote safe movement of traffic. Therefore, the same practice was adopted by placing the ventilation duct at the roof, as shown in Figure 3.4.

The development heading is 2.7 m (8.9 ft) wide, 3 m (9.8 ft) high, and 43.2 m (142 ft) long. It is located at approximately 800 m (2,624 ft) below mean sea level (MSL), where the geothermal gradient is approaching 31°C (87.8°F). Fragmentation of the rock is achieved through conventional drill and blast operation. Jumbo drills are used for drilling blastholes which are then charged and fragmented with emulsion explosives.

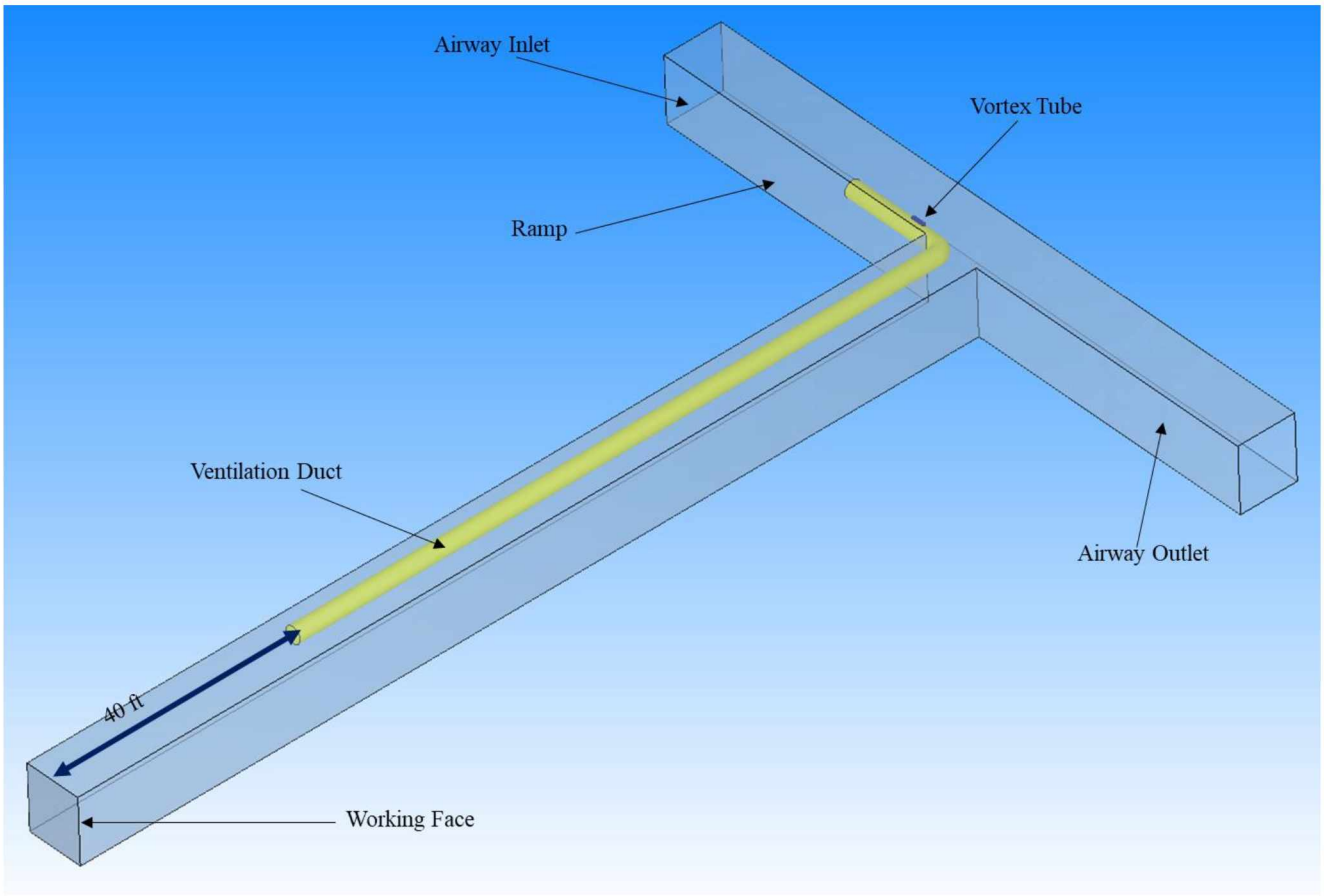

Figure 3.4 3D Model of Development Heading with Ventilation Duct Anchored to the Roof

The first stage of the simulation involved analysis of the airflow in the ventilation duct as cold air from the cold outlet of the VT was injected into the ventilation duct. The cold air was injected parallel to the flow direction of fresh air in the ventilation duct, and hot air from the hot outlet was directed away from the working face into the return airway. The cold air was injected at five different locations, one location at a time. After cold air injection at the various locations, the number of VT was varied from 8 to 20 at Location 3.

3.5 CFD Model

Steady-state simulations were performed using Reynolds averaged Navier-Stokes equations (RANS) with Standard K-ε turbulence model. The flow inside the models was assumed to be incompressible. Many mine ventilation problems can be classified as steady state, incompressible turbulent flow because the ranges of temperature and pressure resulting in variation in air density is fairly limited in most mines [22], [84]. According to McPherson [22], airflow measurements in

mines are normally made to within 5% accuracy. Hence, the assumption of incompressible flow gives acceptable accuracy in most cases. The equations governing the flow are conservation of mass, momentum, and energy [85].

Mass

$$\frac{\partial u_i}{\partial x_i} = 0 \tag{3.1}$$

Momentum

$$\frac{\partial \rho u_i}{\partial t} + \frac{\partial u_j \partial u_i}{\partial x_j} = -\frac{\partial p}{\partial x_i} + \frac{\partial}{\partial x_j} u \left(\frac{\partial u_i}{\partial x_j} + \frac{\partial u_j}{\partial x_i} \right) - \rho G_i \tag{3.2}$$

Energy

$$\frac{\partial \rho C_p T}{\partial t} + \frac{\partial u_j \rho C_p T}{\partial x_i} = \frac{\partial}{\partial x_i} K \frac{\partial T}{\partial x_i} + q \tag{3.3}$$

where u_i is the flow velocity in m/s in x_i direction, t is the time in seconds, ρ is the density in m^3/s, P is the fluid pressure in Pa, μ is the viscosity in Pa, G_i is the gravity in m/s^2, T is the fluid temperature in K, C_P is the specific heat at constant pressure in J/(kg K), K is the thermal conductivity in W/(m K), and q is the heat source in W/m^2.

3.6 Boundary Condition

The boundary conditions for the models include pressure, temperature, and air quantity conditions. Boundary conditions for both ventilation duct and development heading include fix mass flow, at air temperature 28°C (82.4 °F), at the inlet, and zero static pressure at the outlet. The wall of the ventilation duct was smooth and perfectly sealed with no leakage, and there was no heat exchange between the duct and the surroundings (adiabatic condition). The simulation results of the ventilation duct served as the boundary condition for the development heading. The wall of the development heading was rough with 7.62 cm (three in.) equivalent roughness. A no-slip wall condition with a constant wall temperature at 31 °C (87.8 °F) was enforced. The pressure of the compressed air entering the vortex tube was 345 kPa (80 psi) at a temperature of 28 °C (82.4 °F). The volumetric flow rates at cold and hot exits of the vortex tube were 120 cfm and 30 cfm with a temperature of 0 °C (32 °F) and 128 °C (262 °F), respectively. A summary of the boundary condition is provided in Table 3.2.

Table 3.2 Model Boundary Conditions

Computation Boundaries	Condition	Value
Duct and the surroundings	Adiabatic	No heat exchange
Walls of development heading	Rough	7.62 cm (3 in)
Inlet	Pressure inlet	345 kPa (80 psi)
Hot exit	Pressure outlet	Varies with different Cold Mass Fractions (ε)
Walls	Adiabatic wall with no slip	Heat flux = 0 W/m^2

The following assumptions were used in the CFD model:

i. The wall of the ventilation duct was modeled as an adiabatic condition.
ii. A constant rock temperature was maintained along the wall of the development heading.
iii. The ventilation duct was assumed to be perfectly sealed; thus there was no leakage of air in the duct.

3.7 Mesh Independence Study

A mesh independence study was conducted first to determine the appropriate mesh size for the numerical simulations. Unstructured computational mesh was generated in the computational domain using the finite volume method. The mesh independence study started with a coarse mesh that was gradually refined until an acceptable variation was achieved. The unstructured mesh consists of tetrahedral elements, as shown in Figure 3.5. A tetrahedron cell has four vertices, six edges and is bounded by four triangular faces. One advantage of the unstructured mesh is that it is easier to generate and saves time in the overall process as it can be automated compared to structured mesh. But it cannot be easily controlled and modified at specific regions in the flow domain if needed based on the gradient of flow properties in that domain.

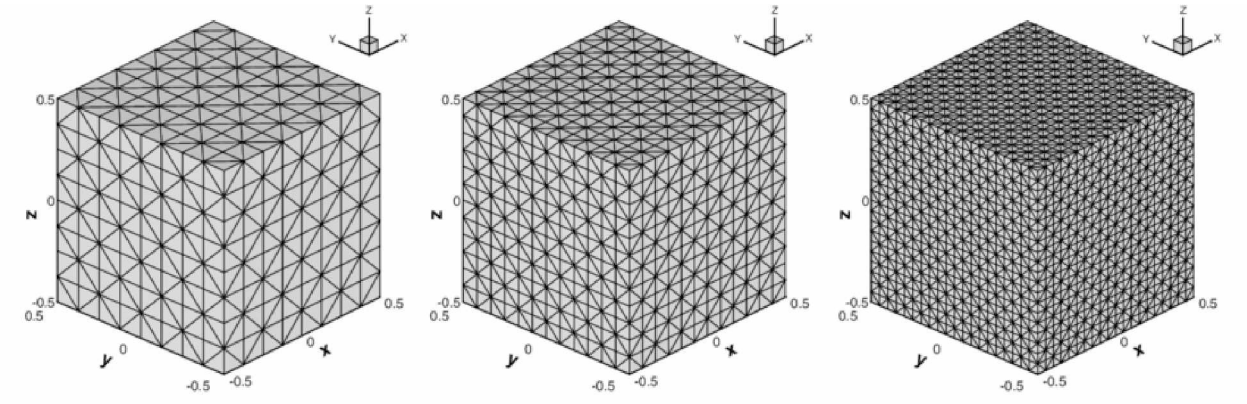

Figure 3.5 Unstructured Mesh with Tetrahedral Cells generated from a Cartesian Mesh [86]

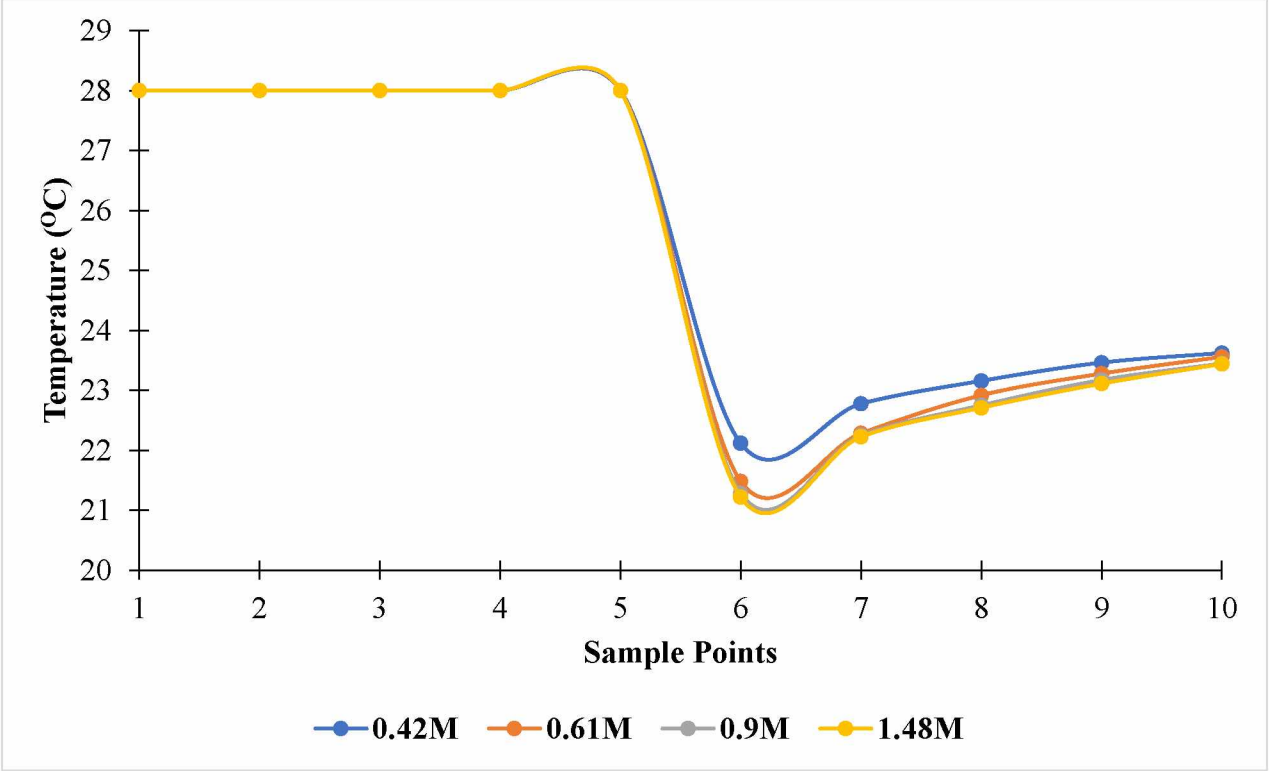

Figure 3.6 Performance of Different Grid Sizes

Generally, a finer mesh is preferred and more desirable for capturing flow properties fluctuations in numerical modeling. However, a very fine mesh requires significantly larger computational resources and time. As the degree of fineness is further increased, the refinement effect on numerical results is diminished, and beyond a certain degree of fineness, the extra computational resources do not contribute much to the refinement effect. The result of the mesh independence study is presented in Figure 3.6, showing the meshing details of different levels of the mesh

fineness (0.42M, 0.61M, 0.9M, and 1.48M). The air temperature was predicted at ten different points for each mesh. The solution was assumed to converge when the average residuals were below 10^{-4} within a cycle, and the mass flow was balanced. It can be seen from Figure 3.6 that there is no observable variation among the different mesh sizes from sample point 1 to sample 5. However, beyond sample point 5, the temperature prediction for coarse mesh sizes (0.42M and 0.61M) was higher than that predicted using finer sizes (0.9M and 1.48M). The difference between 0.9M and 1.48M is not significant. To save computational resources, the mesh with 0.9M element in the computational domain is chosen. In the ventilation duct simulation, the optimal number of elements in the computational domain is 0.98 million, while that of the development heading simulation is 4.25 million.

3.8 Turbulence Model

Different turbulence models were evaluated to determine the most appropriate model for the flow conditions being considered. Four turbulence models (standard k-ε, RNG k-ε, MP k-ε, and Spalart-Allmaras) were analyzed. The air temperature was predicted and compared at ten points in the computational domain. The solution was assumed to converge when the average residuals of all the variables were below 10^{-4} within a cycle, and the mass flow was balanced. An analysis of results indicates a maximum deviation among the four turbulence models of 1.5% from their mean temperature. Figure 3.7 shows the temperature variation of the turbulence model. Therefore, the most used and well-validated turbulence model in engineering, the standard k-ε turbulence model, was chosen for this study. This model is robust, and it also happens to be the most widely applied for modeling fluid flow.

The performance of the different turbulence models is similar. It can be seen from Figure 3.7 that the different models had no variation in temperature from sample point 1 to sample point 5. There was a noticeable difference in temperature beyond sample point 6; however, this variation is not significant.

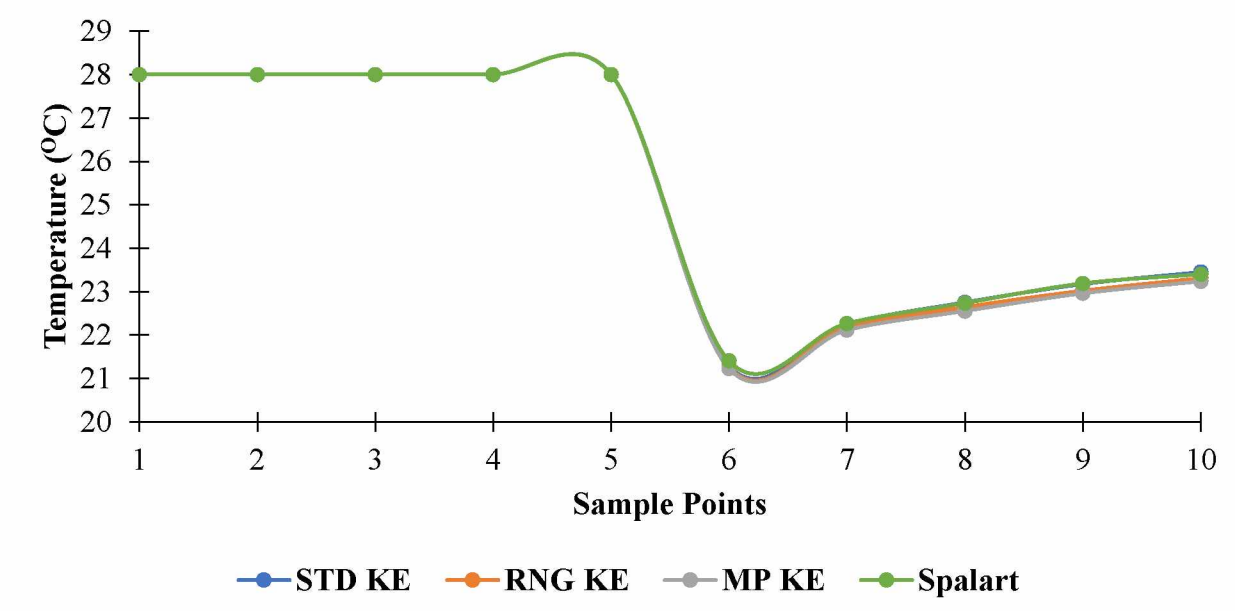

Figure 3.7 Performance of Different Turbulence Models

CHAPTER 4 RESULTS AND DISCUSSION

4.1 Introduction

This chapter presents and discusses the simulation results of the study. The results include inlet and outlet air quantities and temperature and velocity profiles for different ventilation scenarios. The profiles show the behavior of airflow in the ventilation duct and development heading as the number and location of VT were varied.

4.2 Simulation Results

Total fresh airflow entering the ventilation duct is 30 kcfm at 28°C (82.4 °F). Cold airflow from the VT was released at five different locations in the ventilation duct. The cold airflow was released at Location 1, followed by Location 2, 3, and 5, sequentially. About 0.96 kcfm of cold airflow was injected at each location. The cold airflow mixes with the fresh airflow from the auxiliary ventilation as both airflows move toward the face of the development heading. Figure 4.8, Figure 4.9, and Figure 4.10 show temperature gradients for Locations 1, 3, and 5, respectively. The remaining temperature gradients *i.e.,* Locations 2 and 4, and velocity gradients for the five locations are presented in Appendix A. The temperature and velocity gradients were at a mid-section of the ventilation duct.

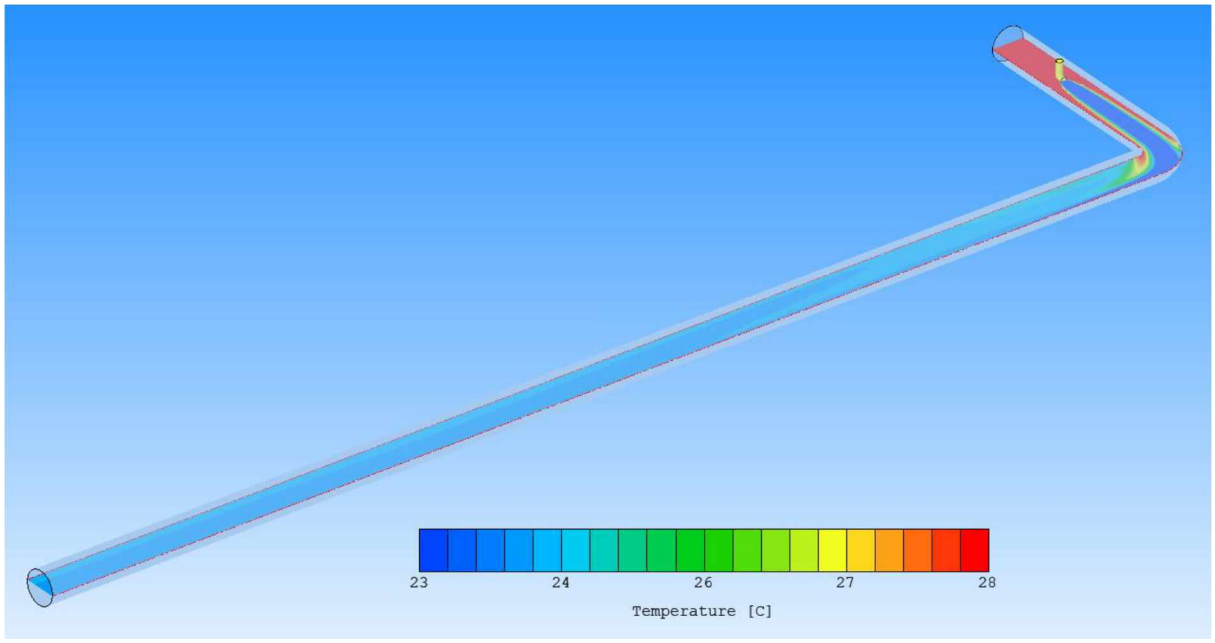

Figure 4.8 Temperature Gradient of Airflow within Ventilation Duct for Location 1

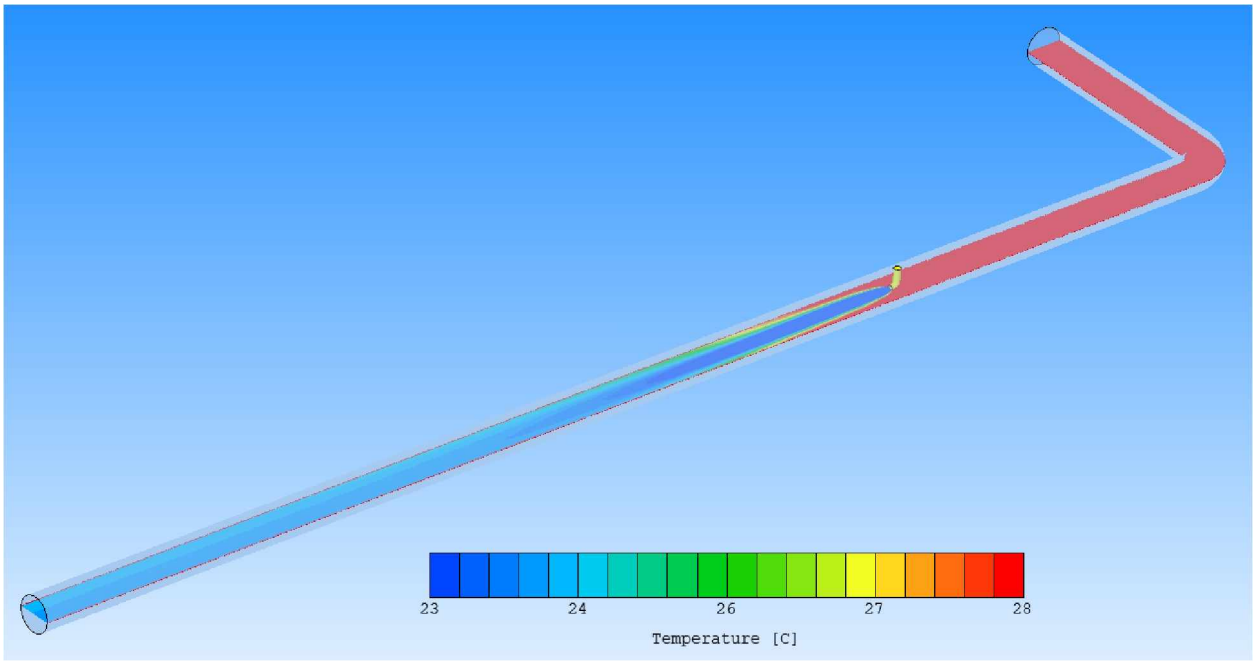

Figure 4.9 Temperature Gradient of Airflow within Ventilation Duct for Location 3

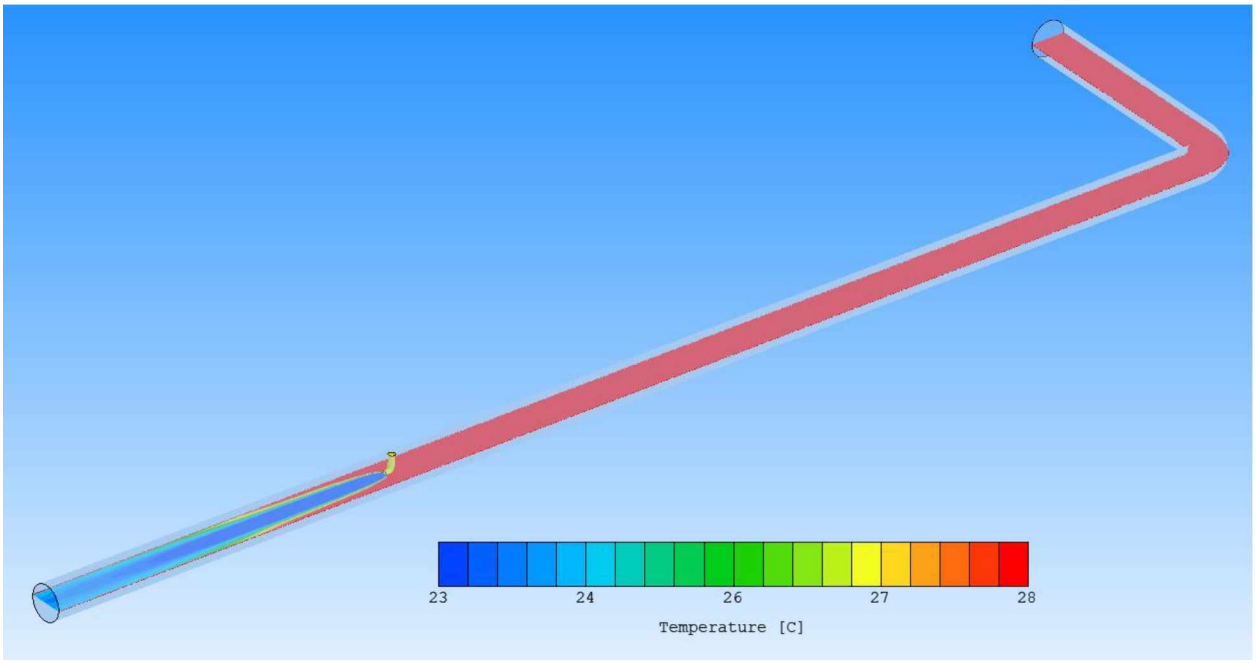

Figure 4.10 Temperature Gradient of Airflow within Ventilation Duct for Location 5

Overall, the location of the VTs seems to have a marginal influence on temperature variation of airflow in the ventilation duct. At Location 1, the airflow travels over a longer distance (about 33 m) before it exits the ventilation duct. The difference between the insertion point temperature and the exit temperature is approximately 1°C (33.8°F). Similarly, Locations 2 (see Appendix A) and

3 exhibited the same temperature changes observed in Location 1. The temperature difference at Location 5 is less than 1°C (33.8°F), as the insertion point is closer to the exit and the airflow travels over a shorter distance (6 m) than the other locations. In the case of velocity gradients (Appendix A), the highest velocities were recorded at the injection point of the cold airflow for the five different locations. However, the velocities decrease as the airflow move towards the exit.

The number of VT was varied to determine how many VTs are required to achieve a decent cooling effect. The number of VTs were varied at only Location 3. The initial number was eight (8). Then it was increased by 2 to 10, 12, 14, 16, 18, and 20. Each increment revealed minor temperature change, as in there was no significant temperature drop between successive number sets. In the first set, the temperature drop was prominent in the middle region of the ventilation duct, as shown in Figure 4.11. Airflow along the contact of the wall of the ventilation duct did not experience any temperature drop. The temperature of the airflow in the middle and exit was approaching 26°C (78.8°F), while along the duct, it was around 28°C (82.4 °F). For 14 VTs (Figure 4.12), the airflow temperature decreased for most of the ventilation duct. There was a noticeable high temperature along the ventilation duct wall, extending a few meters (about 6 m) from the insertion point. The temperature of airflow exiting the ventilation duct was below 26°C (78.8°F).

Given 20 VTs (Figure 4.13), a significant drop in the exit temperature from 26°C (78.8°F) in the initial set to below 24°C (75.2°F) was observed. Additionally, the high-temperature region observed in the previous sets has also decreased significantly to about 1 m from the insertion point. The 20 VTs also generated a more uniform temperature airflow. Appendix B shows the temperature gradients for sets 10, 12, 16, and 18.

The velocity gradients for each number set are presented in Appendix B. Again, the highest velocity of 50 m/s was recorded at the injection point of the cold airflow, while the lowest (38 m/s) was recorded at the ventilation duct outlet. The span of the highest velocity seems to increase with the increasing number of VTs. The 20 VT has the longest span of about 6 m (19.69 ft), and the least span is approximately 2 m (6.56 ft) for 8 VT.

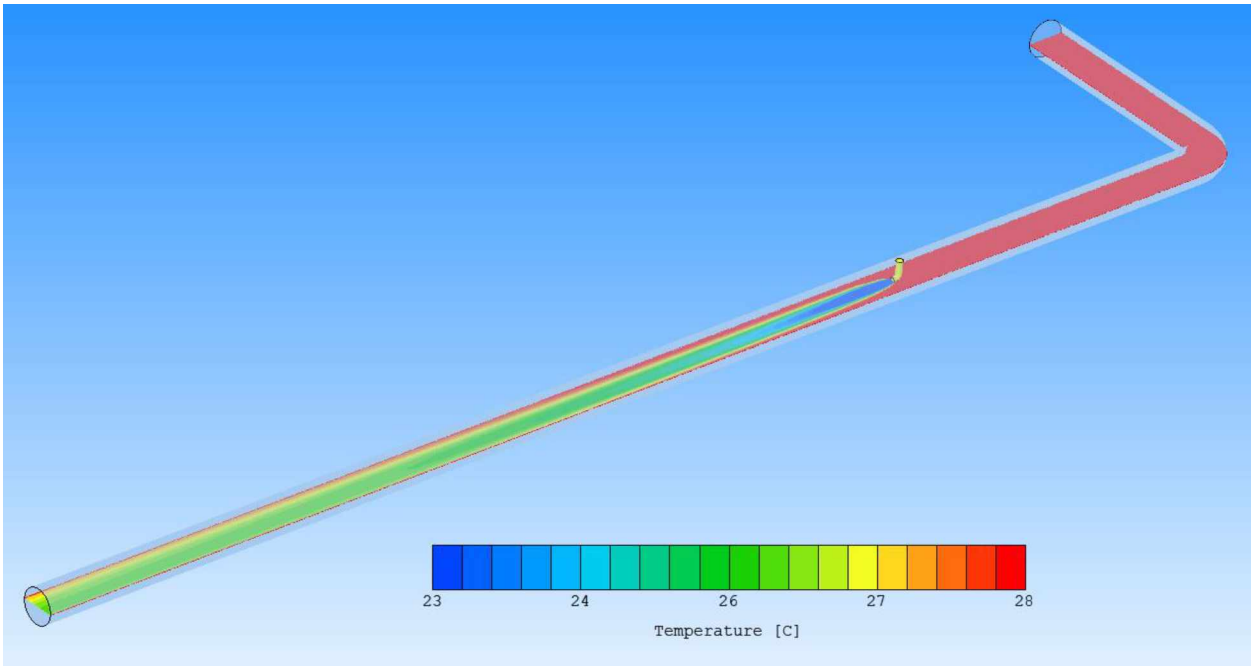

Figure 4.11 Temperature Gradient in Ventilation Duct for 8 VTs

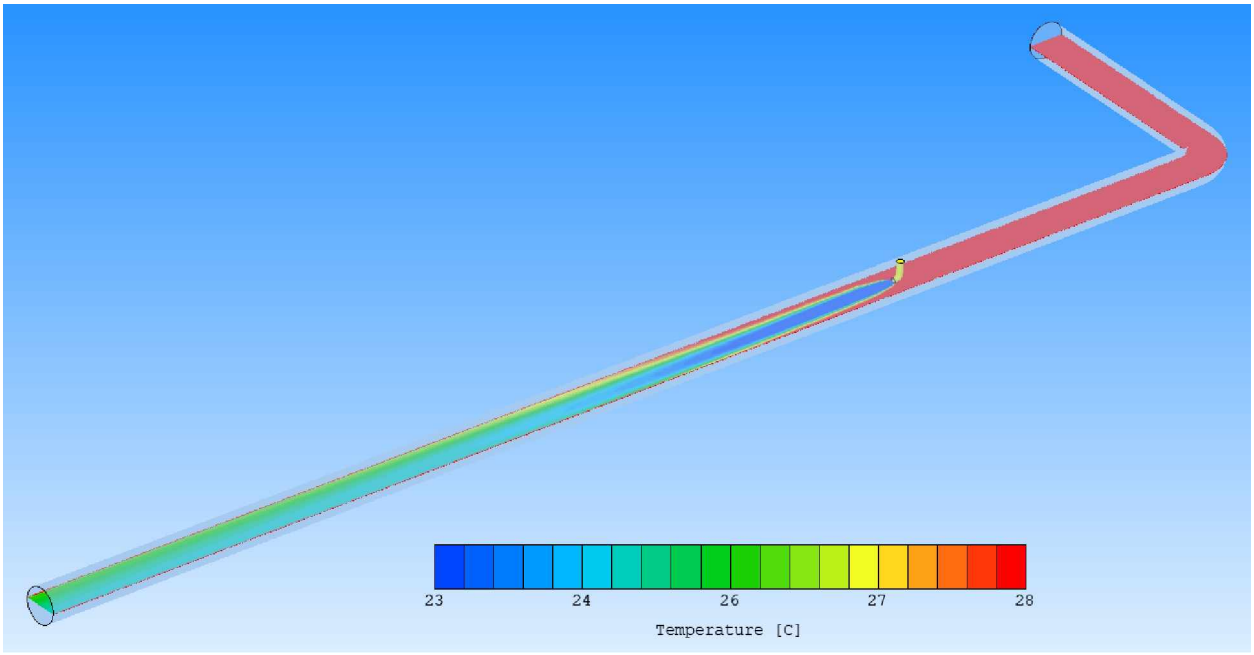

Figure 4.12 Temperature Gradient in Ventilation Duct for 14 VTs

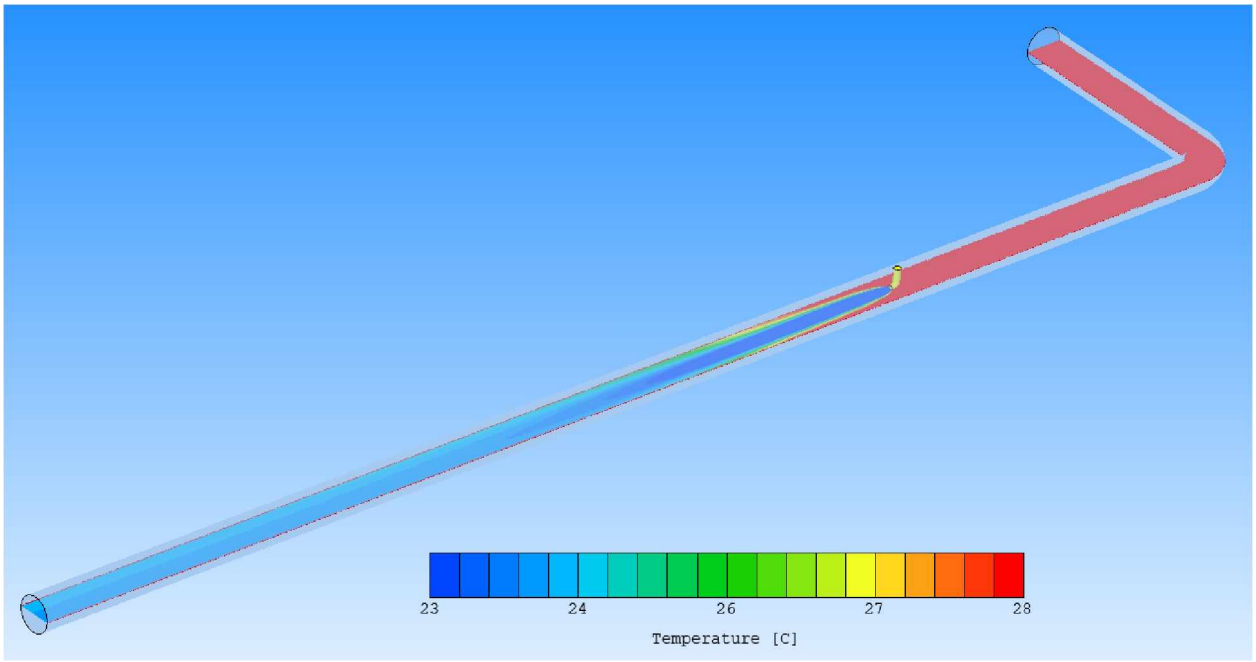

Figure 4.13 Temperature Gradient in Ventilation Duct for 20 VTs

The second stage of the CFD modeling involved simulation airflow from the ventilation duct in the development heading. Here, the scenarios considered in the first stage were also applied, and the results obtained were used as inputs. The simulation run included an evaluation of airflow at the face of the development heading for the different VT locations and the number of VTs. Temperature and velocity gradients presenting the airflow dynamics were captured 2 m from the floor level of the development heading. Airflow from the ventilation duct outlet circulates the face and escapes into the return airway. At location 1 (Figure 4.14), the face temperature averages about 25°C, and the hot airstream from the hot outlet is discharged in the return airway. Locations 3 (Figure 4.15) and 5 (Figure 4.16) also had similar face temperature gradients seen at Location 1; however, the hot airstreams were discharged in the development heading. Though the hot airstream was not close to the face, it could elevate airflow temperature downstream of the development heading. Temperature gradients for Locations 2 and 3 and velocity gradients for each location are presented in Appendix C. Concerning the location of VT, the velocity gradient of airflow ranges from 0 m/s to 10 m/s. The velocities are high at the ventilation duct outlet, and it extends to the face. However, it decreases significantly to less than 4 m/s as the airflow moves towards the return airway. There were a few spots that showed 0 m/s, indicating slow or stagnate airflow.

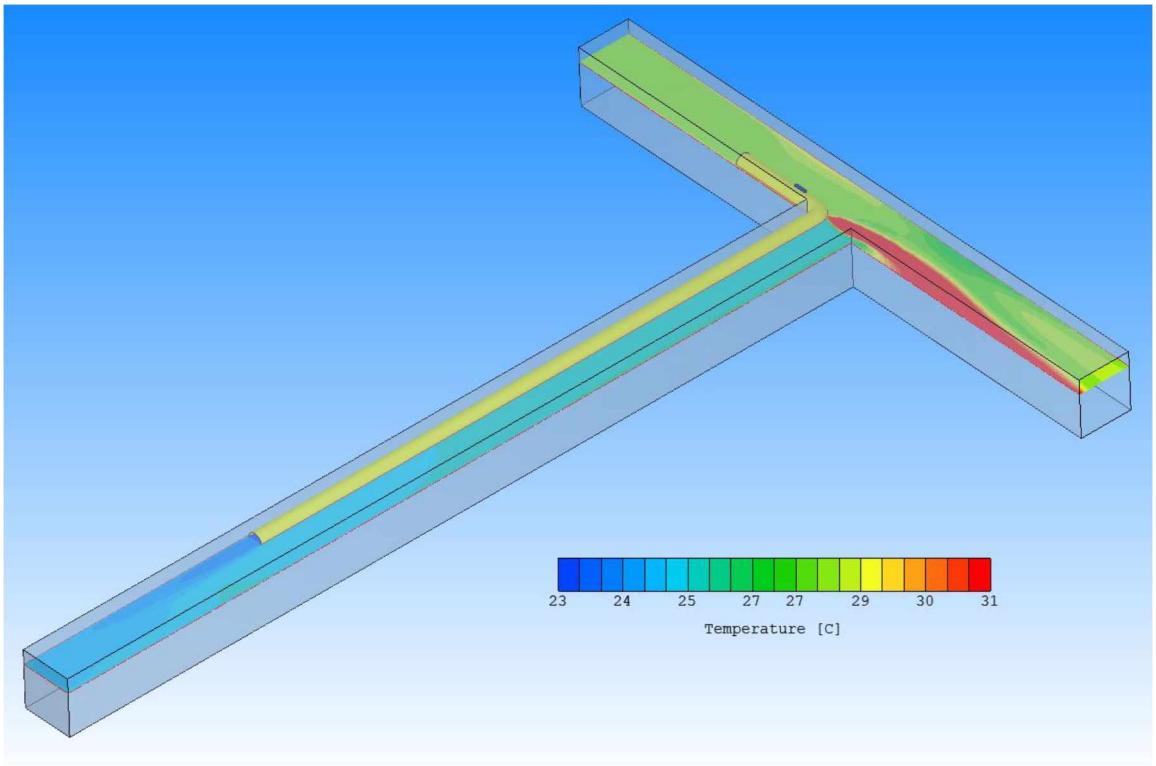

Figure 4.14 Temperature Gradient of Airflow in the Development Heading for VT Location 1

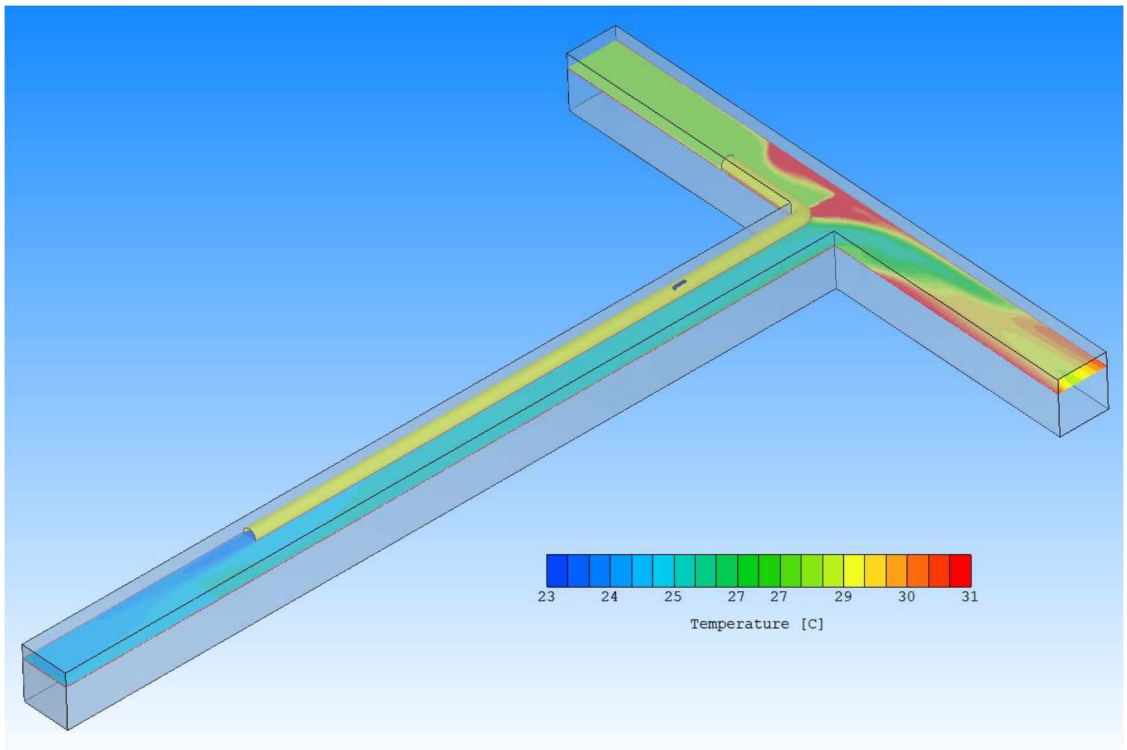

Figure 4.15 Temperature Gradient of Airflow in the Development Heading for VT Location 3

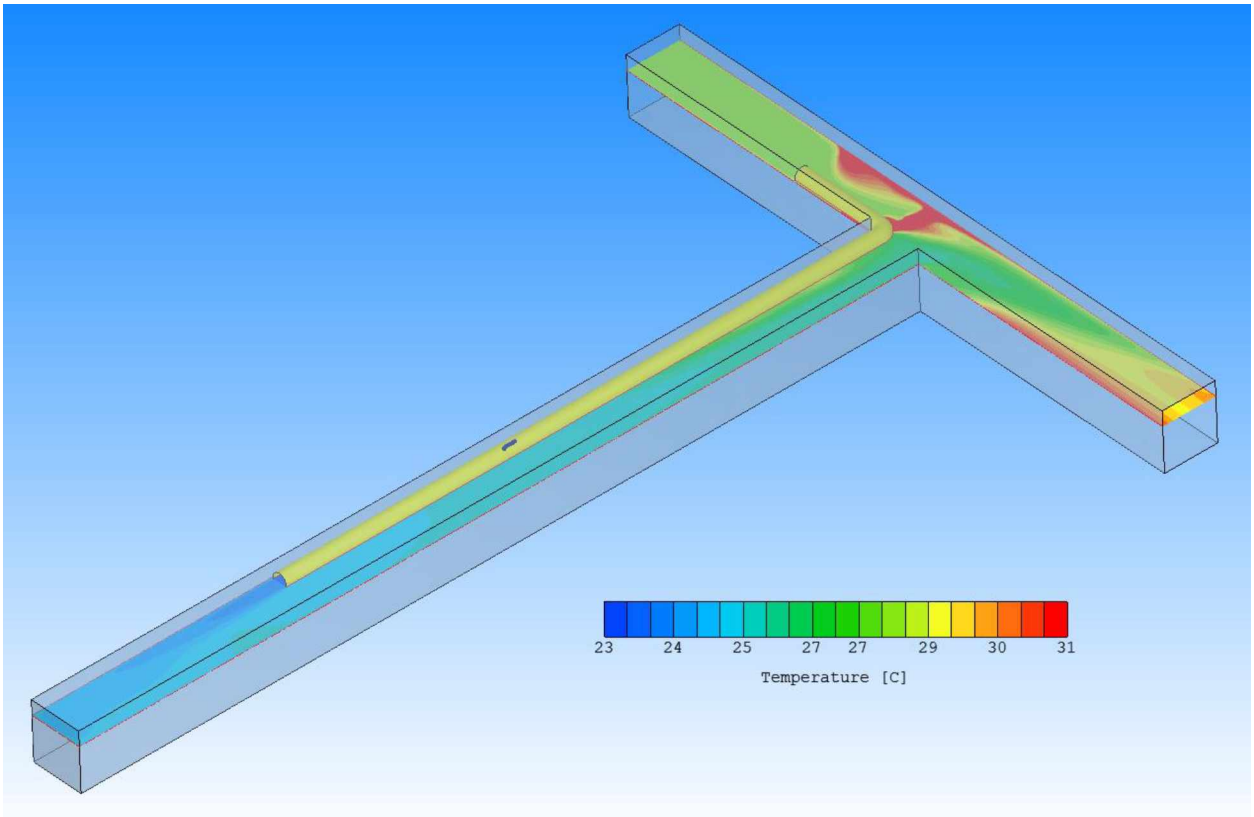

Figure 4.16 Temperature Gradient of Airflow in the Development Heading for VT Location 5

In simulating the number of VT for the development heading, Location 2 was chosen arbitrarily for all the simulation run. Figures 4.17, 4.18, and 4.19 illustrate the temperature gradient of airflow for 8, 14, and 20 VTs. Temperature gradients for 10, 12, 16, and 18 VTs are presented in Appendix D in addition to velocity gradients for each set of VT number. The face temperature was approximately 27ºC for 8 VTs, 26ºC for 14 VTs, and 25ºC for 20 VTs. Similar to the results presented above for the VT locations, the velocity gradient shows that airflow velocity was high at the face and decreases as the airflow moves towards the return airway.

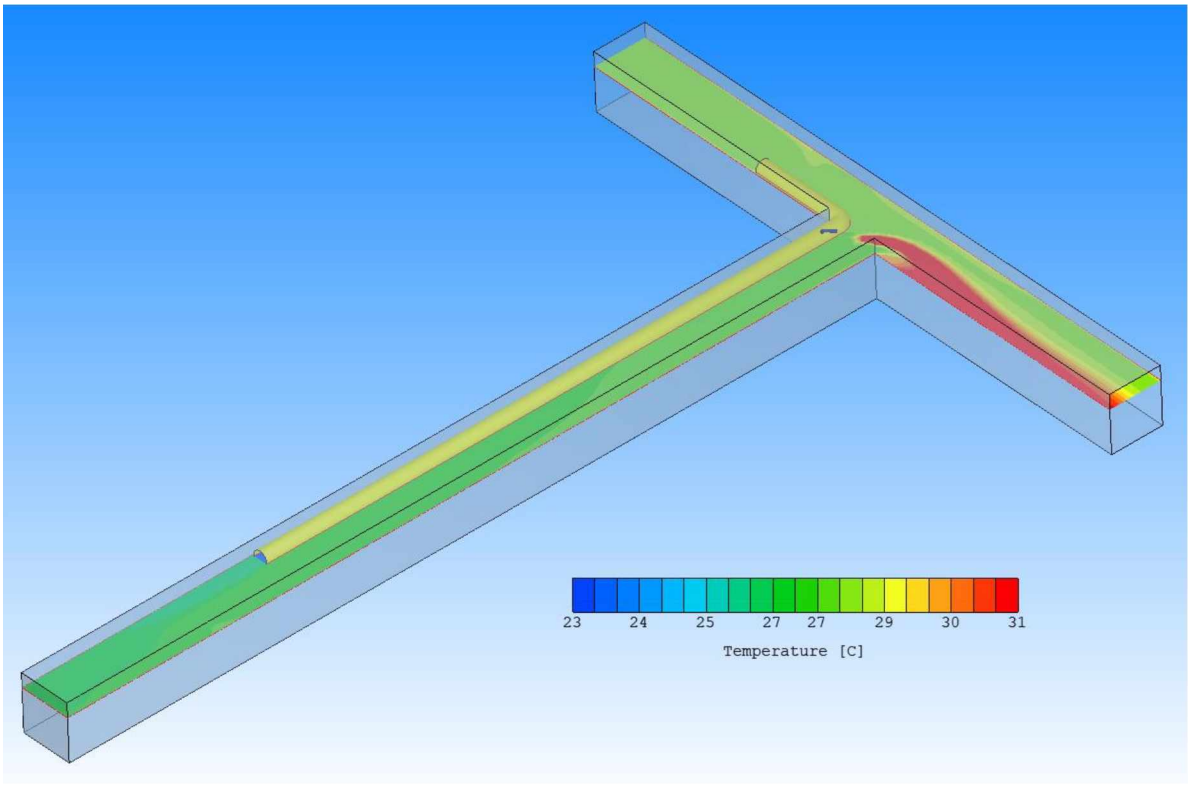

Figure 4.17 Temperature Gradient of Airflow in the Development Heading for 8 VTs

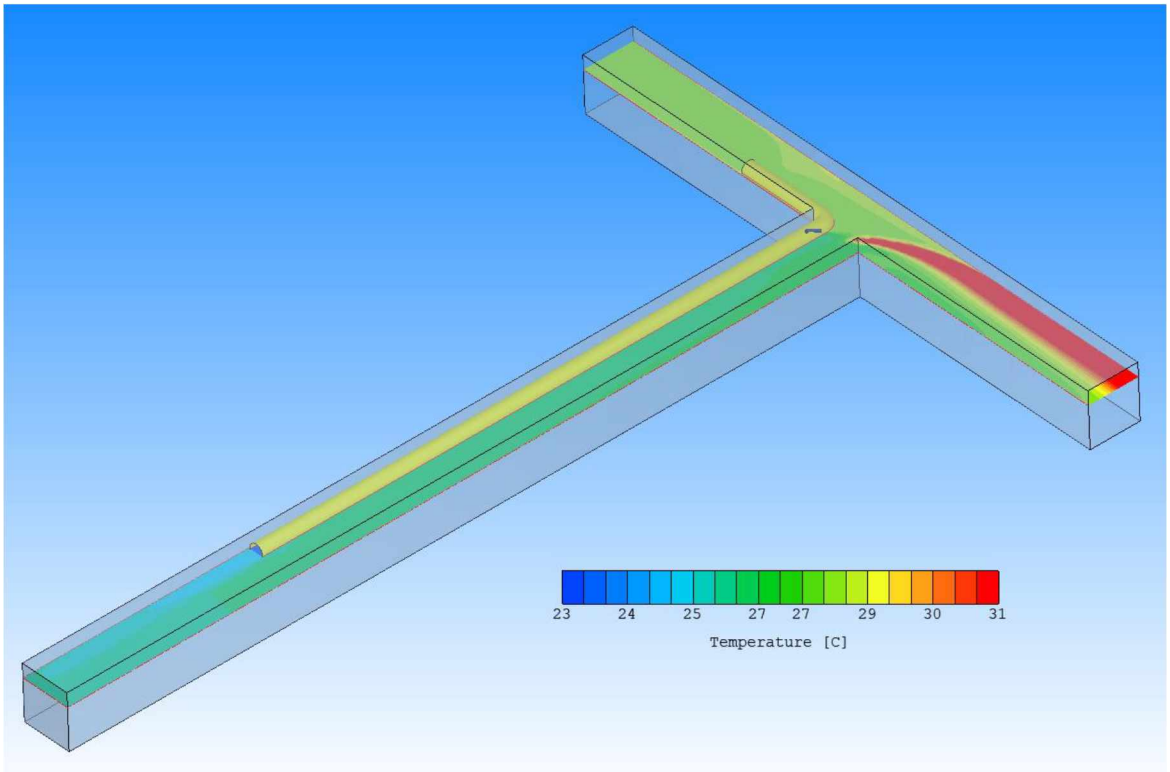

Figure 4.18 Temperature Gradient of Airflow in the Development Heading for 14 VTs

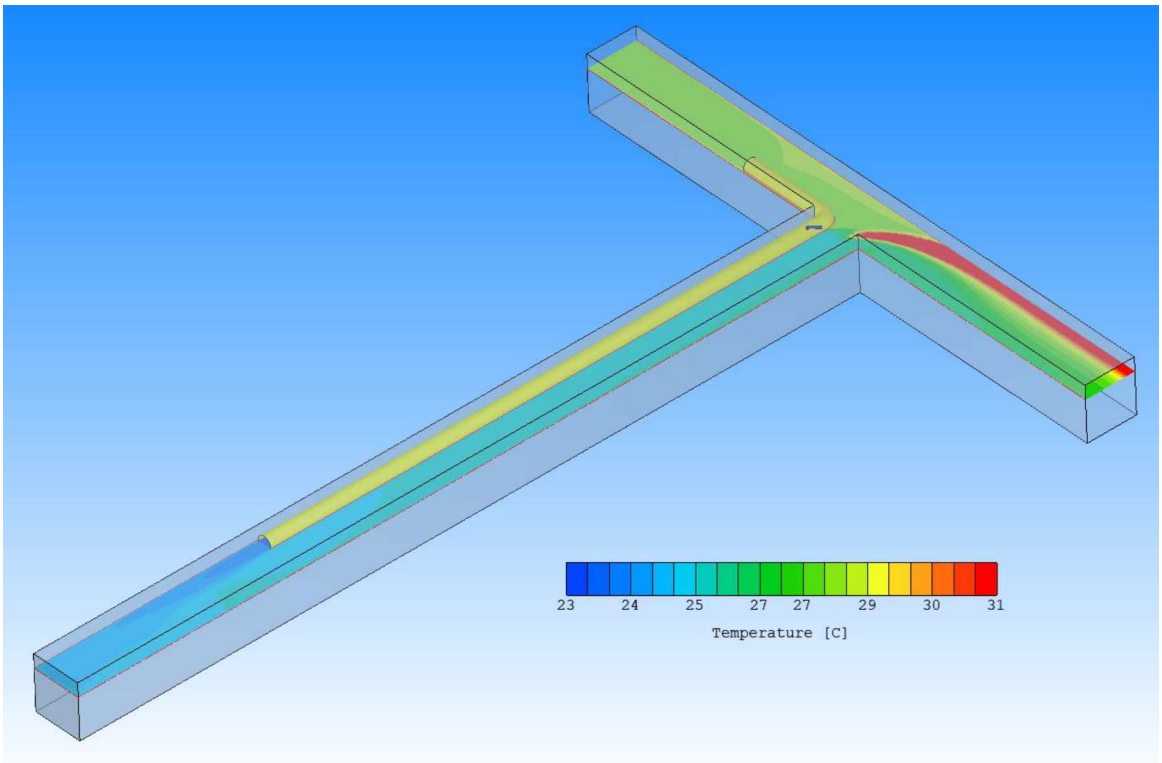

Figure 4.19 Temperature Gradient of Airflow in the Development Heading for 20 VTs

Table 4.3 presents a detailed result of the simulation run for varying numbers of VT in the ventilation duct. As the number of VT increased from 8 to 20; the outlet temperature decreased from 26.3°C to 23.9°C, the outlet air quantity increased from 30.1 kcfm to 32.4 kcfm, the cold air quantity increased from 0.96 kcfm to 2.4 kcfm, and the hot quantity increased from 0.24 kcfm to 0.6 kcfm. The inlet temperature and air quantities were 28°C and 30 kcfm, respectively. The result shows that as the number of VT increases, the cooling effect also increases, causing the ventilation duct outlet temperature to decrease. From Table 4.3, the highest cooling effect was achieved with 20 vortex tubes where temperature decreased from 28°C (82.4°F) to 24°C (75.2°F), which translates into a temperature drop of 4°C (39.2°F).

Table 4.3 Temperature Variation in the Ventilation Duct with varying Number of VT

Location	3	3	3	3	3	3	3
No of vortex tube	20	18	16	14	12	10	8
Inlet temperature (°C)	28	28	28	28	28	28	28
Inlet air quantity (kcfm)	30	30	30	30	30	30	30
Outlet temperature (°C)	23.9	24.3	24.7	25.1	25.4	25.8	26.3
Outlet air quantity (kcfm)	32.4	32.16	31.92	31.68	31.44	31.2	30.1
Cold Air quantity (kcfm)	2.4	2.16	1.92	1.68	1.44	1.2	0.96
Hot air quantity (kcfm)	0.6	0.54	0.48	0.42	0.36	0.3	0.24

4.3 Discussion

The results presented are reasonably accurate considering the simplifications made in the CFD model. The study shows VT location does not have any effect on the ventilation duct outlet temperature. The temperature remained the same irrespective of the location. This can be attributed to the absence of air leakage in the ventilation system, preventing interaction with surrounding air in the ventilation duct. Another contributing factor could be the adiabatic boundary condition. Under the adiabatic condition, no heat is exchanged between a system and its environment [87], [88]. In other words, no external heat enters or leaves the ventilation duct. The ventilation duct is considered to be perfectly insulated so heat from the surroundings does not flow into the duct or vice versa, except the cold air from the VT. Additionally, the velocity profile for the VT locations shows that airflow velocity decreases as it moves towards the ventilation duct exit, as illustrated in Appendix C.

The number of VT was varied to determine the optimal vortex tube number for desired cooling effect. Figure 4.11, Figure 4.12, and Figure 4.13 show that as the number of VTs increases, the cooling effect also increases, causing the ventilation duct outlet temperature to decrease. This observation is evident in Table 4.3 as the number of VT increased from 8 to 20. The highest cooling effect was achieved with 20 VT where temperature decreased by 4°C from 28°C (82.4°F) to 24°C (75.2°F). Stanton [40] posits that in mine ventilation, there are only five degrees difference between "heaven" and "hell." At 27.5°C, the environment is heaven with no adverse effects to productivity or human health while at 32.5°C, the environment is "hell" with poor output and a high propensity to adverse human health. Hence, even a 1°C drop in temperature is of immense value to the cooling regime employed in a mine.

The earlier assertion that irrespective of the VT location, the ventilation duct outlet temperature remains constant holds for the development heading as well. Thus, VT location does have significant effect on temperature drop in the development heading. There was no noticeable temperature change at the development heading face as the positions of VT was varied from Location 1 to Location 5. However, vortex tube location can dictate where the hot air from the hot outlet of the vortex tube will be released. The hot air can raise the airflow temperature in the working area if it is not handled properly. For instance, Figure 4.14 and Appendix C show that at

Locations 1 and 2, the hot air was ejected directly into the return airway. But at Locations 3, 4, and 5, the hot air was being released into the development heading. Having hot air in the development heading can elevate the ambient temperature, making the work area unconducive with associated adverse health issues for miners. Therefore, Locations 1 and 2 would be the most appropriate locations to consider for VT installation. Increasing the number of vortex tubes in the development heading also seems to follow the trend observed in the ventilation duct. The temperature gradients shown in Figure 4.17, Figure 4.18 and Figure 4.19 suggest that as the VT number increases, the temperature at the face decreases.

In all the scenarios considered, the velocity gradients show airflow velocity is highest at the insertion point and the center of the ventilation duct. The velocity is lower along the wall and decreases as it moves towards the exit point. This behavior of the velocity profile is similar to observations made by Cui et al. [89] about the velocity of airflow in a mine tunnel. With a series of cross-sectional velocity profiles of an arched tunnel, the airflow velocity reached its maximum value in the center of the tunnel and decreased from the center to the tunnel wall. Below average airflow velocities decrease more quickly when closer to the tunnel wall. Therefore, the airway shape and wall are critical factors influencing the airflow velocity distribution.

Clearly, VT can be applied in underground workings to control the face temperature. However, a potential concern with the VT cooling system is noise pollution from the compressed air system and exhausts of the VTs. Compressed air generates sudden blowing noise when it expands out from the compressed air system. The noise level can be louder if the compressed air is allowed to expand freely. Thus, silencers and mufflers can be connected to the compressed air inlet and exhausts of the vortex tubes to control and reduce the noise level to an acceptable threshold.

CHAPTER 5 CONCLUSION AND FUTURE WORK

5.1 Conclusion

This study examined the application of vortex tube cooling technology in mine ventilation, using an underground metal mine in Ghana, West Africa as a case study. This type of thermal management method falls under a spot cooling strategy in mine ventilation, where the required cold air is released directly at the working face. The cooling device is located close to the face. A numerical experiment was conducted using the CFD modeling technique to model and simulate the ventilation system at the development heading of the mine. CFD has found wide applications in real-world problems involving complex flow structures. First, the vortex tube and ventilation duct were simulated, and the result obtained was used as a boundary condition to simulate airflow in the development heading.

The simulated airflow shows that with 20 vortex tubes, the working face temperature decreased from 28°C (82.4°F) to 24°C (75.2°F), resulting in the highest cooling effect. The number of vortex tubes can be increased as cooling demand increases. The location of the vortex tube does not affect the temperature gradient at the working face. However, it influences the temperature of the exhaust air in the development heading. To avoid the discharge of hot air in the development heading, the VT should be installed close to the return airway. Preferably, the vortex tubes should be placed at Location 1 or 2 since hot air is ejected directly into the return airway at either location.

5.2 Future Work

Future works of the current study should incorporate different model scenarios, including heat exchange and/or air leakage through the ventilation duct, validation of the model with existing underground spot cooling systems, and feasibility of vortex tube installation in underground mine workings. Also, an experimental study can be conducted using commercial VTs and ventilation network models to validate the current CFD model.

REFERENCES

[1] M. J. McPherson, *Subsurface Ventilation and Environmental Engineering*. Springer Netherlands, 1993.

[2] K. A. Scalise, M. B. Teixeira, and K. C. Kocsis, "Managing Heat in Underground Mines: the Importance of Incorporating the Thermal Flywheel Effect into Climatic Modeling," *Mining, Metall. Explor.*, vol. 38, no. 1, pp. 575–579, 2021, doi: 10.1007/s42461-020-00323-5.

[3] T. Maurya, K. Karena, H. Vardhan, M. Aruna, and M. G. Raj, "Effect of Heat on Underground Mine Workers," *Procedia Earth Planet. Sci.*, 2015, doi: 10.1016/j.proeps.2015.06.049.

[4] M. Sunkpal, P. Roghanchi, and K. C. Kocsis, "A Method to Protect Mine Workers in Hot and Humid Environments," *Saf. Health Work*, 2018, doi: 10.1016/j.shaw.2017.06.011.

[5] A. Kamyar, S. Mostafa Aminossadati, C. Leonardi, and A. Sasmito, "Current Developments and Challenges of Underground Mine Ventilation and Cooling Methods," 2016.

[6] A. Greth, P. Roghanchi, and K. C. Kocsis, "A review of cooling system practices and their applicability to deep and hot underground US mines," *16th North Am. Mine Vent. Symp.*, 2017.

[7] S. Eiamsa-ard and P. Promvonge, "Review of Ranque–Hilsch effects in vortex tubes," *Renew. Sustain. Energy Rev.*, vol. 12, no. 7, pp. 1822–1842, 2008, doi: https://doi.org/10.1016/j.rser.2007.03.006.

[8] M. Yilmaz, M. Kaya, S. Karagoz, and S. Erdogan, "A review on design criteria for vortex tubes," *Heat Mass Transf.*, vol. 45, no. 5, pp. 613–632, 2009, doi: 10.1007/s00231-008-0447-8.

[9] K. I. Matveev and J. Leachman, "Numerical investigation of vortex tubes with extended vortex chambers," *Int. J. Refrig.*, vol. 108, pp. 145–153, 2019, doi: https://doi.org/10.1016/j.ijrefrig.2019.08.030.

[10] J. Wang, X. Gao, and S. Jiao, "The application of vortex tube in deep mine cooling," 2009, doi: 10.1109/ICEET.2009.102.

[11] X. Zhai, "Research on the application of vortex tube type of cooling jacket in coal mine," 2017, doi: 10.1063/1.4993037.

[12] R. L. Bullock, "Subsurface Mine Development," 3rd ed., P. Darling, Ed. SME, pp. 1203–1221.

[13] L. Dong, X. Tong, X. Li, J. Zhou, S. Wang, and B. Liu, "Some developments and new insights of environmental problems and deep mining strategy for cleaner production in mines," *J. Clean. Prod.*, vol. 210, pp. 1562–1578, 2019.

[14] B. H. G. Brady and E. T. Brown, *Rock mechanics: for underground mining*. Springer science & business media, 1993.

[15] N. K. Dumakor-Dupey, "Selection of Underground Mining Method Using Analytic Network Process – A Case Study," University of Mines and Technology, 2018.

[16] A. Pronk, J. Coble, and P. A. Stewart, "Occupational exposure to diesel engine exhaust: A literature review," *Journal of Exposure Science and Environmental Epidemiology*. 2009, doi: 10.1038/jes.2009.21.

[17] A. M. Donoghue, M. J. Sinclair, and G. P. Bates, "Heat exhaustion in a deep underground metalliferous mine," *Occup. Environ. Med.*, 2000, doi: 10.1136/oem.57.3.165.

[18] A. Ryan and D. S. Euler, "Heat stress management in underground mines," *Int. J. Min. Sci. Technol.*, 2017, doi: 10.1016/j.ijmst.2017.05.020.

[19] R. Brake, "The Importance of Underground Mine Ventilation," *AusIMM Bulletin*, 2006.

[20] K. Carpenter, P. Roghanchi, and C. K. Kocsis, "Investigating the importance of climatic monitoring and modeling in deep and hot US underground mines," in *Proceedings of 15th North American Mine Ventilation Symposium, Virginia Tech, Virginia*, 2015, pp. 1–4.

[21] X. Nie, X. Wei, X. Li, and C. Lu, "Heat Treatment and Ventilation Optimization in a Deep Mine," *Adv. Civ. Eng.*, vol. 2018, p. 1529490, 2018, doi: 10.1155/2018/1529490.

[22] M. J. Mcpherson, *Subsurface Ventilation Engineering*. 2009.

[23] T. Maurya, K. Karena, H. Vardhan, M. Aruna, and M. G. Raj, "Potential Sources of Heat in Underground Mines – A Review," *Procedia Earth Planet. Sci.*, vol. 11, pp. 463–468, 2015, doi: https://doi.org/10.1016/j.proeps.2015.06.046.

[24] S. Zhu, S. Wu, J. Cheng, S. Li, and M. Li, "An underground air-route temperature prediction model for ultra-deep coal mines," *Minerals*, vol. 5, no. 3, pp. 527–545, 2015.

[25] G. L. Danko, "Subsurface flow and transport process model for time dependent mine ventilation simulations," *Min. Technol.*, vol. 122, no. 3, pp. 134–144, 2013.

[26] P. Lazaro and M. Momayez, "Heat Stress in Hot Underground Mines: a Brief Literature Review," *Mining, Metall. Explor.*, vol. 38, no. 1, pp. 497–508, 2021, doi: 10.1007/s42461-020-00324-4.

[27] L. O'Connor, "An Investigation into the Development of Thermal Management Policies for Underground Metal Mines in the United States," University of Nevada, 2018.

[28] E. De Souza, "Cost saving strategies in mine ventilation," in *Canadian Institute of Mining, Metallurgy and Petroleum (CIM) 2015 Convention, Montreal*, 2015, pp. 10–12.

[29] A. P. Sasmito, J. C. Kurnia, E. Birgersson, and A. S. Mujumdar, "Computational evaluation of thermal management strategies in an underground mine," *Appl. Therm. Eng.*, 2014, doi: 10.1016/j.applthermaleng.2015.01.062.

[30] P. Roghanchi, "Managing and Controlling the Thermal Environment in Underground Metal Mines," *ProQuest Diss. Theses*, 2017.

[31] B. Belle and M. Biffi, "Cooling pathways for deep Australian longwall coal mines of the future," *Int. J. Min. Sci. Technol.*, vol. 28, no. 6, pp. 865–875, 2018.

[32] P. Guo, Y. Wang, M. Duan, D. Pang, and N. Li, "Research and application of methods for effectiveness evaluation of mine cooling system," *Int. J. Min. Sci. Technol.*, vol. 25, no. 4, pp. 649–654, 2015.

[33] V. T. M. Ngô, S. Nadeau, and S. Hallé, "Validation of ergonomic criteria of a cooling vest for deep and ultra-deep mining," *Int. J. Ind. Ergon.*, vol. 78, p. 102980, 2020.

[34] V. T. M. Ngô, S. Nadeau, and S. Hallé, "Ergonomic design of a cooling vest in deep and ultra-deep mining environments," *Occup. Ergon.*, vol. 13, no. S1, pp. 115–126, 2017.

[35] C. Al Sayed, L. Vinches, O. Dupuy, W. Douzi, B. Dugue, and S. Hallé, "Air/CO2 cooling garment: Description and benefits of use for subjects exposed to a hot and humid climate during physical activities," *Int. J. Min. Sci. Technol.*, vol. 29, no. 6, pp. 899–903, 2019.

[36] C. Al Sayed, L. Vinches, and S. Hallé, "Towards optimizing a personal cooling garment for hot and humid deep mining conditions," *Open J. Optim.*, vol. 5, no. 01, p. 35, 2016.

[37] T. C. Ernst and S. Garimella, "Demonstration of a wearable cooling system for elevated ambient temperature duty personnel," *Appl. Therm. Eng.*, 2013, doi: 10.1016/j.applthermaleng.2013.06.019.

[38] R. Potgieter and M. Van Eldik, "Operational advantages of mobile refrigeration using a closed loop heat rejection configuration," 2018.

[39] M. Van Eldik, "An investigation into the DSM and energy efficiency potential of a modular underground air cooling unit applied in the South African mining industry." North-West University, 2006.

[40] D. J. Stanton, "Development and testing of an underground remote refrigeration plant." North-West University, 2004.

[41] T. Karthikeya Sharma, G. Amba Prasad Rao, and K. Madhu Murthy, "Numerical Analysis of a Vortex Tube: A Review," *Arch. Comput. Methods Eng.*, 2017, doi: 10.1007/s11831-016-9166-3.

[42] Y. T. Wu, Y. Ding, Y. B. Ji, C. F. Ma, and M. C. Ge, "Modification and experimental research on vortex tube," *Int. J. Refrig.*, vol. 30, no. 6, pp. 1042–1049, 2007, doi: https://doi.org/10.1016/j.ijrefrig.2007.01.013.

[43] Y. Xue, M. Arjomandi, and R. Kelso, "The working principle of a vortex tube," *Int. J. Refrig.*, vol. 36, no. 6, pp. 1730–1740, 2013, doi: https://doi.org/10.1016/j.ijrefrig.2013.04.016.

[44] C. M. Gao, K. J. Bosschaart, J. C. H. Zeegers, and A. T. A. M. de Waele, "Experimental study on a simple Ranque–Hilsch vortex tube," *Cryogenics (Guildf).*, vol. 45, no. 3, pp. 173–183, 2005, doi: https://doi.org/10.1016/j.cryogenics.2004.09.004.

[45] S. Y. Im and S. S. Yu, "Effects of geometric parameters on the separated air flow temperature of a vortex tube for design optimization," *Energy*, vol. 37, no. 1, pp. 154–160, 2012, doi: https://doi.org/10.1016/j.energy.2011.09.008.

[46] Bsbergmann, "The Theory of the Vortex Tube," *Exair.com*, 2018.

https://blog.exair.com/2018/10/31/the-theory-of-the-vortex-tube/ (accessed Aug. 12, 2020).

[47] K. V. C. Balakumar, "Analysis of Energy Separation in Vortex Tube using RANS based CFD," University of Cincinnati, 2020.

[48] M. H. Saidi and M. R. Allaf Yazdi, "Exergy model of a vortex tube system with experimental results," *Energy*, vol. 24, no. 7, pp. 625–632, 1999, doi: https://doi.org/10.1016/S0360-5442(98)00076-0.

[49] N. F. Aljuwayhel, G. F. Nellis, and S. A. Klein, "Parametric and internal study of the vortex tube using a CFD model," *Int. J. Refrig.*, vol. 28, no. 3, pp. 442–450, 2005, doi: https://doi.org/10.1016/j.ijrefrig.2004.04.004.

[50] H. Khazaei, A. R. Teymourtash, and M. Malek-Jafarian, "Effects of gas properties and geometrical parameters on performance of a vortex tube," *Sci. Iran.*, vol. 19, no. 3, pp. 454–462, 2012, doi: https://doi.org/10.1016/j.scient.2012.03.003.

[51] M. Mirjalili and K. Ghorbanian, "Numerical investigation of transient thermo-fluid processes in a Ranque-Hilsch vortex tube," *Int. J. Refrig.*, 2021, doi: https://doi.org/10.1016/j.ijrefrig.2021.07.025.

[52] Y. Xue, M. Arjomandi, and R. Kelso, "A critical review of temperature separation in a vortex tube," *Exp. Therm. Fluid Sci.*, vol. 34, no. 8, pp. 1367–1374, 2010, doi: https://doi.org/10.1016/j.expthermflusci.2010.06.010.

[53] F. Liang *et al.*, "Experimental investigation on improving the energy separation efficiency of vortex tube by optimizing the structure of vortex generator," *Appl. Therm. Eng.*, vol. 195, p. 117222, 2021, doi: https://doi.org/10.1016/j.applthermaleng.2021.117222.

[54] N. Bej and K. P. Sinhamahapatra, "Numerical analysis on the heat and work transfer due to shear in a hot cascade Ranque–Hilsch vortex tube," *Int. J. Refrig.*, vol. 68, pp. 161–176, 2016.

[55] U. Behera, P. J. Paul, K. Dinesh, and S. Jacob, "Numerical investigations on flow behaviour and energy separation in Ranque–Hilsch vortex tube," *Int. J. Heat Mass Transf.*, vol. 51, no. 25–26, pp. 6077–6089, 2008.

[56] Y. Xue, M. Arjomandi, and R. Kelso, "Energy analysis within a vortex tube," *Exp. Therm. fluid Sci.*, vol. 52, pp. 139–145, 2014.

[57] M. Kurosaka, "Acoustic streaming in swirling flow and the Ranque—Hilsch (vortex-tube) effect," *J. Fluid Mech.*, vol. 124, pp. 139–172, 1982.

[58] M. H. Saidi and M. S. Valipour, "Experimental modeling of vortex tube refrigerator," *Appl. Therm. Eng.*, vol. 23, no. 15, pp. 1971–1980, 2003.

[59] R. G. Deissler and M. Perlmutter, "Analysis of the flow and energy separation in a turbulent vortex," *Int. J. Heat Mass Transf.*, vol. 1, no. 2, pp. 173–191, 1960, doi: https://doi.org/10.1016/0017-9310(60)90021-1.

[60] H. M. Skye, G. F. Nellis, and S. A. Klein, "Comparison of CFD analysis to empirical data

in a commercial vortex tube," *Int. J. Refrig.*, vol. 29, no. 1, pp. 71–80, 2006.

[61] T. Dutta, K. P. Sinhamahapatra, and S. S. Bandyopdhyay, "Comparison of different turbulence models in predicting the temperature separation in a Ranque–Hilsch vortex tube," *Int. J. Refrig.*, vol. 33, no. 4, pp. 783–792, 2010.

[62] S. E. Rafiee and M. M. Sadeghiazad, "Three-dimensional and experimental investigation on the effect of cone length of throttle valve on thermal performance of a vortex tube using k–ε turbulence model," *Appl. Therm. Eng.*, vol. 66, no. 1–2, pp. 65–74, 2014.

[63] V. Bianco, A. Khait, A. Noskov, and V. Alekhin, "A comparison of the application of RSM and LES turbulence models in the numerical simulation of thermal and flow patterns in a double-circuit Ranque-Hilsch vortex tube," *Appl. Therm. Eng.*, vol. 106, pp. 1244–1256, 2016.

[64] R. Shamsoddini and A. H. Nezhad, "Numerical analysis of the effects of nozzles number on the flow and power of cooling of a vortex tube," *Int. J. Refrig.*, vol. 33, no. 4, pp. 774–782, 2010, doi: https://doi.org/10.1016/j.ijrefrig.2009.12.029.

[65] J. M. Alexander, J. J. Croley Jr, and R. R. Messick, "Use of Vortex Tube for Cooling Wearers of Industrial Protective Clothing," Du Pont de Nemours (EI) & Co. Savannah River Plant, Aiken, SC, 1963.

[66] Bestech Australia, "H-6826 Vortex Tube Refrigerator," 2021. https://www.bestech.com.au/product/h-6826-vortex-tube-refrigerator/ (accessed Sep. 02, 2021).

[67] VortTech UK, "Vortex Enclosure Coolers," 2021. https://www.vortextube.co.uk/enclosure-coolers (accessed Sep. 02, 2021).

[68] B. Boswell, "Use of air cooling and its effectiveness in dry machining processes." Curtin University, 2008.

[69] Nex Flow Air Products Corp., "DRY MACHINING AND THE USE OF VORTEX COOLING," 2021. https://www.nexflow.com/blog/dry-machining-use-vortex-cooling/ (accessed Sep. 02, 2021).

[70] M. Lorey, J. Steinle, and K. Thomas, "Industrial application of vortex tube separation technology utilizing the Ranque-Hilsch effect," 1998.

[71] M. B. Laique and T. Hussain, "Comparison Between Traditional Air Conditioning System and Wearable Cooling/Heating Devices," *Int. J. Eng. Res. Technol.*, vol. 7, no. 1, pp. 111–113, 2018.

[72] G. Xu, K. D. Luxbacher, S. Ragab, J. Xu, and X. Ding, "Computational fluid dynamics applied to mining engineering: a review," *Int. J. Mining, Reclam. Environ.*, vol. 31, no. 4, pp. 251–275, 2017, doi: 10.1080/17480930.2016.1138570.

[73] S. Song, G. Zhou, J. Duan, Q. Meng, B. Sun, and Y. Wang, "CFD simulation of multi-phase and multi-component diffusion of air-dust-gas in a fully mechanized mining face," *Environ. Sci. Pollut. Res.*, vol. 28, no. 14, pp. 18260–18275, 2021, doi: 10.1007/s11356-020-11850-5.

[74] G. Zhang, G. Zhou, S. Song, L. Zhang, and B. Sun, "CFD investigation on dust dispersion pollution of down/upwind coal cutting and relevant countermeasures for spraying dustfall in fully mechanized mining face," *Adv. Powder Technol.*, vol. 31, no. 8, pp. 3177–3190, 2020, doi: https://doi.org/10.1016/j.apt.2020.06.009.

[75] G. Zhang, B. Sun, S. Song, H. Wang, and G. Zhou, "CFD comparative analysis on the pollution characteristics of coal dust under turbulent airflow from coal cutting in the fully mechanized mining face," *Process Saf. Environ. Prot.*, vol. 146, pp. 515–530, 2021, doi: https://doi.org/10.1016/j.psep.2020.11.044.

[76] S. Arya, J. Sottile, and T. Novak, "Development of a flooded-bed scrubber for removing coal dust at a longwall mining section," *Saf. Sci.*, vol. 110, pp. 204–213, 2018, doi: https://doi.org/10.1016/j.ssci.2018.08.003.

[77] J. C. Kurnia, A. P. Sasmito, and A. S. Mujumdar, "CFD simulation of methane dispersion and innovative methane management in underground mining faces," *Appl. Math. Model.*, vol. 38, no. 14, pp. 3467–3484, 2014, doi: https://doi.org/10.1016/j.apm.2013.11.067.

[78] T. Feroze and B. Genc, "Estimating the effects of line brattice ventilation system variables in an empty heading in room and pillar mining using CFD," *J. South. African Inst. Min. Metall.*, vol. 116, no. 12, pp. 1143–1152, 2016.

[79] F. Fernández-Alaiz, A. M. Castañón, F. Gómez-Fernández, and M. Bascompta, "Mine Fire Behavior under Different Ventilation Conditions: Real-Scale Tests and CFD Modeling," *Appl. Sci.*, vol. 10, no. 10, 2020, doi: 10.3390/app10103380.

[80] R. Singh and F. D. Ardejani, "Finite volume discretisation for solving acid mine drainage problems," *Arch. Min. Sci.*, vol. 49, no. 4, pp. 531–556, 2004.

[81] M. Narasimha, A. N. Mainza, P. N. Holtham, M. S. Powell, and M. S. Brennan, "A semi-mechanistic model of hydrocyclones — Developed from industrial data and inputs from CFD," *Int. J. Miner. Process.*, vol. 133, pp. 1–12, 2014, doi: https://doi.org/10.1016/j.minpro.2014.08.006.

[82] T. Ren and R. Balusu, "The use of CFD modelling as a tool for solving mining health and safety problems," 2010.

[83] K. G. Wallace, B. S. Prosser, S. Ampiah, and E. Gyawu, "Ventilation System Design for the Prestea Underground Mine BT - Proceedings of the 11th International Mine Ventilation Congress," 2019, pp. 829–837.

[84] M. Semin and L. Levin, "Theoretical study of partially return air flows in vertical mine shafts," *Therm. Sci. Eng. Prog.*, vol. 23, p. 100884, 2021.

[85] S. Arya and T. Novak, "Numerical Investigation of the Effect of a Novel Wet Scrubber on Dust Reduction in an Underground Coal Mine," *Mining, Metall. Explor.*, 2020, doi: 10.1007/s42461-019-00135-2.

[86] M. Dumbser, M. Käser, V. A. Titarev, and E. F. Toro, "Quadrature-free non-oscillatory finite volume schemes on unstructured meshes for nonlinear hyperbolic systems," *J. Comput. Phys.*, vol. 226, no. 1, pp. 204–243, 2007.

[87] R. Legg, “Chapter 1 - Properties of Humid Air,” R. B. T.-A. C. S. D. Legg, Ed. Butterworth-Heinemann, 2017, pp. 1–28.

[88] D. E. Stevens and F. X. Crum, “Meteorology, Dynamic (Troposphere),” R. A. B. T.-E. of P. S. and T. (Third E. Meyers, Ed. New York: Academic Press, 2003, pp. 629–659.

[89] C. Ding, X. He, and B. Nie, “Numerical simulation of airflow distribution in mine tunnels,” *Int. J. Min. Sci. Technol.*, vol. 27, no. 4, pp. 663–667, 2017, doi: https://doi.org/10.1016/j.ijmst.2017.05.017.

APPENDICES

Appendix A: Temperature and Velocity Gradient for VT Locations

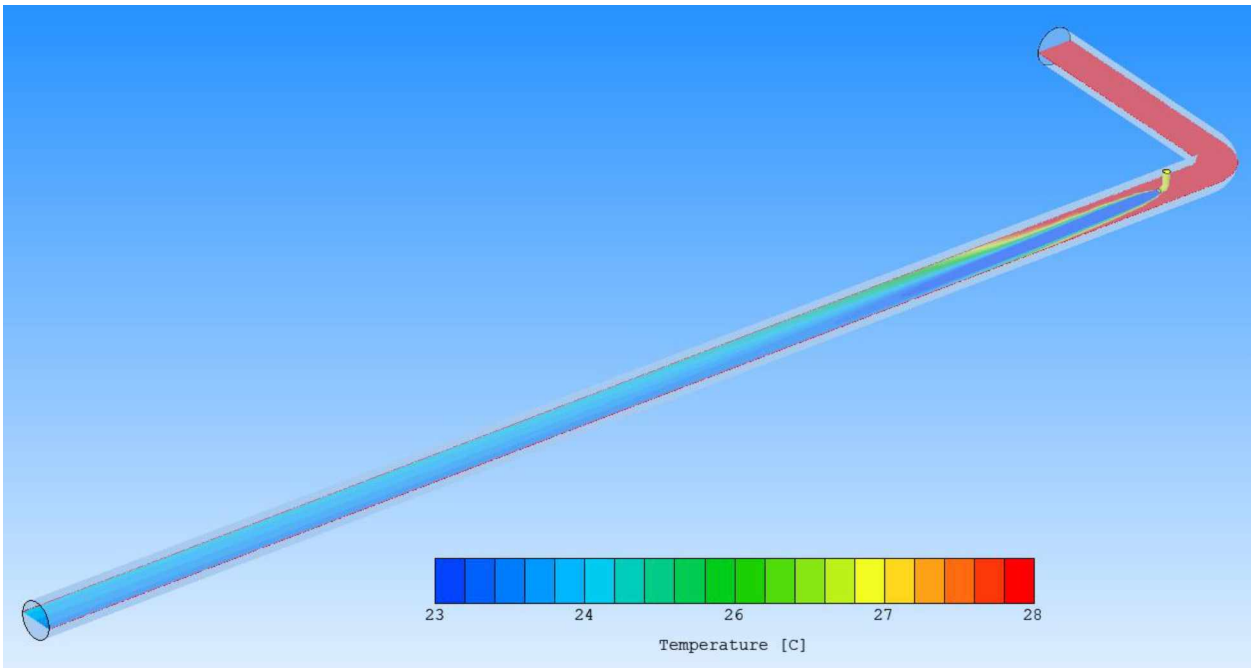

Figure A1 Temperature Gradient of Airflow within Ventilation Duct for Location 2

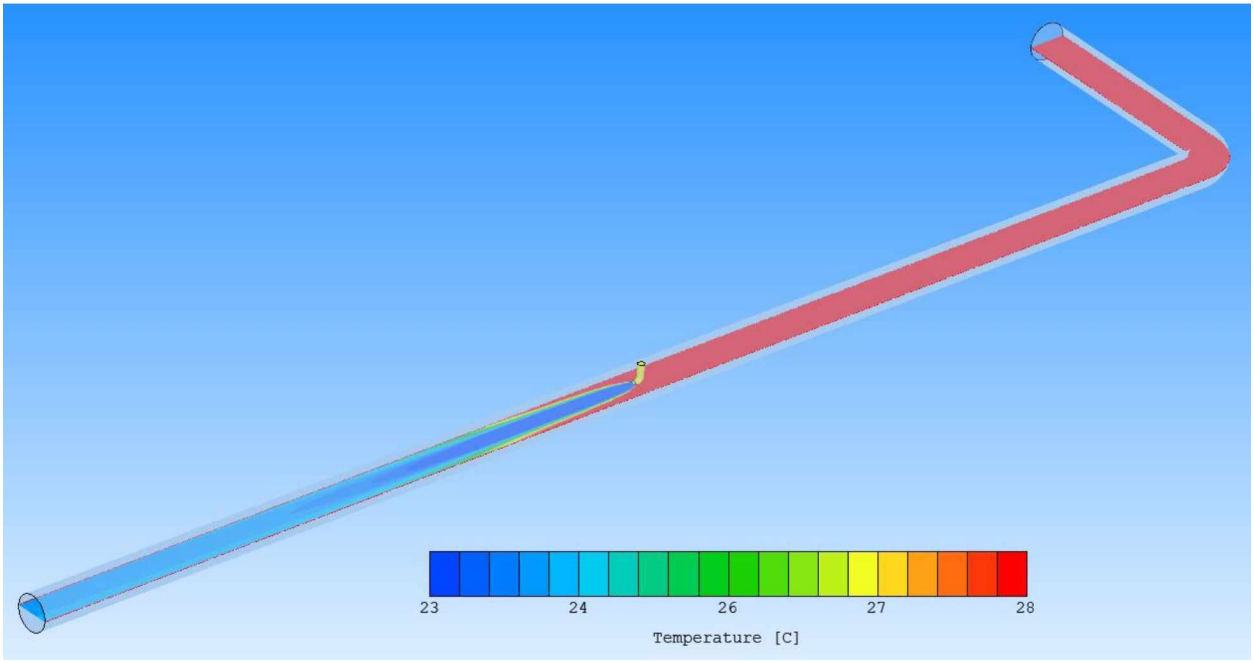

Figure A2 Temperature Gradient of Airflow within Ventilation Duct for Location 4

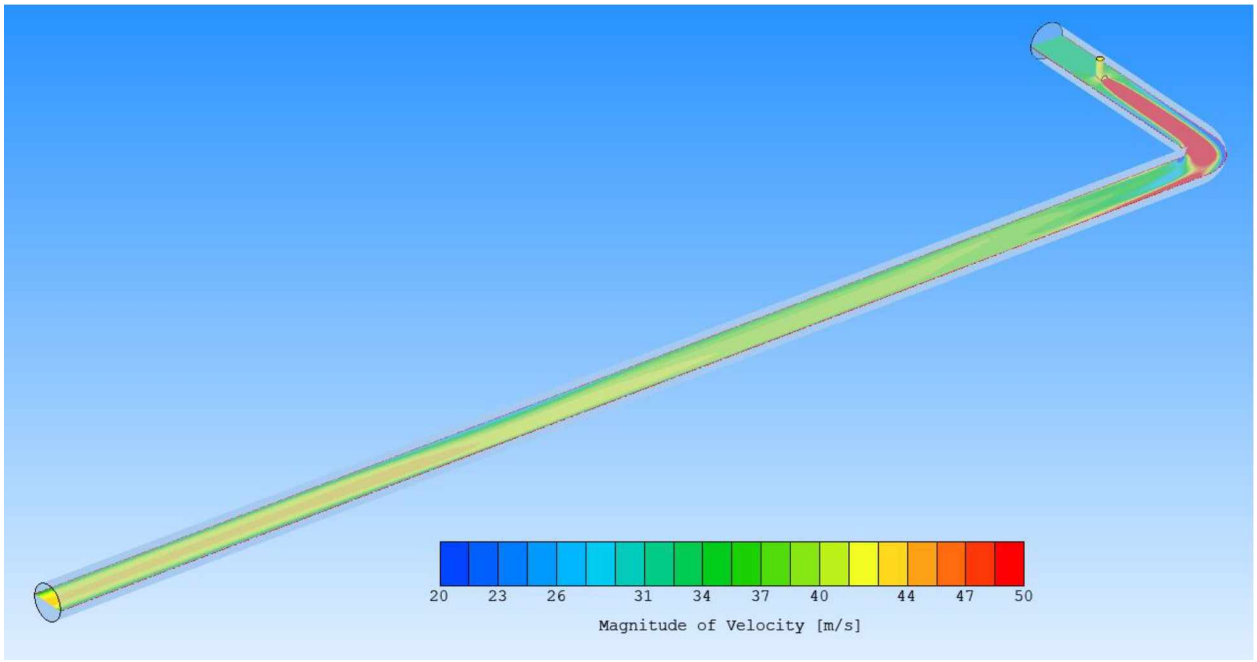

Figure A3 Velocity Gradient of Airflow within Ventilation Duct for Location 1

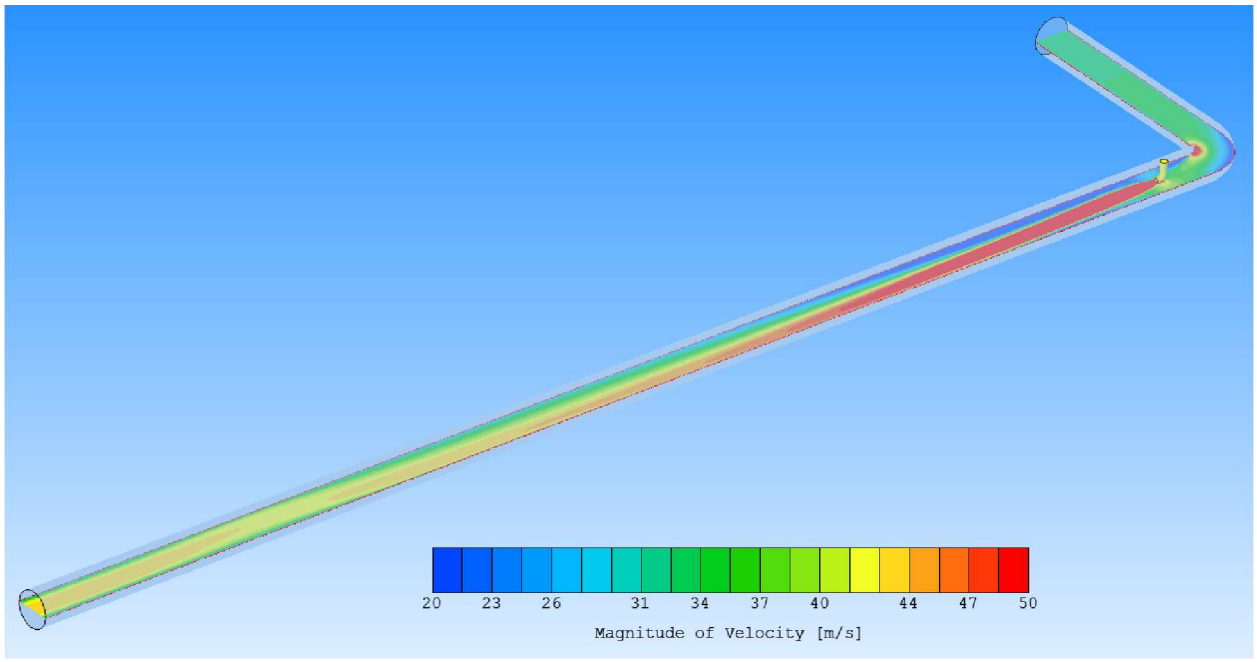

Figure A4 Velocity Gradient of Airflow within Ventilation Duct for Location 2

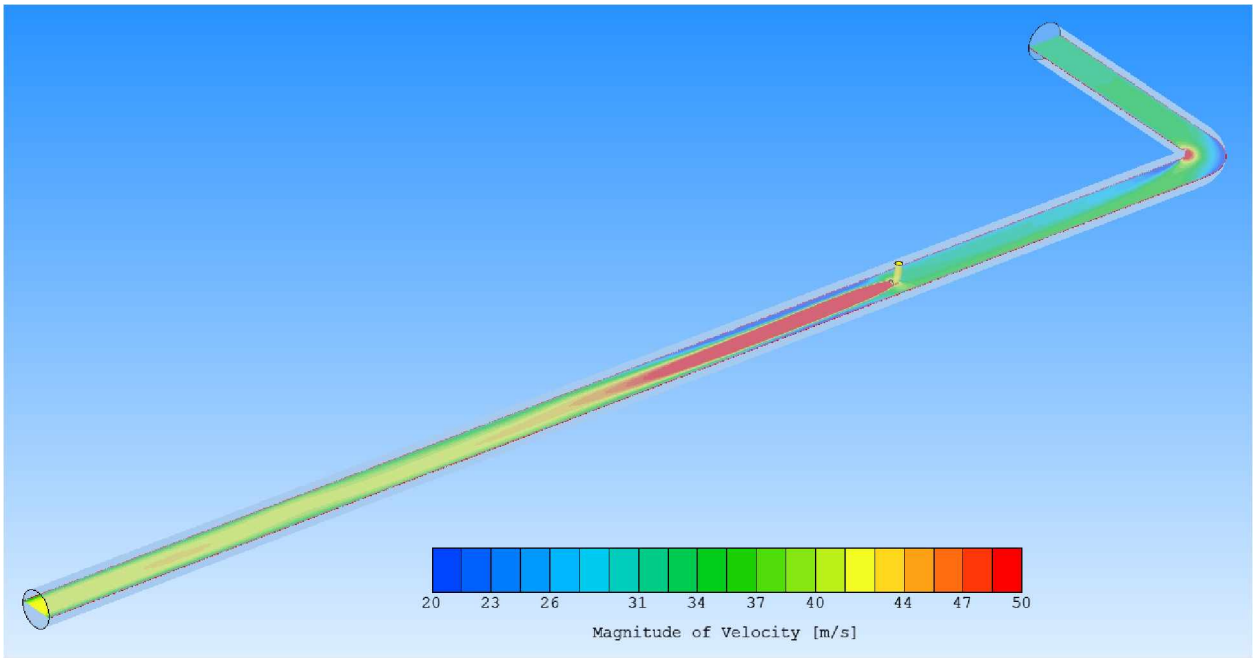

Figure A5 Velocity Gradient of Airflow within Ventilation Duct for Location 3

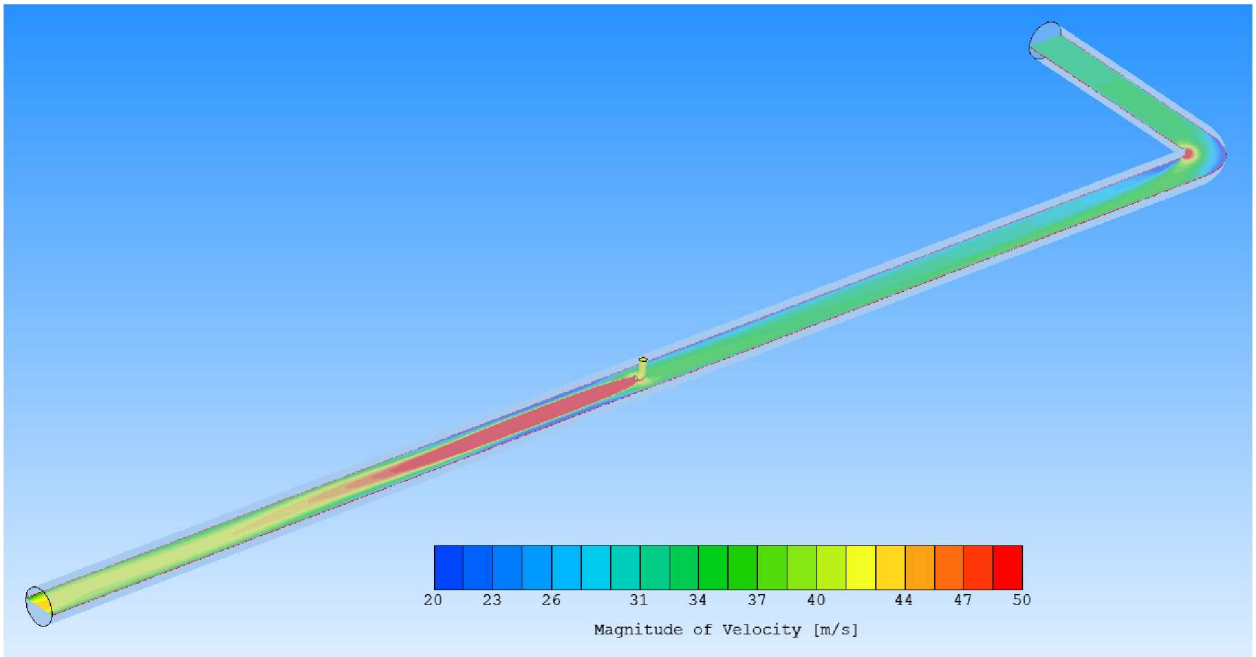

Figure A6 Velocity Gradient of Airflow within Ventilation Duct for Location 4

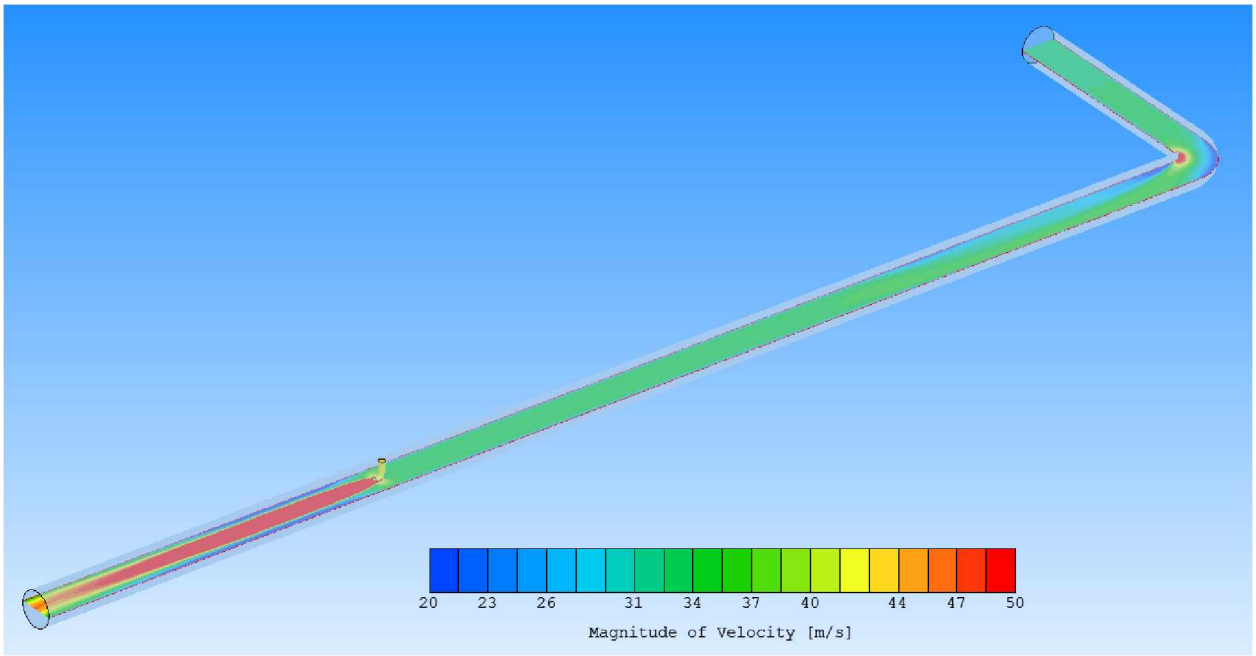

Figure A7 Velocity Gradient of Airflow within Ventilation Duct for Location 5

Appendix B: Temperature and Velocity Gradient for Number of VTs

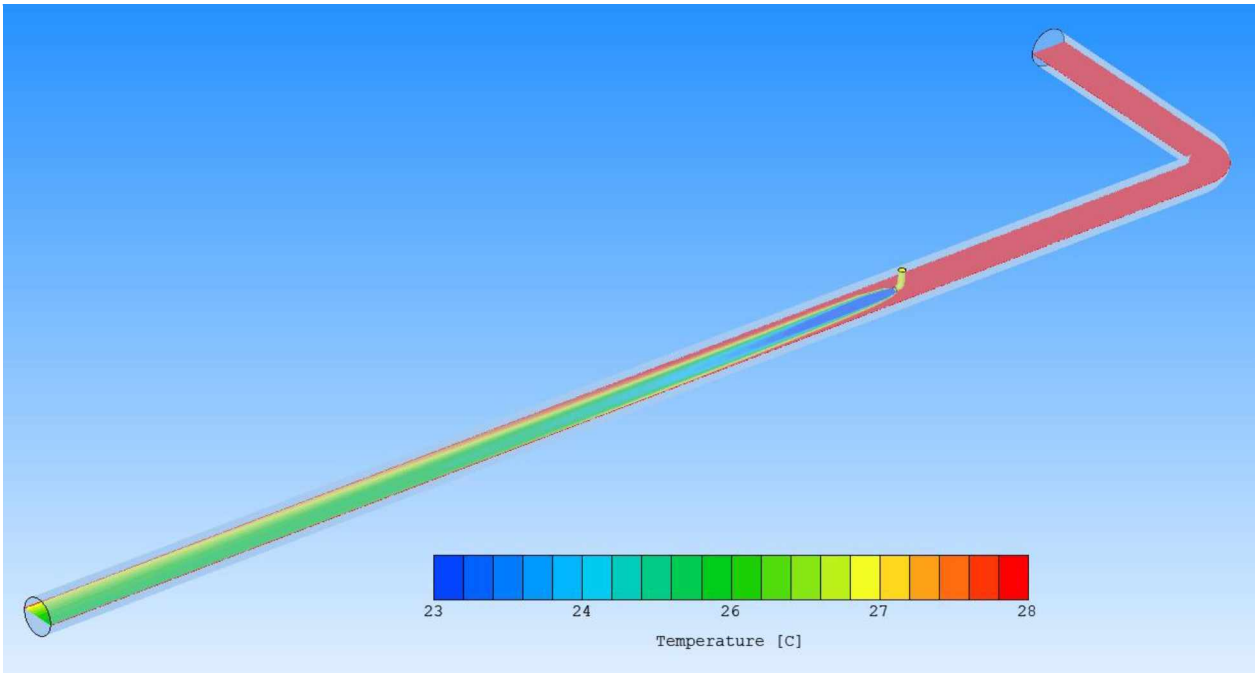

Figure B1 Temperature Gradient in Ventilation Duct for 10 VTs

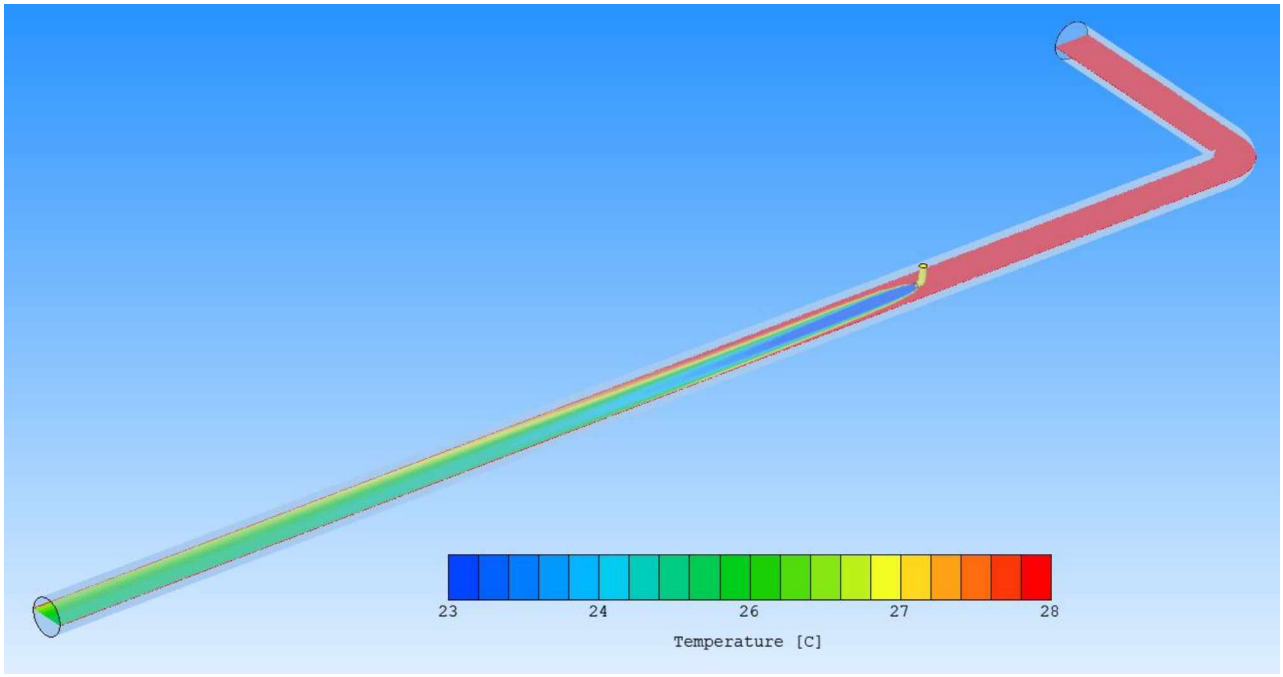

Figure B2 Temperature Gradient in Ventilation Duct for 12 VTs

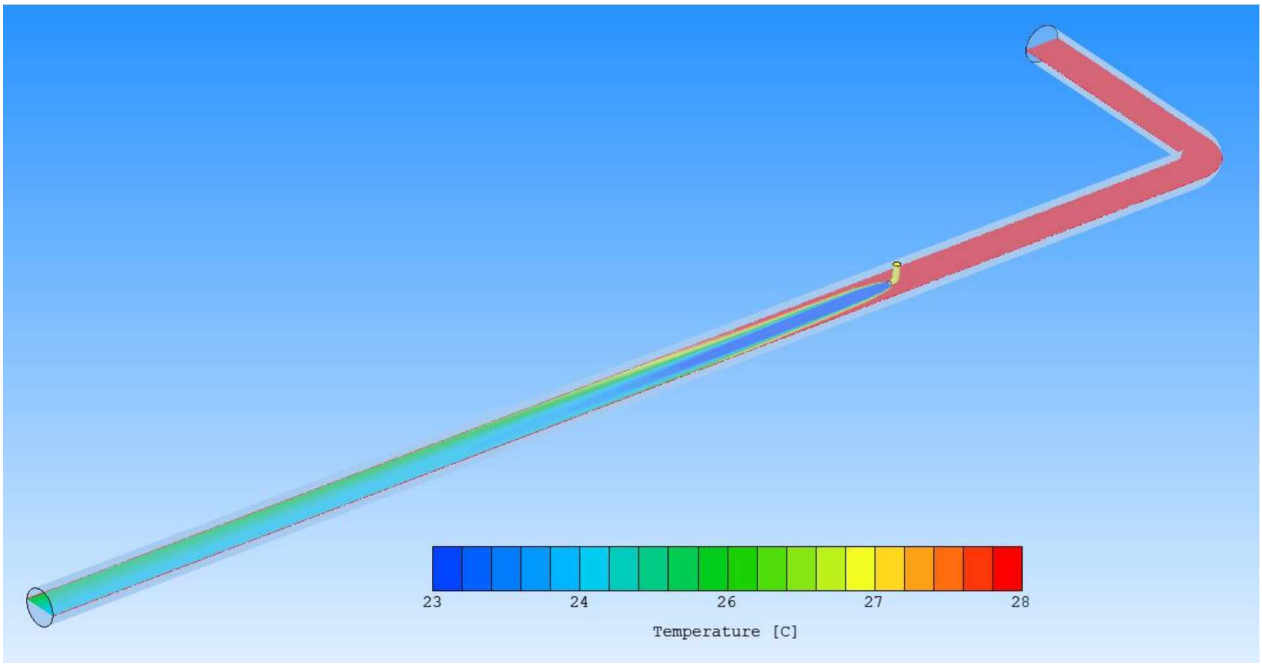

Figure B3 Temperature Gradient in Ventilation Duct for 16 VTs

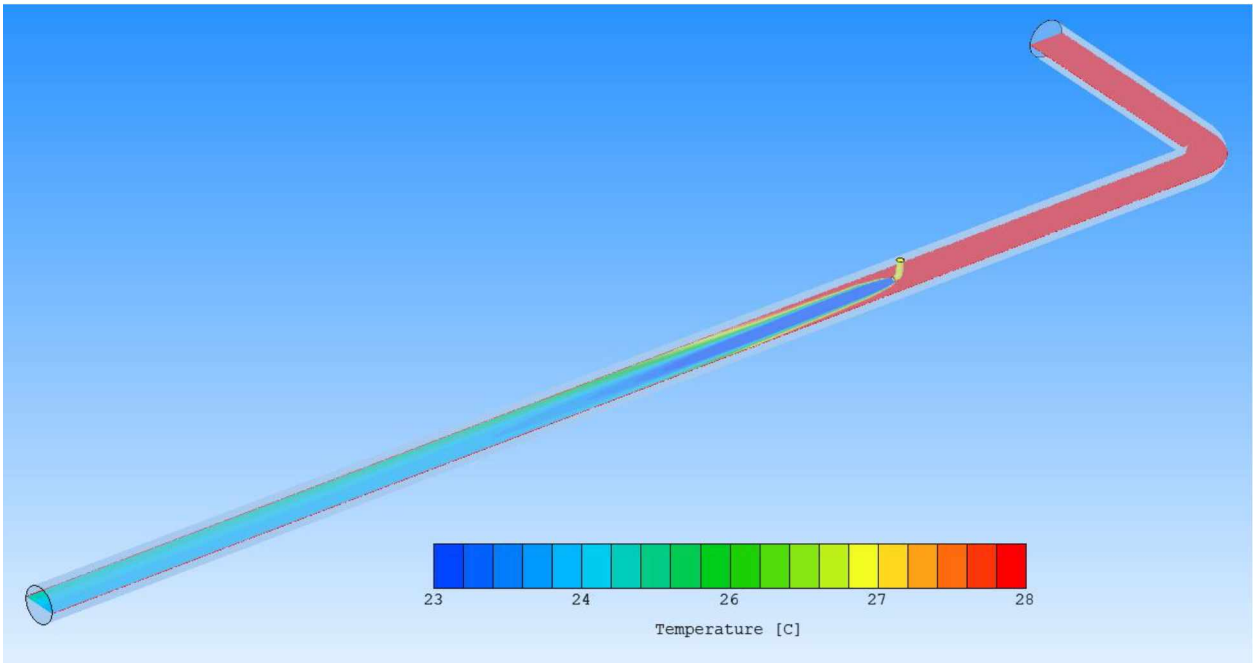

Figure B4 Temperature Gradient in Ventilation Duct for 18 VTs

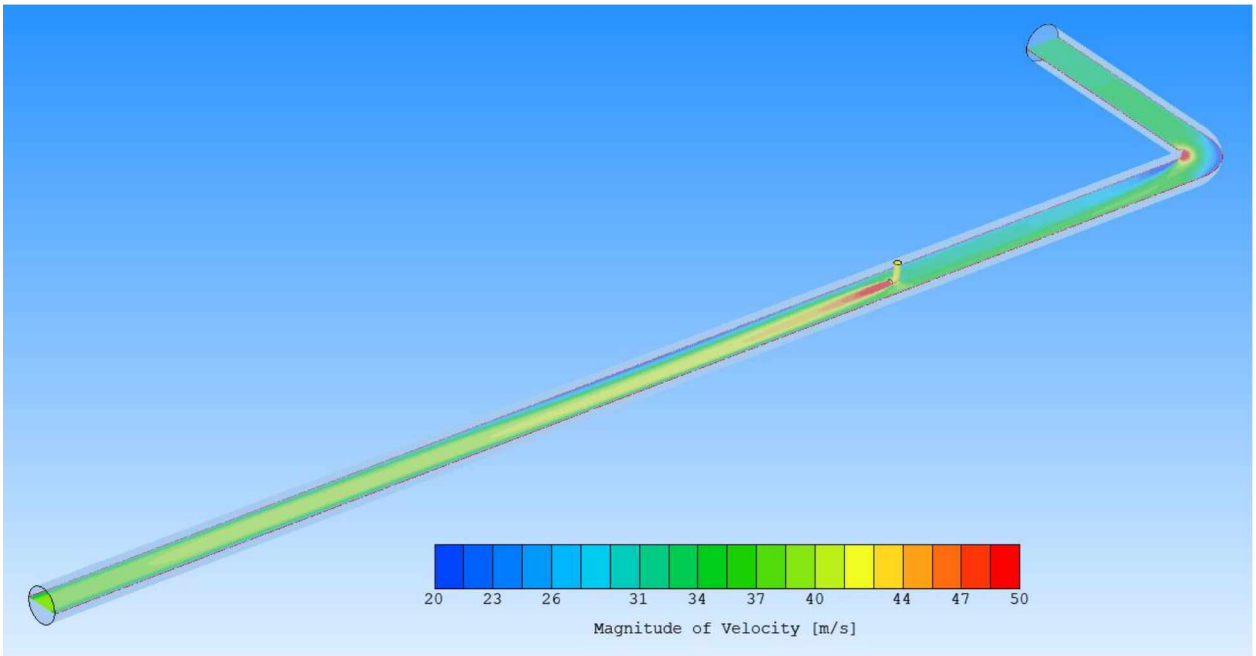

Figure B5 Velocity Gradient in Ventilation Duct for 8 VTs

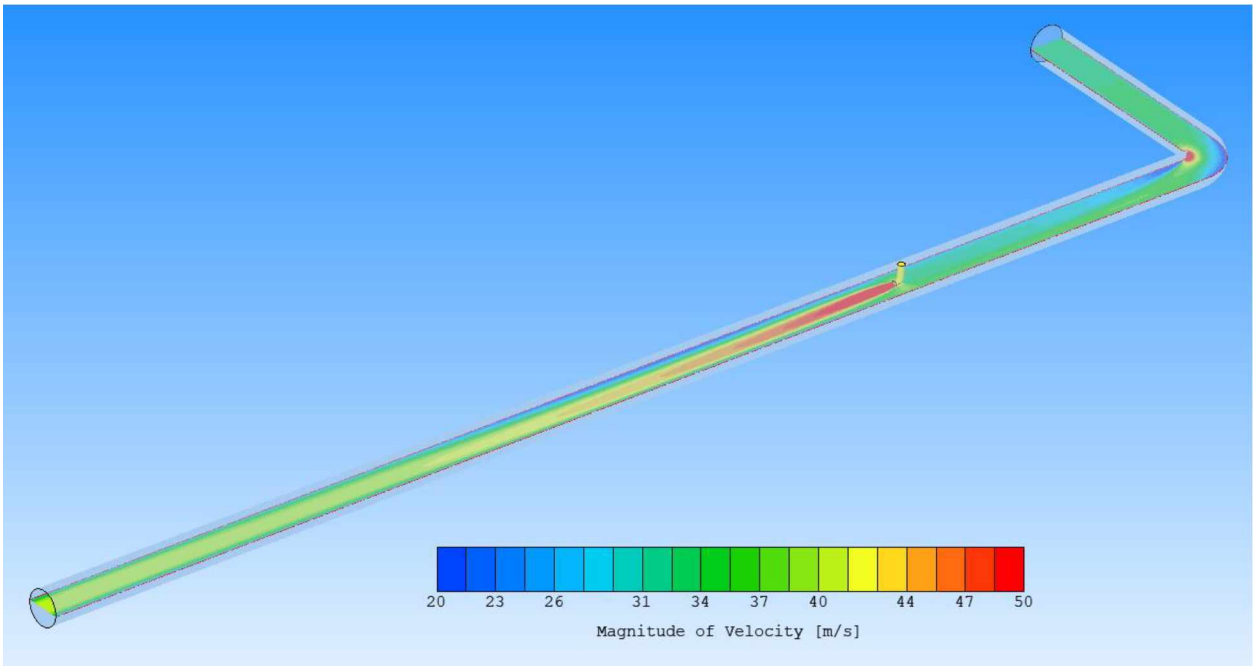

Figure B6 Velocity Gradient in Ventilation Duct for 10 VTs

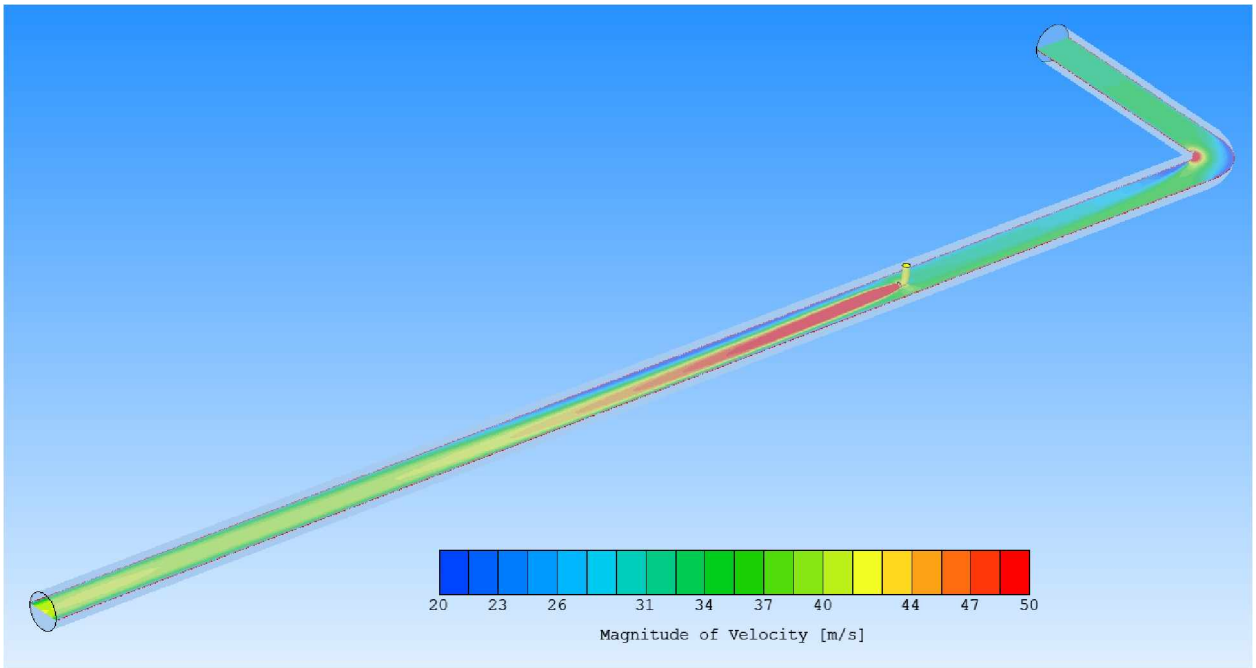

Figure B7 Velocity Gradient in Ventilation Duct for 12 VTs

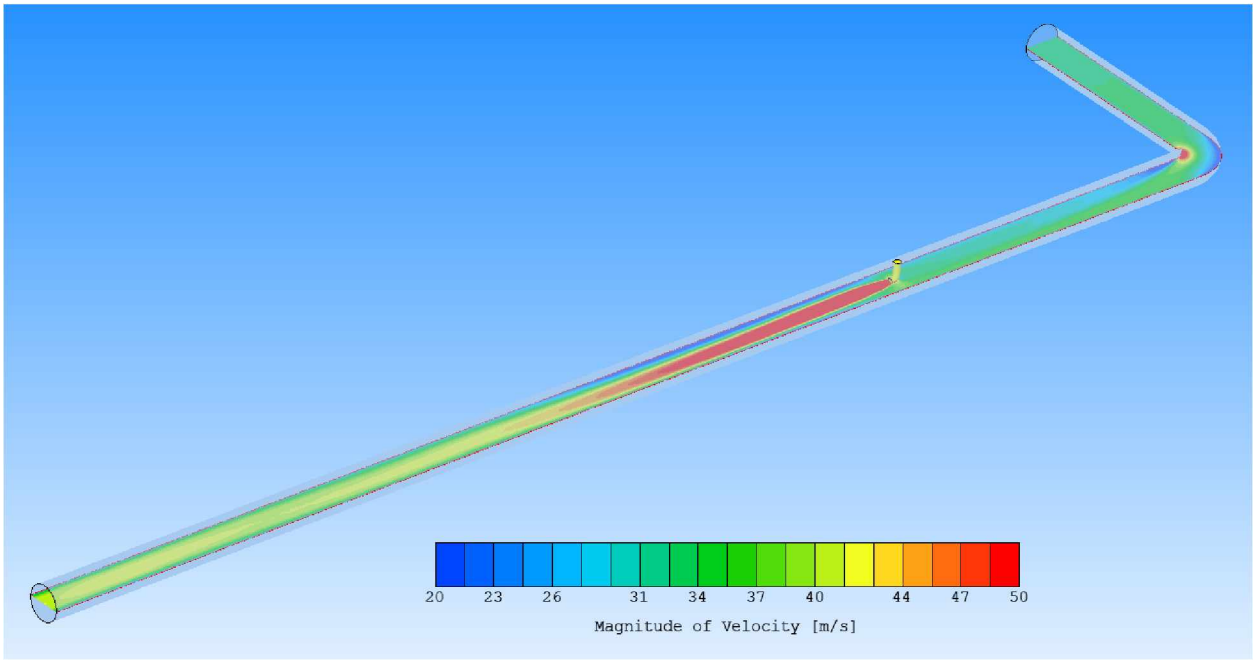

Figure B8 Velocity Gradient in Ventilation Duct for 14 VTs

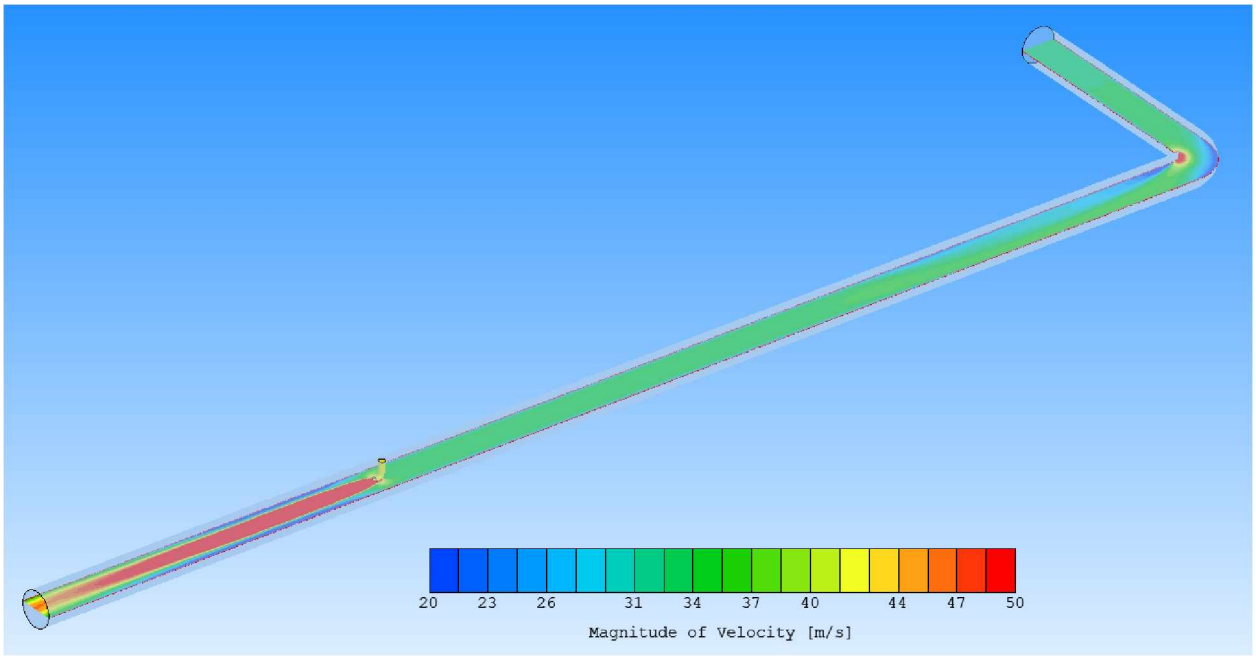

Figure B10 Velocity Gradient in Ventilation Duct for 16 VTs

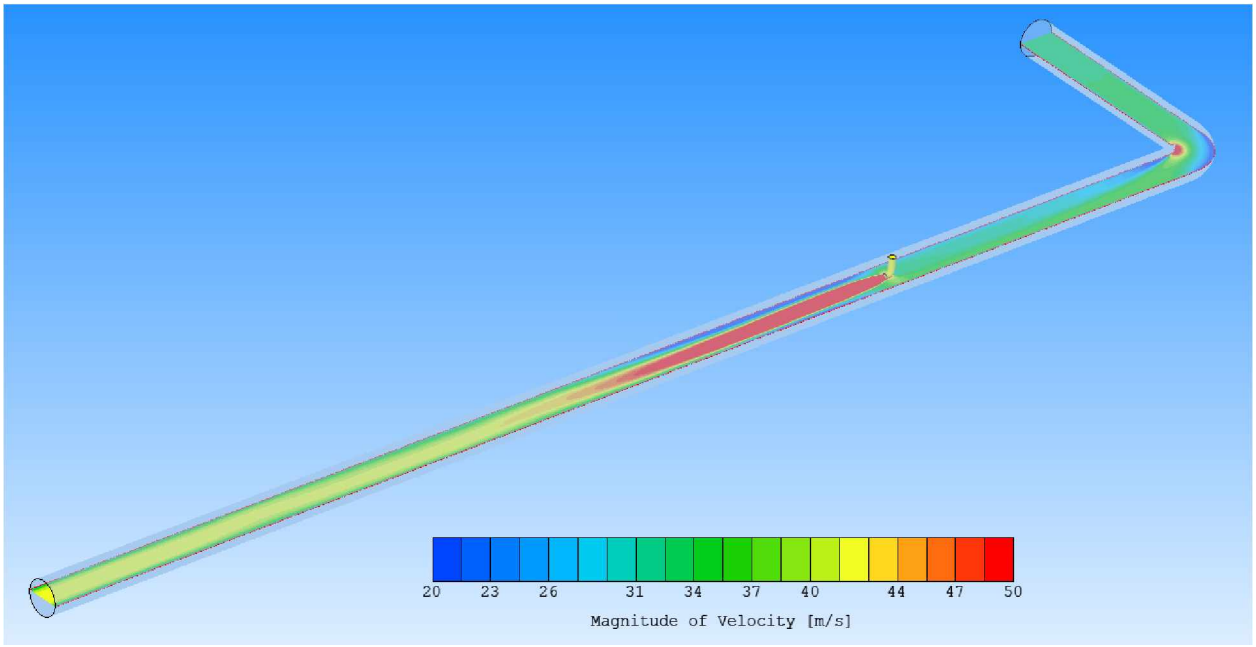

Figure B11 Velocity Gradient in Ventilation Duct for 18 VTs

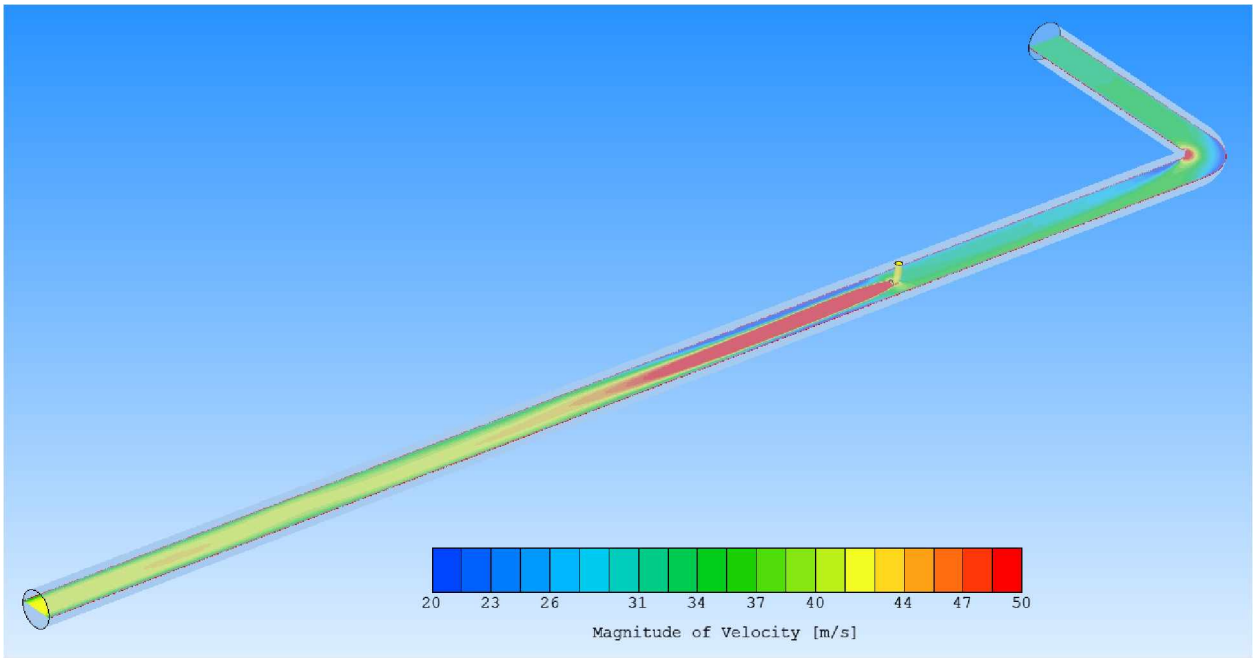

Figure B12 Velocity Gradient in Ventilation Duct for 20 VTs

Appendix C: Temperature and Velocity Gradient for VT Locations in Development Heading

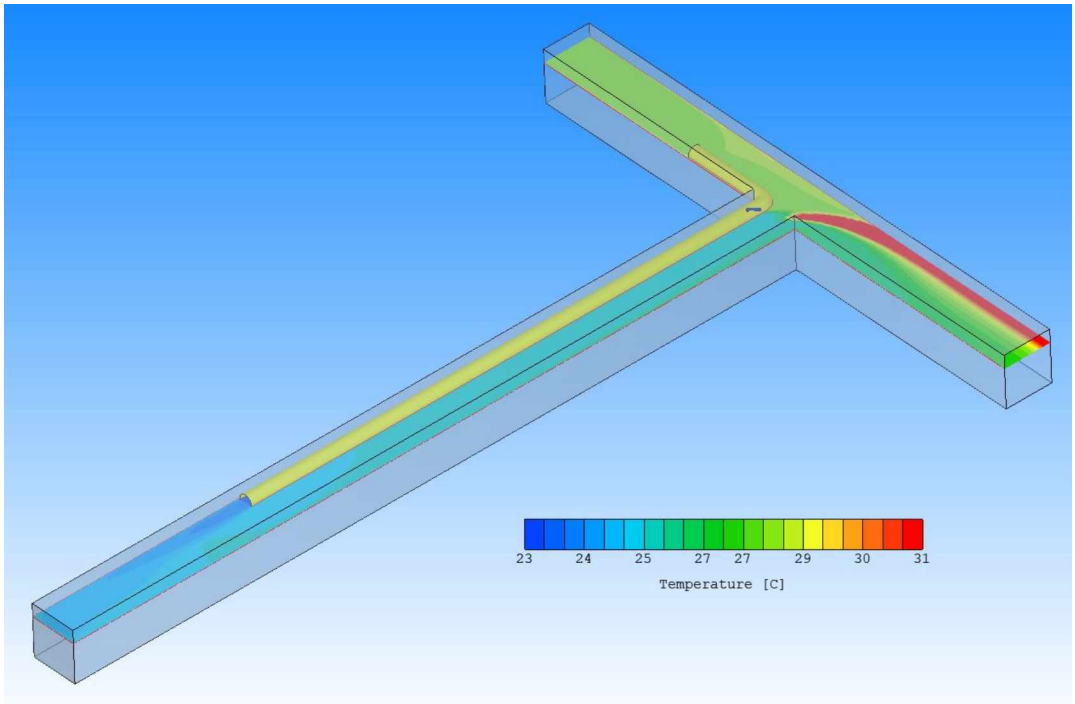

Figure C1 Temperature Gradient of Airflow in the Development Heading for VT Location 2

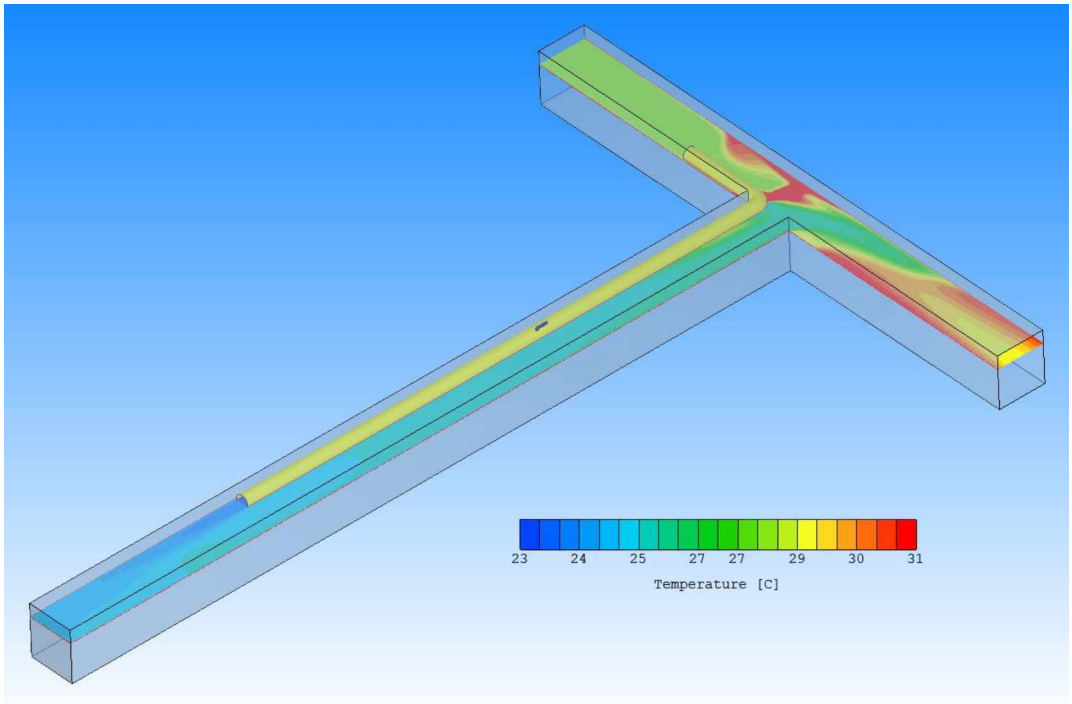

Figure C2 Temperature Gradient of Airflow in the Development Heading for VT Location 4

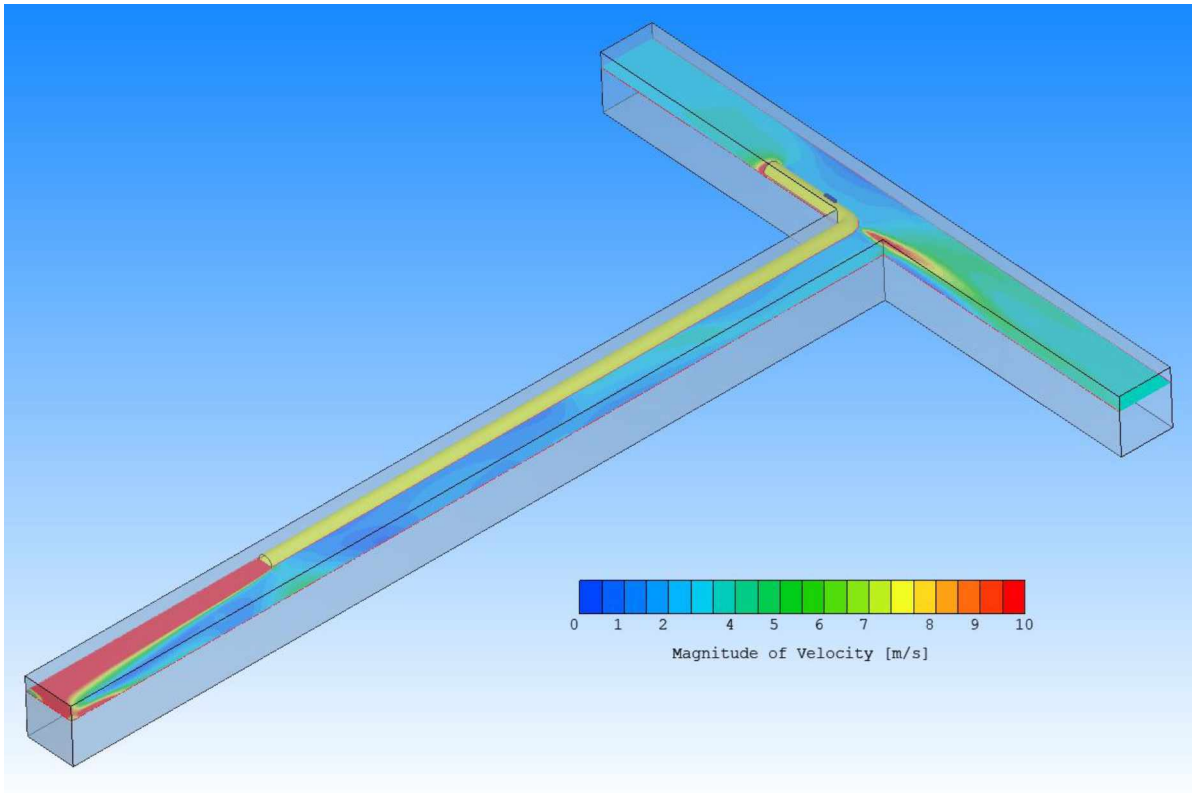

Figure C3 Velocity Gradient of Airflow in the Development Heading for VT Location 1

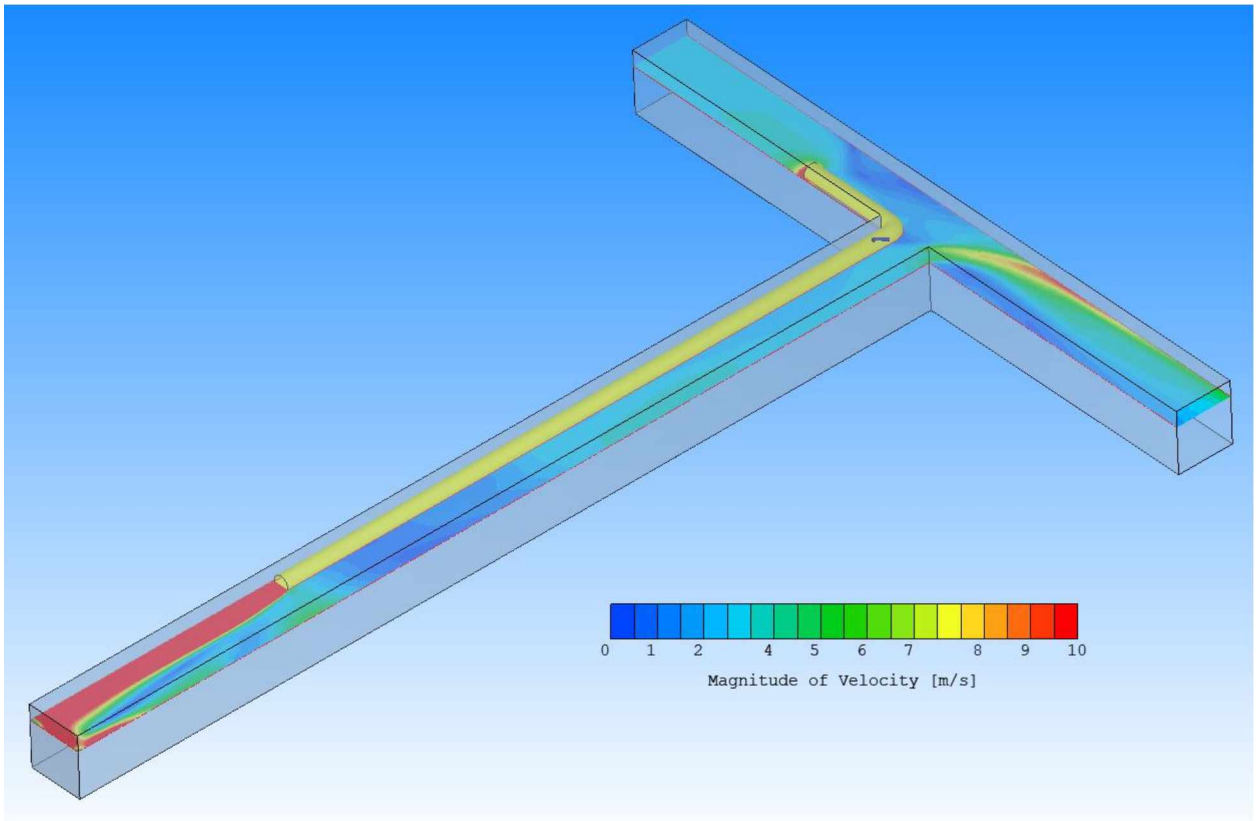

Figure C4 Velocity Gradient of Airflow in the Development Heading for VT Location 2

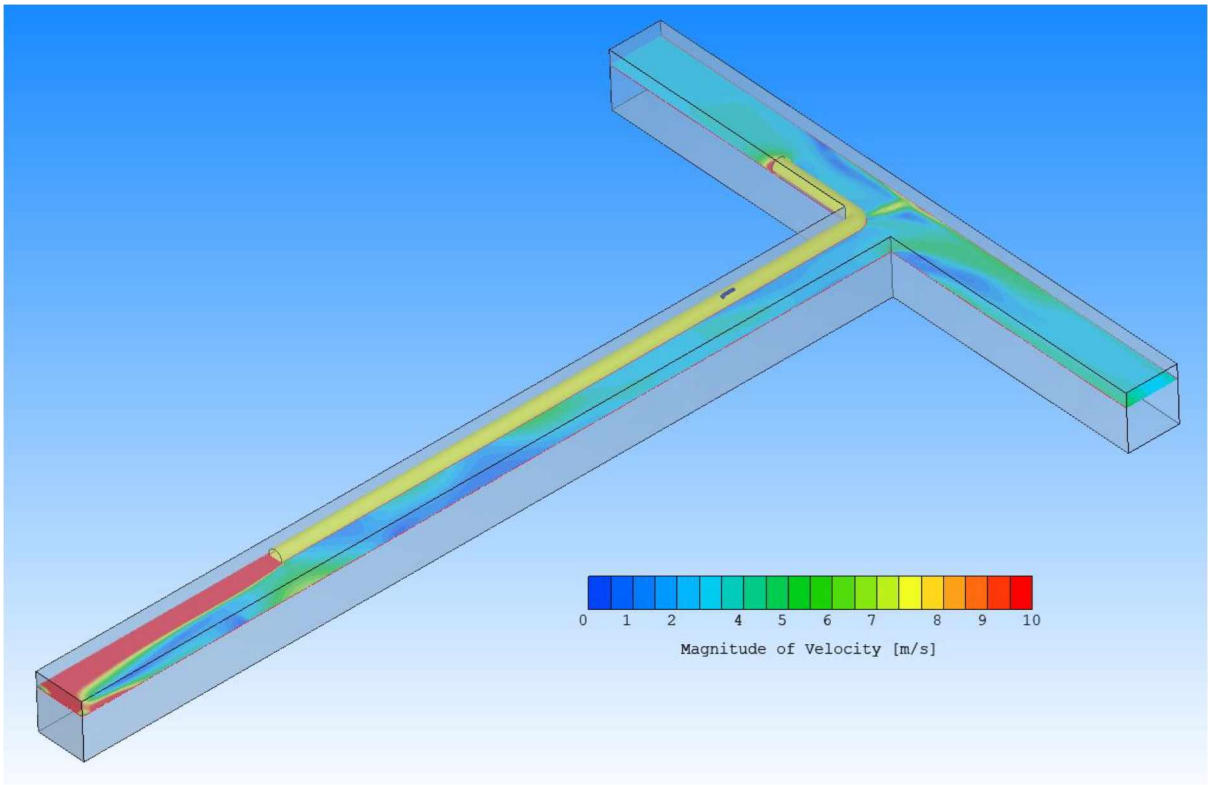

Figure C5 Velocity Gradient of Airflow in the Development Heading for VT Location 3

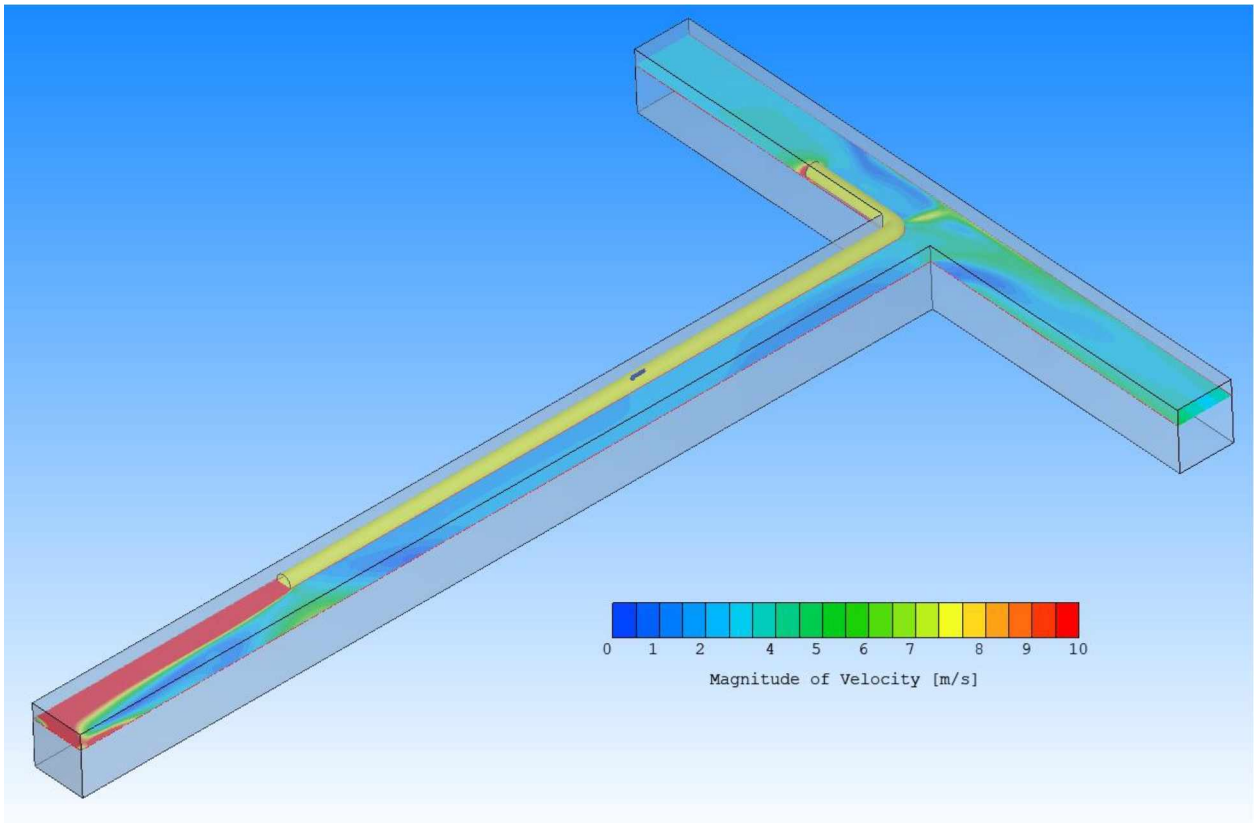

Figure C6 Velocity Gradient of Airflow in the Development Heading for VT Location 4

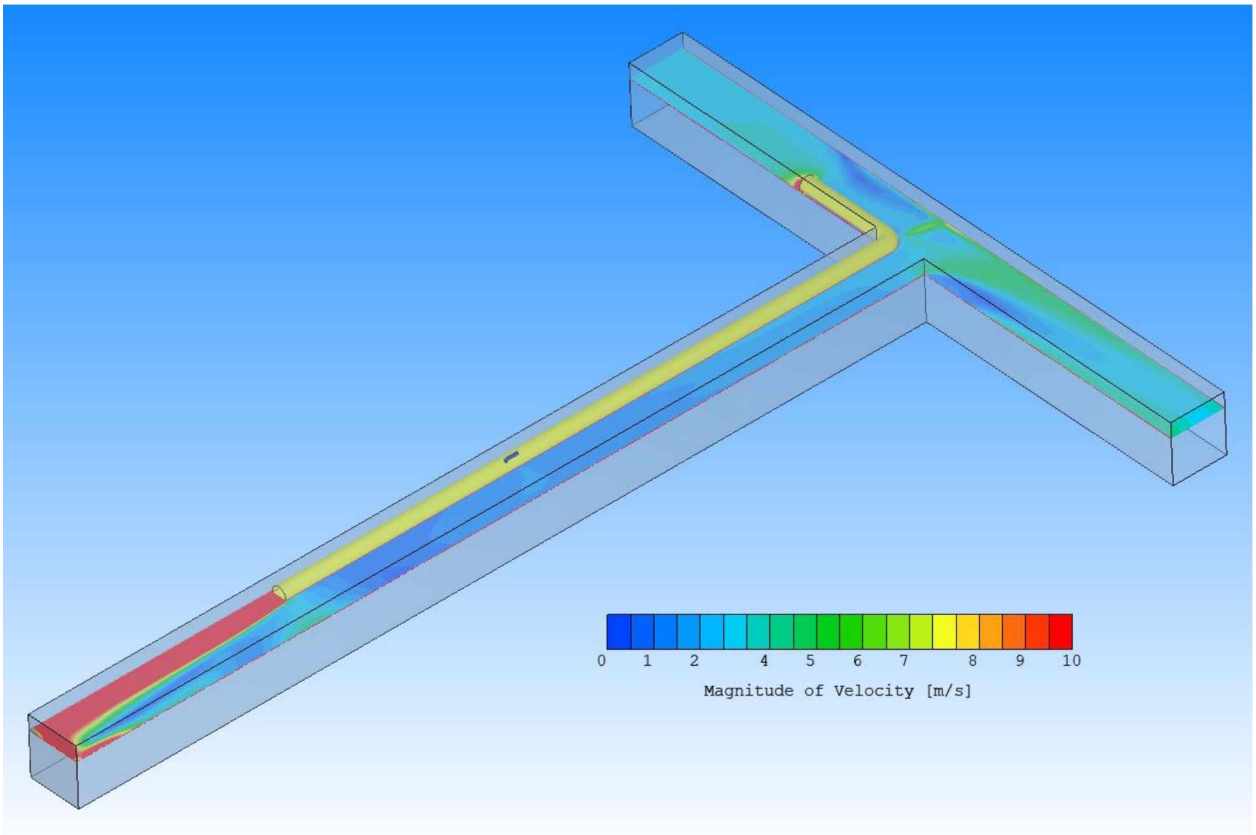

Figure C7 Velocity Gradient of Airflow in the Development Heading for VT Location 5

Appendix D: Temperature and Velocity Gradient for Number of VT in Development Heading

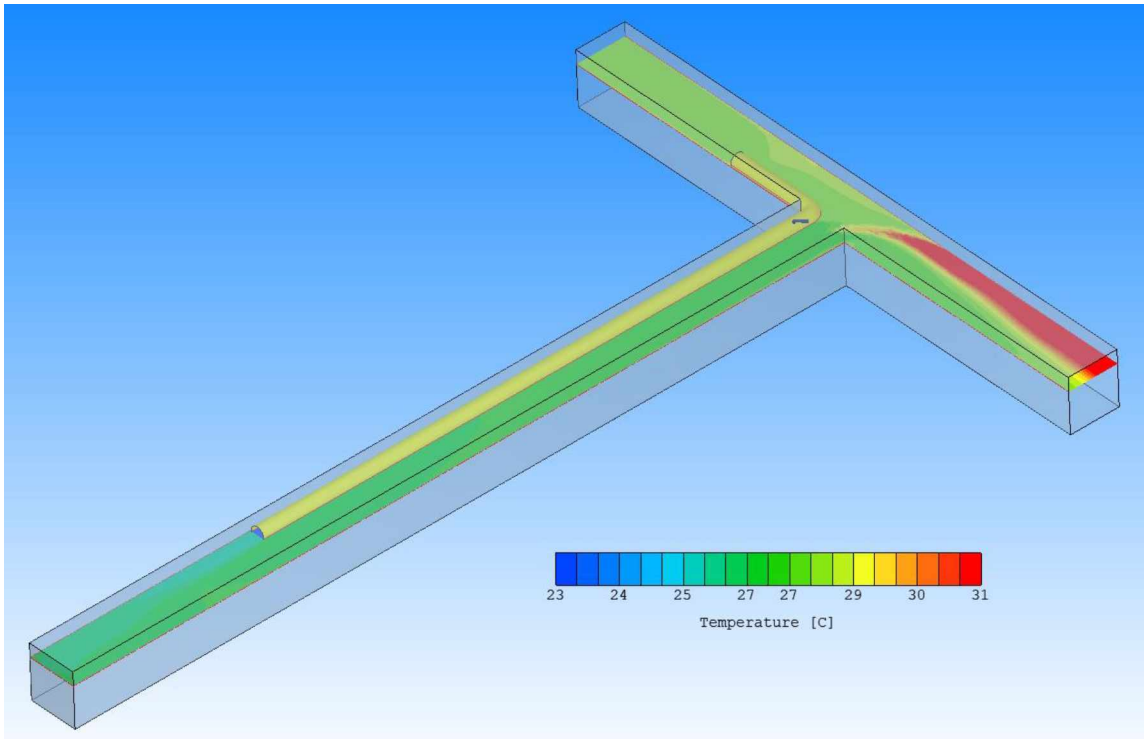

Figure D1 Temperature Gradient of Airflow in the Development Heading for 10 VTs

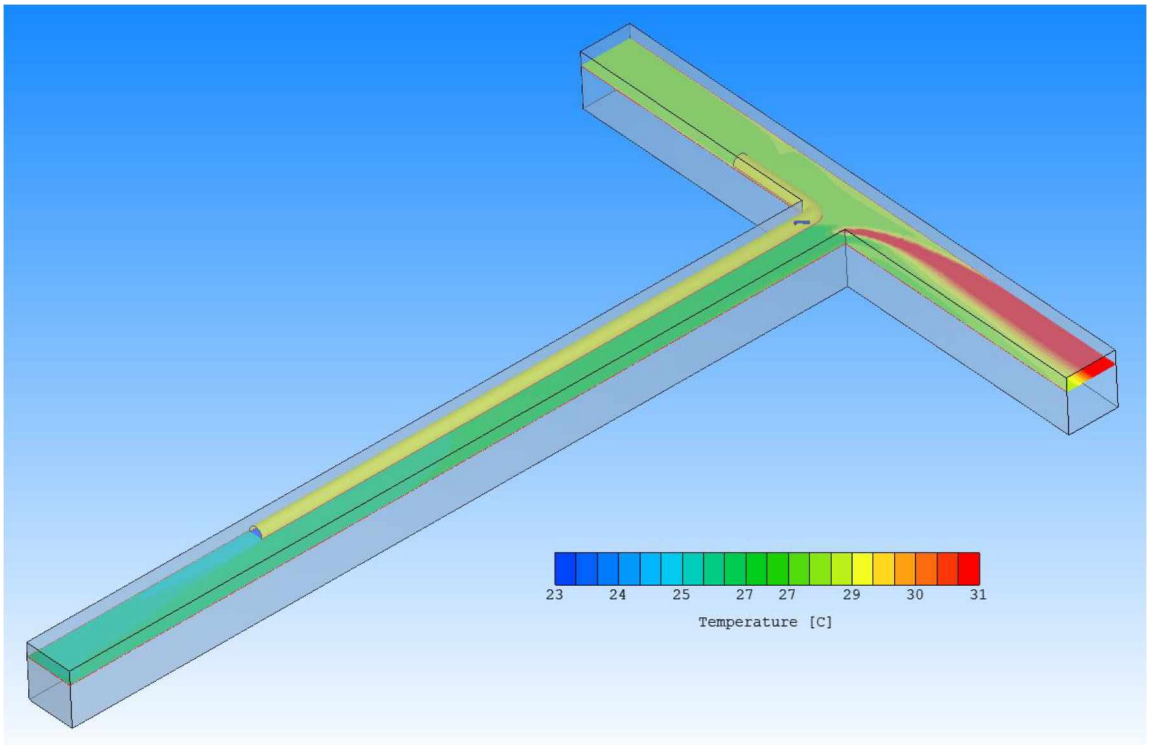

Figure D2 Temperature Gradient of Airflow in the Development Heading for 12 VTs

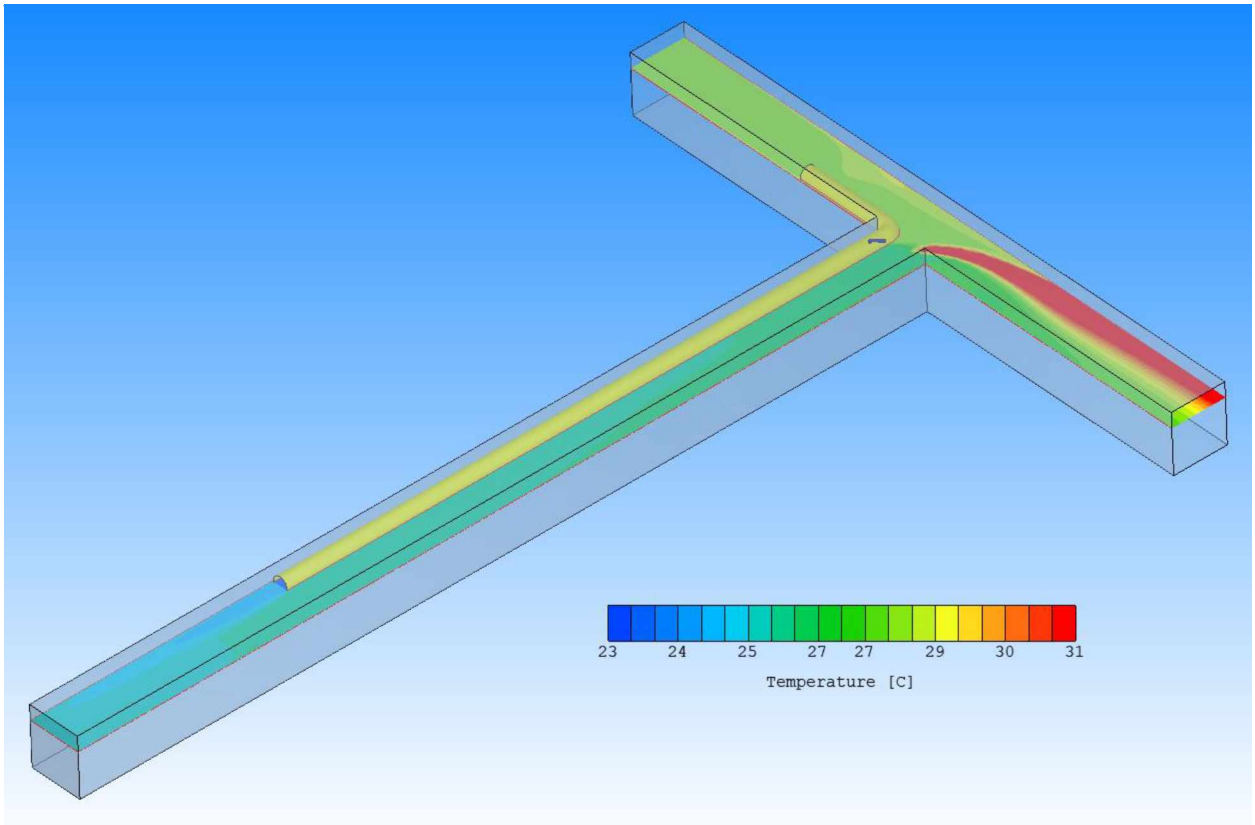

Figure D3 Temperature Gradient of Airflow in the Development Heading for 16 VTs

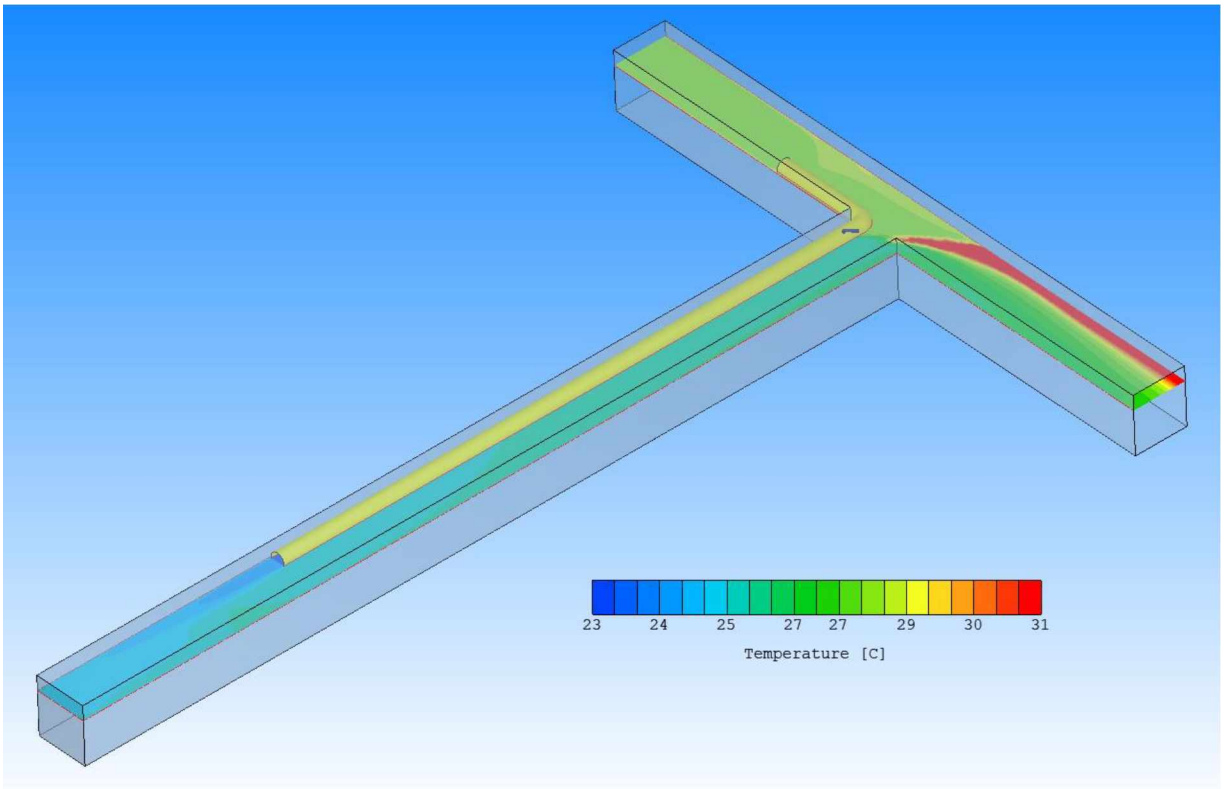

Figure D4 Temperature Gradient of Airflow in the Development Heading for 18 VTs

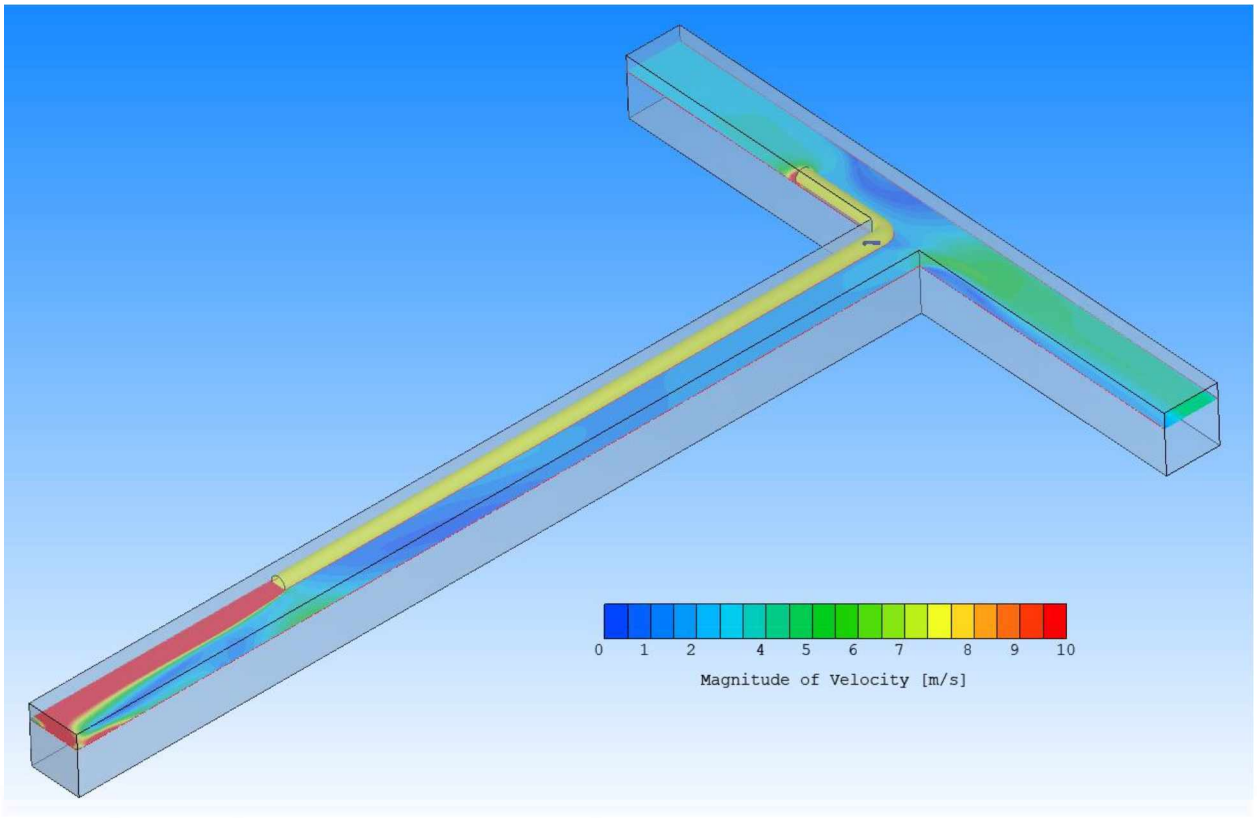

Figure D5 Velocity Gradient of Airflow in the Development Heading for 8 VTs

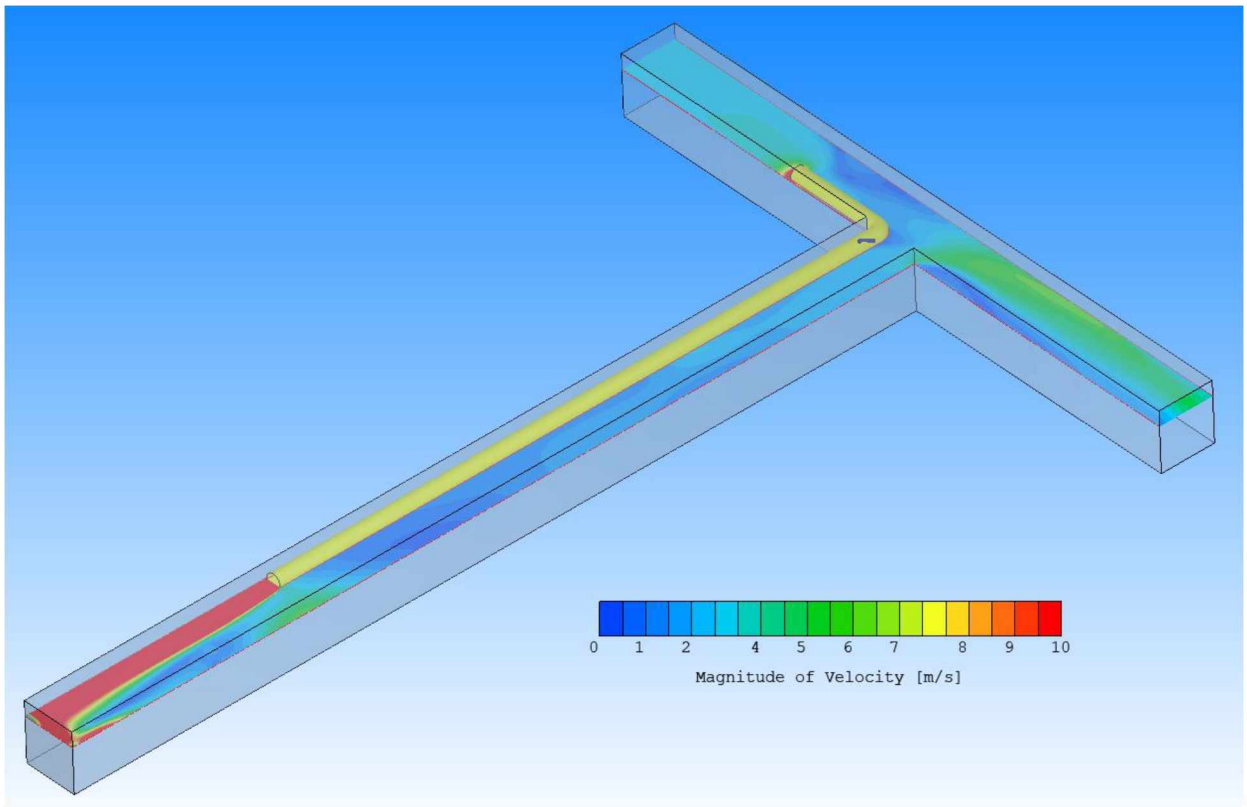

Figure D6 Velocity Gradient of Airflow in the Development Heading for 10 VTs

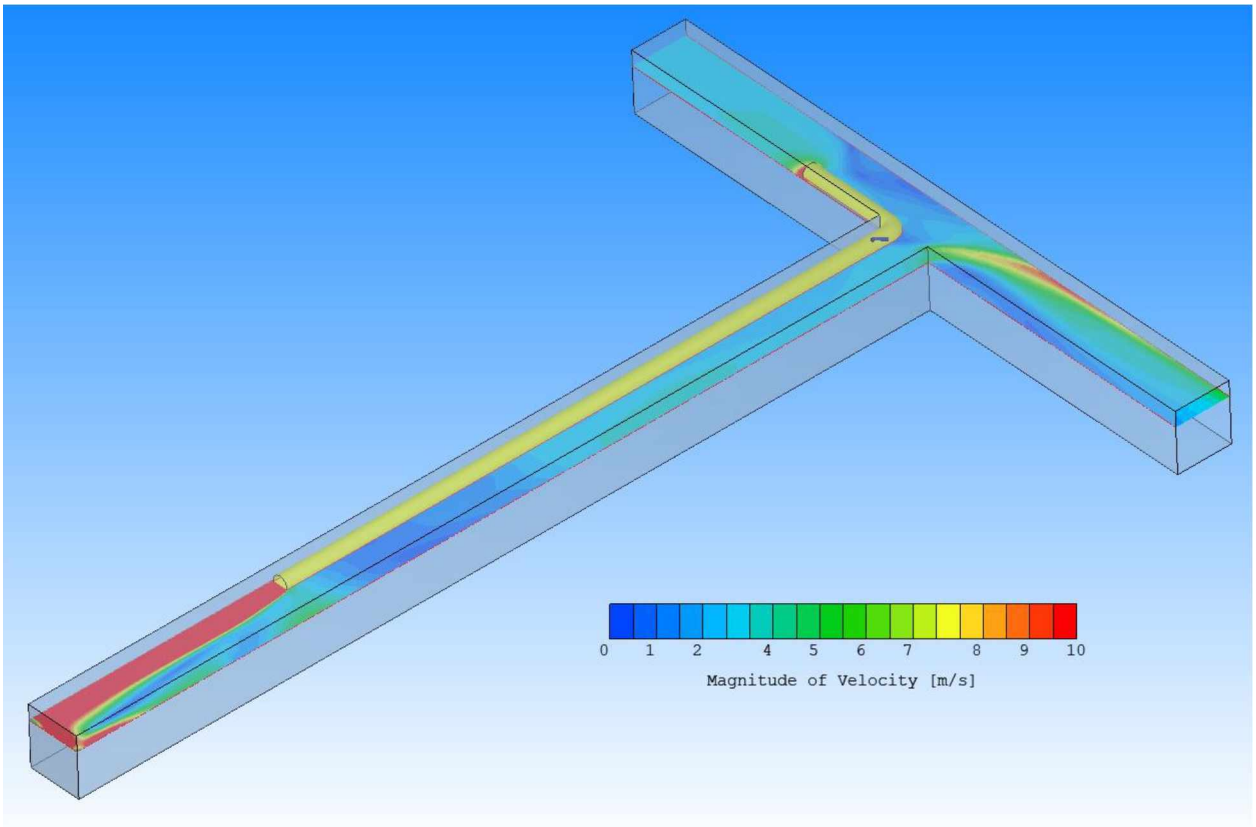

Figure D7 Velocity Gradient of Airflow in the Development Heading for 12 VTs

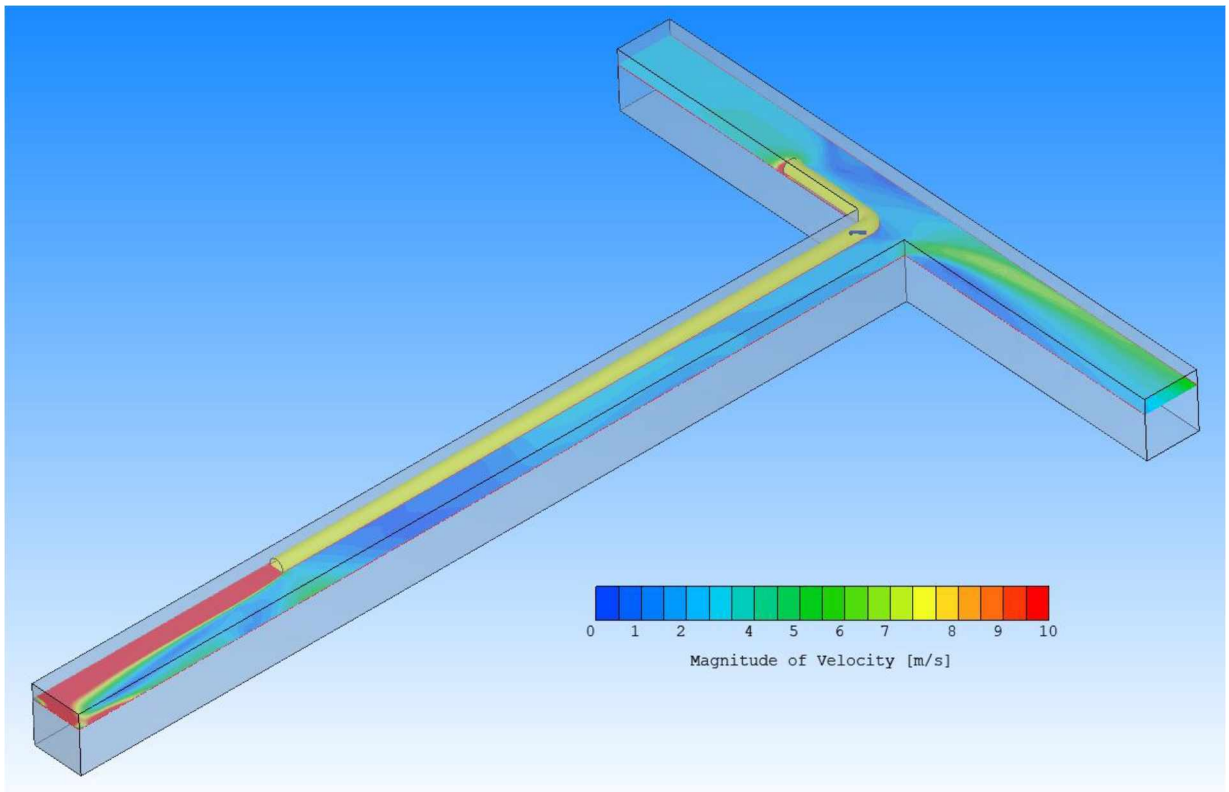

Figure D8 Velocity Gradient of Airflow in the Development Heading for 14 VTs

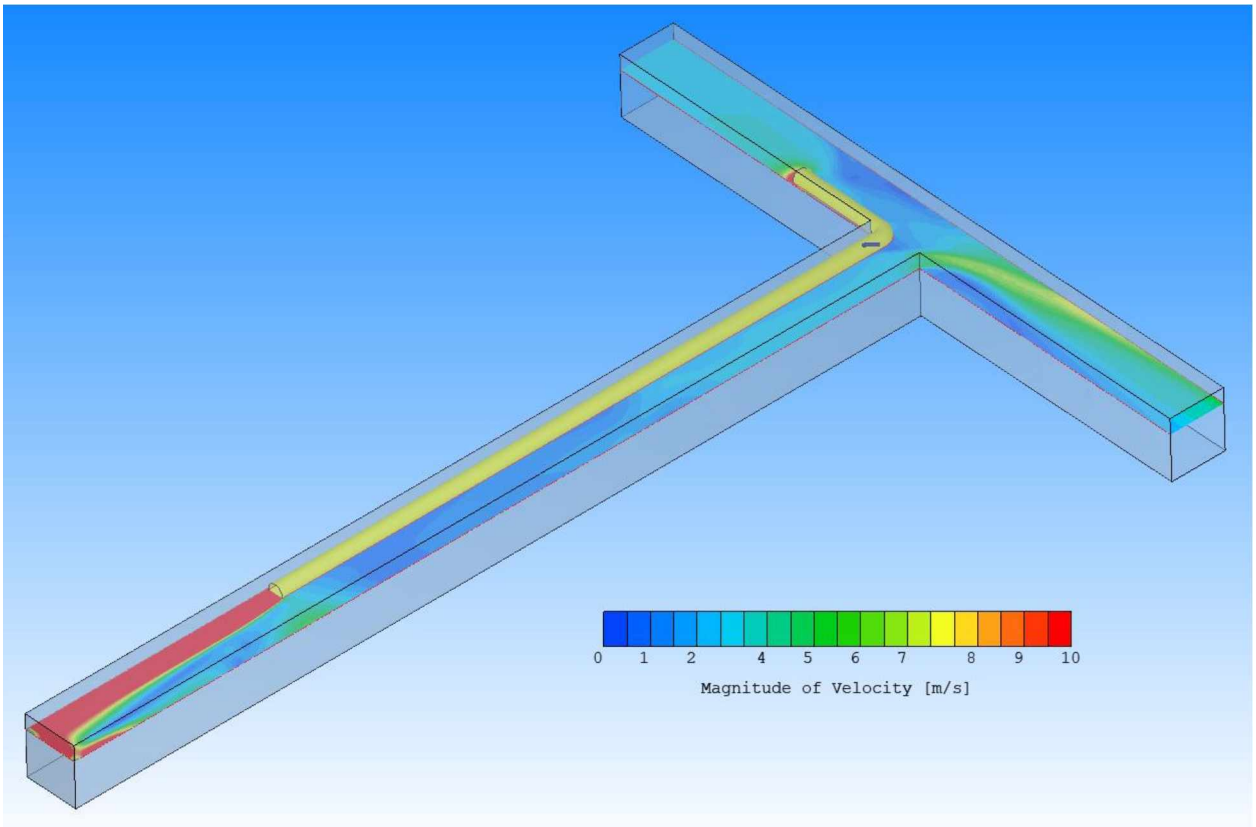

Figure D9 Velocity Gradient of Airflow in the Development Heading for 16 VTs

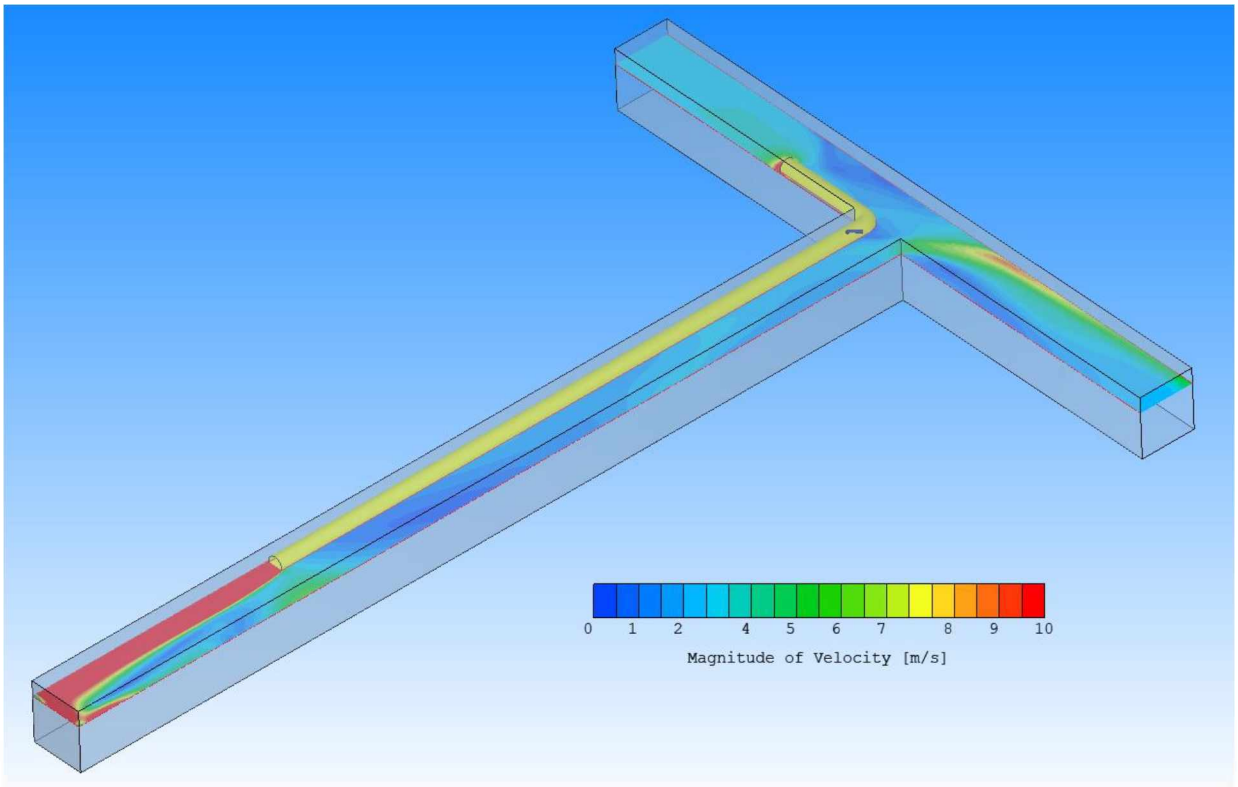

Figure D10 Velocity Gradient of Airflow in the Development Heading for 18 VTs

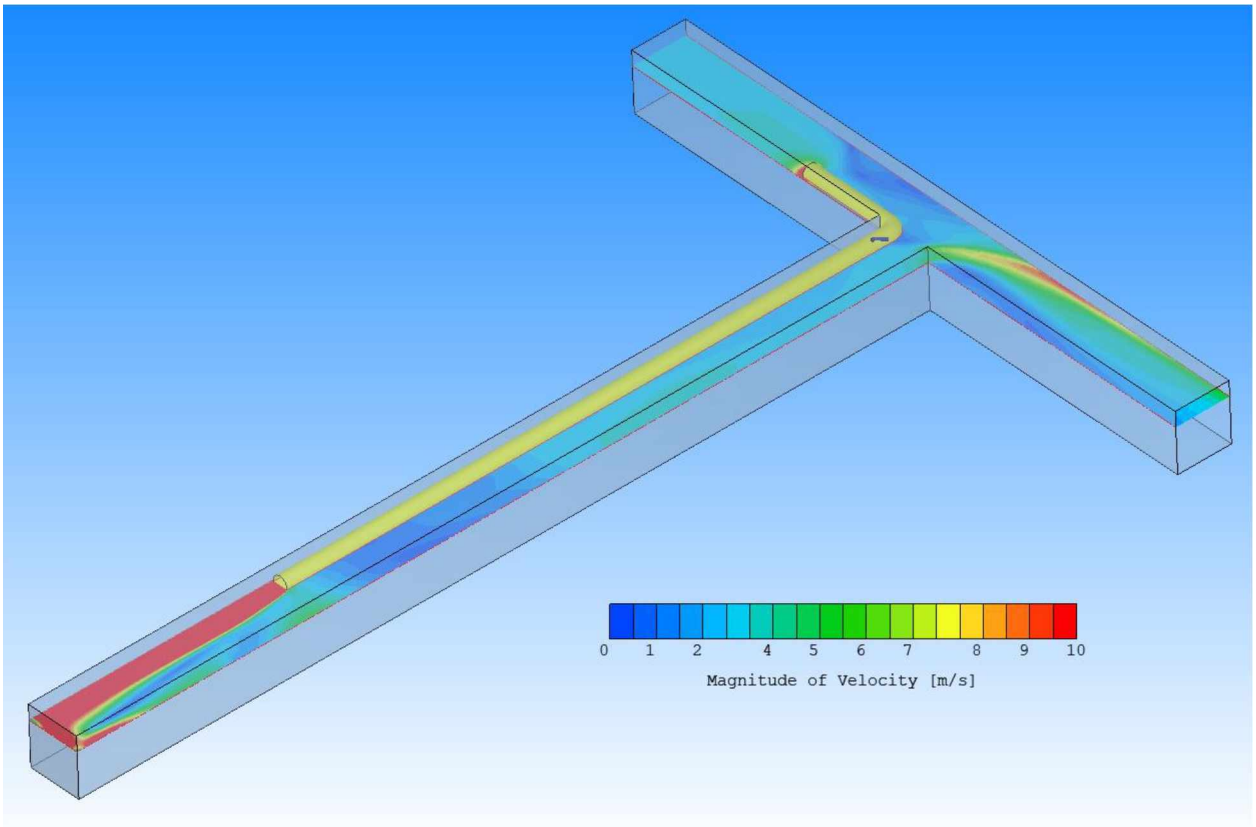

Figure D11 Velocity Gradient of Airflow in the Development Heading for 20 VTs